

Standard Penetration Test in Predicting the Shear Strength and the Cyclic Mobility of Fine Grained Soils

Rebin Sardar Husain

Submitted to the
Institute of Graduate Studies and Research
in partial fulfillment of the requirement for the degree of

Master of Science
in
Civil Engineering

Eastern Mediterranean University
July 2016
Gazimağusa, North Cyprus

Approval of the Institute of Graduate Studies and Research

Prof. Dr. Mustafa Tümer
Acting Director

I certify that this thesis satisfies the requirements as a thesis for the degree of Master of Science in Civil Engineering.

Prof. Dr. Özgür Eren
Chair, Department of Civil Engineering

We certify that we have read this thesis and that in our opinion it is fully adequate in scope and quality as a thesis for the degree of Master of Science in Civil Engineering.

Prof. Dr. Zalihe Sezai
Supervisor

Examining Committee

1. Prof. Dr. Zalihe Sezai

2. Assoc. Prof. Dr. Huriye Bilsel

3. Asst. Prof. Dr. Eriş Uygur

ABSTRACT

The evaluation of liquefaction susceptibility of soils and the related failures during earthquakes are one of the important aspects in geotechnical engineering. The liquefied soil will not only cause instability on substructure, but it will also cause failure on superstructure, resulting in catastrophic fatalities. Therefore, it is very important to be able to predict the liquefaction susceptibility of soils during earthquakes. There are different methods used for determining the liquefaction susceptibility of soils. In the present study, 20 boreholes in Basra city in Iraq were considered and the seismicity and the liquefaction susceptibility of the fine grained soils in these boreholes were studied by using the measured Atterberg limits, shear strength parameters and the standard penetration test, SPT N values. Because of the uncertainty and the confusion of the fine grained soils due to cyclic loading, the reliability of using the SPT values in predicting the Atterberg limits and the shear strength parameters of fine grained soils was also evaluated. According to the findings, Seed et al., (2003) and Bray et al., (2004) criteria's were found to be more applicable for predicting the liquefaction susceptibility of Basra soil based on Atterberg limits data. The calculated factor of safety, FS against liquefaction based on cyclic stress ratio, CSR and cyclic resistance ratio, CRR gave a high liquefaction potential for Basra soil. Strong correlations between the shear strength parameters and the SPT values were obtained whereas for the prediction of cone penetration resistance, q_c from SPT is not promising.

Keywords: Chinese criteria, cyclic mobility, cyclic resistance ratio, cyclic stress ratio, liquefaction susceptibility, seismicity, sensitivity.

ÖZ

Depremler sırasında toprakta sıvılaşma duyarlılığının ve ilgili göçmelerin değerlendirilmesi geoteknik mühendisliğin önemli yönlerinden biridir. Sıvılaşmış toprak yalnızca altyapı üzerinde istikrarsızlığa neden olmayıp, aynı zamanda felaket ölümlerle sonuçlanan, üstyapı üzerinde yetmezliğe de neden olur. Bu nedenle, deprem sırasında zemin sıvılaşma duyarlılığını tahmin edebilmek çok önemlidir. Zeminlerin sıvılaşma duyarlılığını belirlemek için kullanılan farklı yöntemler vardır. Bu çalışmada, Irak Basra kentinde 20 adet sondaj kuyusu dikkate alınıp, bu noktadaki ince taneli zeminlerin deprensellik ve sıvılaşma duyarlılığı, ölçülen kıvam limitleri, kayma mukavemeti parametreleri ve standard penetrasyon deneyi, N değeri kullanılarak incelendi. İnce taneli zeminlerin tekrarlı yükleme altındaki davranışlarındaki belirsizlik nedeniyle, ince taneli zeminlerin kıvam limitleri ve kayma mukavemeti parametrelerinin SPT değerleri kullanılarak tahminindeki güvenilirliği de değerlendirilmiştir. Elde edilen bulgulara göre, Seed ve diğerleri (2003) ve Bray ve diğerleri (2004) kriterleri, kıvam limitleri verilerine dayanarak Basra toprağının sıvılaşma duyarlılığı tahmininde daha uygun olduğu bulunmuştur. Tekrarlı gerilme oranı, TGO ve tekrarlı direnç oranları, TDO esas alınarak sıvılaşmaya karşı hesaplanan güvenlik faktörü, Basra toprağı için yüksek sıvılaşma potansiyeli verdi. Kayma direnci parametreleri ve SPT değerleri arasında kuvvetli korelasyon elde edilirken SPT kullanılarak koni penetrasyon direnci, qc tahmini umut verici değildir.

Anahtar kelimeler: Çin kriteri, tekrarlı hareketlilik, tekrarlı direnç oranı, tekrarlı gerilme oranı, sıvılaşma duyarlılığı, deprensellik, duyarlılık.

This thesis is dedicated to

The blessed soul of my beloved father, who rests in the
heavens

My parents

My darling wife Mrs. Rekan

Both my daughters, (Layn & Lare)

ACKNOWLEDGMENT

I would like to express my sincere gratitude to my supervisor Prof. Dr. Zalihe Sezai for her guidance, patience, support, and invaluable advices throughout this study and for her corrections in the text. In fact, she is a great advisor. I was so lucky to have her as my supervisor. Also special thanks to the other members of my graduate committee, Assoc. Prof. Dr. Huriye Bilsel and Asst. Prof. Dr. Eriş Uygur.

I would like to express my appreciation to ANDREA Company especially Dr. Azad to give me the data for my thesis. Moreover, many thanks to my lovely Mom and dear Uncle Ali and my best brother Darbaz and my lovely friend Ranjdar for their emotional supports and encouragements for me to continue in graduate studies.

Finally, I wish to express my deepest appreciations to my true treasures in life, my wife, dear Mrs. Rekan for her love, endless patience, encouragement, and all kind of support during this study. My dear daughters Layn and Lare, I am so thankful to God for giving me such gifts. My life would have never been complete without you. I hope one day, I will see you both at this stage.

TABLE OF CONTENTS

ABSTRACT	iii
ÖZ.....	iv
DEDICATION	v
ACKNOWLEDGMENT.....	vi
LIST OF TABLES	xi
LIST OF FIGURES.....	xiii
1 INTRODUCTION	1
1.1 Introduction.....	1
1.2 Objectives of the Study	4
1.3 Organization of the Study	5
2 SEISMICITY OF IRAQ	5
2.1 Introduction.....	6
2.2 Development of the Arabian Plate.....	6
2.3 Seismic Tectonics and Seismicity of Iraq.....	8
2.3.1 Regional Seismicity.....	10
2.3.2 Macro and Microseismicity of Iraq	12
2.4 Seismic Hazard Analysis	14
3 LITERATURE REVIEW.....	16
3.1 Introduction.....	16
3.2 Fundamentals of Liquefaction.....	19
3.2.1 Cyclic Mobility	20
3.2.2 Flow Liquefaction.....	21
3.3 Effects of Liquefaction.....	22

3.4 Remedies of Liquefaction.....	24
3.4.1 Soil Replacement	24
3.4.2 Water Pumping	24
3.4.3 Solidification.....	24
3.4.4 Gravel Drains.....	25
3.4.5 Enhancing Resistance to Liquefaction.....	25
3.4.6 Resistant Structures	25
3.5 Liquefaction and Nanoparticles	25
3.6 Structural Designs and Liquefaction	27
3.7 Soil Susceptibility and Liquefaction	28
3.8 Detection of Liquefaction	29
3.8.1 Standard Penetration Test (SPT)	31
3.8.2 Cone Penetration Test (CPT).....	32
4 METHODOLOGY.....	34
4.1 Introduction.....	34
4.2 Liquefaction Evaluation Based on Index Properties	34
4.2.1 The Polito and Martin (2001) Criteria	35
4.2.2 The Seed et al. (2003) Criteria.....	36
4.2.3 The Chinese Criteria (1982)	36
4.2.4 The Bray and Sancio (2004) Criteria.....	37
4.2.5 Boulanger and Idriss (2004 and 2006) Criteria	37
4.3 Soil Parameters Obtained from Field Tests.....	38
4.3.1 The Standard Penetration Test (SPT)	38
4.4 Soil Parameters Obtained from Laboratory Test	39
4.4.1 The Unconfined Compression Test	39

4.4.2 Atterberg Limits.....	40
4.5 Soil Liquefaction Potential Assessment.....	41
4.5.1 Evaluation of Cyclic Stress Ratio (CSR).....	42
4.5.2 Evaluation of Liquefaction Resistance (CRR).....	43
4.6 Calculation of Factor of Safety (FS) Against Liquefaction	45
4.6.1 Magnitude Scaling Factor, MSF	46
4.7 The Liquefaction Potential Index (LPI).....	47
4.8 Probability of Liquefaction.....	48
4.9 Coefficient of Determination, R^2 : SPT versus LL, PI, Shear Strength Parameters.....	50
4.10 Predicting q_c from the SPT N Number	51
4.11 Estimating the Undrained Shear Strength (S_u) by SPT N Value	51
5 RESULTS AND DISCUSSIONS	53
5.1 Soil Classification in Boreholes.....	53
5.2 Assessment of Liquefaction by Index Properties	60
5.2.1 The Polito and Martin (2001) Criteria	61
5.2.2 Seed et al. (2003) Criteria.....	61
5.2.3 Chinese Criteria (1982).....	62
5.2.1 Bray and Sancio (2004) Criteria	63
5.2.2 Boulanger and Idriss (2004 and 2006) Criteria	63
5.3 In-situ and Laboratory Tests Results Used for Predicting the Liquefaction Susceptibility of Basra Soils.....	64
5.3.1 Sensitivity	64
5.3.2 Factor of Safety Determination Based on SPT N Value	66
5.3.3 Liquefaction Potential Index, LPI Based on SPT	68

5.3.4 Liquefaction Severity Index Based on SPT.....	71
5.4 Correlations between SPT and Shear Strength Parameters.....	75
5.4.1 Measured Atterberg Limits and SPT N Values	75
5.4.2 Correlation between SPT, Atterberg Limits and the Shear Strength Parameters.....	78
5.4.3 Predicting Cone Penetration Resistance q_c by Using SPT N Number.....	81
5.4.4 Estimating Undrained Shear Strength (S_u) by SPT Value.....	82
6 CONCLUSION	85
REFERENCES.....	88
APPENDICES	101
Appendix A: Laboratory Test Result	102
Appendix B: Borehole Logs.....	113

LIST OF TABLES

Table 4.1: Classifications of sensitivity (Rosenqvist, 1953).....	40
Table 4.2: MSF value defined by various researchers (Youd and Noble, 1997a).	46
Table 4.3: Groupings of liquefaction potential index (Sonmez, 2003).....	48
Table 4.4: The Liquefaction severity classification (Sönmez and Gökçeoğlu, 2005).	50
Table 4.5: Correlation between q_u and SPT by (Terzaghi and Peck, 1987).....	52
Table 5.1: Value of SPT, Atterberg limit and soil classification for borehole 1.....	53
Table 5.2: Value of SPT, Atterberg limit and soil classification for borehole 2.....	54
Table 5.3: Value of SPT, Atterberg limit and soil classification for borehole 3.....	54
Table 5.4: Value of SPT, Atterberg limit and soil classification for borehole 4.....	54
Table 5.5: Value of SPT, Atterberg limit and soil classification for borehole 5.....	55
Table 5.6: Value of SPT, Atterberg limit and soil classification for borehole 6.....	55
Table 5.7: Value of SPT, Atterberg limit and soil classification for borehole 7.....	56
Table 5.8: Value of SPT, Atterberg limit and soil classification for borehole 8.....	56
Table 5.9: Value of SPT, Atterberg limit and soil classification for borehole 9.....	56
Table 5.10: Value of SPT, Atterberg limit and soil classification for borehole 10....	57
Table 5.11: Value of SPT, Atterberg limit and soil classification for borehole 11....	57
Table 5.12: Value of SPT, Atterberg limit and soil classification for borehole 12....	57
Table 5.13: Value of SPT, Atterberg limit and soil classification for borehole 13....	58
Table 5.14: Value of SPT, Atterberg limit and soil classification for borehole 14....	58
Table 5.15: Value of SPT, Atterberg limit and soil classification for borehole 15....	58
Table 5.16: Value of SPT, Atterberg limit and soil classification for borehole 16....	59
Table 5.17: Value of SPT, Atterberg limit and soil classification for borehole 17....	59

Table 5.18: Value of SPT, Atterberg limit and soil classification for borehole 18....	59
Table 5.19: Value of SPT, Atterberg limit and soil classification for borehole 19....	60
Table 5.20: Value of SPT, Atterberg limit and soil classification for borehole 20....	60
Table 5.21: Result of sensitivity values of Basra soil	65
Table 5.22: Sensitivity classification of Basra soils according to (Rosenqvist, 1953).	66
Table 5.23: Calculated factor of safeties against liquefaction using SPT $(N_1)_{60cs}$ values.	67
Table 5.24: SPT based Liquefaction Potential Index, LPI classification at $M_w= 6.0$ and $a_{max} = 0.2$	68
Table 5.25: SPT based Liquefaction Potential Index, LPI classification at $M_w= 6.5$ and $a_{max} = 0.2g$	69
Table 5.26: SPT based Liquefaction Potential Index, LPI classification at $M_w= 7.0$ and $a_{max} = 0.2g$	70
Table 5.27: SPT based Liquefaction Potential Index, LPI classification at $M_w= 7.5$ and $a_{max} = 0.2g$	71
Table 5.28: SPT based liquefaction severity index and the classification at $M_w= 6.0$ and $a_{max} = 0.2g$	72
Table 5.29: SPT based liquefaction severity index and the classification at $M_w= 6.5$ and $a_{max} = 0.2g$	73
Table 5.30: SPT based liquefaction severity index and the classification at $M_w= 7.0$ and $a_{max} = 0.2g$	74
Table 5.31: SPT based liquefaction severity index and the classification at $M_w= 7.5$ and $a_{max} = 0.2g$	75

LIST OF FIGURES

Figure 2.1: Movement of the Arabian Plate in relation to Africa (Johnson, 1998)	7
Figure 2.2: The stratigraphic column of Kurdistan Region of Iraq (Karim, 2009).....	8
Figure 2.3: Intraplate and interpolate Seismicity (Ghalib et al., 1985).....	9
Figure 2.4: Historical Seismic map of Iraq (Alsinawi and Ghalib, 1975a).....	11
Figure 2.5: Borehole locations for study area.....	12
Figure 2.6: Seismicity of Iraq Zone (Alsinawi and Qasrani, 2003).....	13
Figure 2.7: Seismic acceleration map with design period of 100 years (Geology of Iraq, 2006).....	15
Figure 3.1: Stress path to failure for dense saturated sand (Elgamal et al., 2007).....	20
Figure 3.2: Flow liquefaction (Lopez and Blazquez, 2006)	21
Figure 3.3: Adjustment path of flow liquefaction (Lopez and Blazquez, 2006).....	22
Figure 3.4: Destruction in buildings as a result of liquefaction (Madabhushi, 2007)	23
Figure 3.5: Loss of property due to liquefaction (USA Geological Survey)	23
Figure 3.6: Liquefaction effects on pile designs Mitchell (2006).....	27
Figure 3.7: SPT clean-sand base curves for earthquake magnitudes of 7.5 (Youd et al., 2001)	31
Figure 3.8: Estimate CRR by CPT Data (Youd et al., 2001).....	33
Figure 4.1: Recommendations of Polito and Martin (2001) for the assessment of liquefaction.....	35
Figure 4.2: Seed et al. (2003) criteria for the assessment of liquefaction potential of fine grained soils.	36
Figure 4.3: Bray and Sancio (2004) criteria for liquefaction susceptibility of fine grained soils.	37

Figure 4.4: Boulanger and Idriss (2004 - 2006) criteria for the assessment of liquefaction potential.....	38
Figure 4.5: The correction factor $\Delta (N_1)_{60}$ for fines content (Boulanger and Idriss, 2006).....	44
Figure 5.1: Liquefaction behaviour of Basra soils based on Polito (2001) criteria ...	61
Figure 5.2: Liquefaction behaviour of Basra soils based on Seed et al. (2001).....	62
Figure 5.3: Basra soils susceptible to liquefaction according to Chinese criteria.....	62
Figure 5.4: Basra soils susceptible to liquefaction according to Bray and Sancio (2004)	63
Figure 5.5 Basra soils susceptible to liquefaction according to Boulanger and Idriss (2006).....	64
Figure 5.6: Liquid limit values with changing depth	76
Figure 5.7: Plastic limit values with changing depth	76
Figure 5.8: Plasticity index versus depth	77
Figure 5.9: Depth versus corrected SPT N_{60} values.....	77
Figure 5.10: SPT N_{60} value versus liquid limit.....	78
Figure 5.11: SPT N_{60} value versus plastic limit.....	79
Figure 5.12: SPT N_{60} value versus plasticity index	79
Figure 5.13: SPT N_{60} value versus cohesion.....	80
Figure 5.14: SPT N_{60} values versus angle of internal friction	80
Figure 5.15: Correlation between N_{60} and the angle of internal friction for silty sand.	81
Figure 5.16: Correlation between $(N_1)_{60}$ and angle of internal friction for silty sand.	81
Figure 5.17: Correlation between SPT and the cone penetration resistance, q_c	82

Figure 5.18: Relationships between SPT N_{60} and S_u 83

Figure 5.19: The SPT, N_{60} versus S_u proposed by some researchers..... 84

Chapter 1

INTRODUCTION

1.1 Introduction

Liquefaction is one of the problems in geotechnical earthquake engineering. It is a phenomena which takes place in saturated cohesionless soils due to the increase of pore water pressure and a decrease in effective stress because of dynamic loading. It is a failure condition in soil in which the stiffness and the strength decrease by earthquake shaking or other cyclic loading.

Liquefaction takes place in saturated loose sand and silt. Saturated soils are the soils in which the pore space between the individual soil particles is totally filled with water. The water pressure is moderately low before earthquake shaking. During earthquake, the ground shaking may cause the pore water pressure to increase to the point where the effect stress in the soil becomes equal to zero and liquefaction occurs.

The most recent earthquake is the Kocaeli earthquake in 1999 ($M_w=7.5$) in Turkey. It caused to more than 1200 buildings were damaged, and 1000 structures as outcome of ground softening and liquefaction (Sanico et al., 2002). Also Kobe earthquake in Japan in 1995 caused more than one billion dollars in total damage (Hamada et al., 1999).

The growing numbers and the intensity of earthquakes around the world has placed governments and other major organizations to be at loggerheads as to what exactly can

be done to prevent the detrimental effects of earthquakes (USGS, 2016). Despite the occurrence of life threatening and property ravishing due to liquefaction, insignificant improvements in remedies have been witnessed. Most studies are still advocating traditional liquefaction solutions. The most dominant liquefaction remedies include water pumping, gravel drains, solidification, soil replacement and grouting (Gallagher et al., 2002). Major shifts were however observed when nanoparticles were first introduced as a remedy of liquefaction. The adoption of nanoparticles includes the use of colloidal silica, bentonite, and laponite (Gallagher et al., 2007). The use of nanoparticles has gone a long way in mitigating consequential effects of liquefaction. However, if the world is to remain on the safe side of potential and actual liquefaction consequences, then new and refined understanding of the concepts and surrounding issues of liquefaction have to be established (Coduto, 1999).

The most puzzling fact is that improvements have been made in building structures but still the occurrence of liquefaction is ‘leaving no stone unturned’ as the effects continue to demolish and tear down the strongest structures. Lopez and Blazquez (2006) outlined that engineers have done a lot in addressing liquefaction problems but they still need to continue furthering their insights and ‘dig deeper into the mystery’ of liquefaction.

Others argue that the major improvements made by engineers are mainly biased towards building structures and do not significantly focus on the natural aspect of the environment (Mollamahmutoglu and Yilmaz, 2010). This is reinforced by compelling evidence which has shown that significant damages also occur to infrastructure such as roads and people’s assets such as motor vehicles. The main question to be answered

is “what is the most effective and universal remedy that can be adopted so that all the consequences of liquefaction can be mitigated?”

It is also prevalent that environmental protection bodies are strongly against the adoption of certain liquefaction remedies. Environmental protection measures may impose a ban on the use of methods that are effective in dealing with liquefaction. Such remedies may impose threats to the ecosystem and may disturb the natural balance of the geological systems. These remedies may encompass the use of engineered nanoparticles and grouting which can significantly hinder and alter the effect of water table on the liquefiable soil (Gallagher et al., 2002).

Under strong earthquake, the liquefaction resistance of sand and silty sand have been studied widely. Also during earthquake calculation factor of safety for liquefaction was developed (Yuod et al., 2001). Cyclic failure of sensitive clays was studied by Yuod (1998) and discussed that:

- Liquefaction cyclic failure is susceptible if the sensitivity of the soil is bigger than 4,
- Soils are classify as CL-ML and have $(N_1)_{60}$ less than 5,
- Water content is bigger than 0.99LL, and
- The Liquidity index more than 0.6.

Chinese criteria was developed by Seed et al. (1983) for evaluation of liquefaction of fine grained soil based on natural water content, clay fraction and liquid limit. According to Perlea (2000), any kind of soils include sensitive clays and cohesive soil may liquefy depending on the magnitude of earthquake. Also it was discussed that

liquefaction is not occur in fine grained soil with local magnitude $M_w < 7.2$. Furthermore, Seed et al. (2003), Bray et al. (2004) and Polito (2001) studied the effect of plasticity index on liquefaction of fine grained soils. Susceptibility of liquefaction and cyclic failure of fine grained soils, silt and silty clay are still being studied. According to Boulanger and Idriss (2004 and 2006) criteria, soil sample should be sorted into "clay like" and "sand-like". Fine-grained soils can confidently be expected to display clay-like characteristic if they possess a plasticity index equal or greater than seven ($PI \geq 7$) and soils considered as sand-like if the plasticity index is smaller than 7 ($PI < 7$).

In this study, the liquefaction susceptibility of Basra soil in Iraq was studied. Basra is one of the city in southern Iraq. Due to many researches on the seismicity of Iraq, Iraq has a good documented history of seismic activity. Iraq located in a relatively active seismic zone at the northern and eastern boundary of the Arabian plate (Saad at el., 2006). In this thesis, 20 boreholes were used. All data and borehole logs were obtained from ANDREA Company. It is one of the big geotechnical engineering company in Iraq. Appendix A and B show all the results of laboratory and field tests and boreholes were used for this study.

1.2 Objectives of the Study

The objective of this thesis is to estimate the liquefaction potential of Basra soil in Iraq by using the field and laboratory test data. The main objectives of this study are herein specified as follows:

1. Estimating the liquefaction potential based on SPT N values,
2. Determining the liquefaction potential based on index properties of soils,

3. Calculating the liquefaction potential index, LPI based on SPT for evaluating the liquefaction susceptibility of Basra region.
4. Correlating the SPT N value to depth, Atterberg limits and shear strength parameters.
5. Determining the cone penetration resistance, q_c from the SPT N value.

1.3 Organization of the Study

This study is structured into six chapters. Chapter one provides a description of the problem and what the study seeks to accomplish by addressing the problem. Chapter two of this study looks at an overview of geographical features and seismicity of Iraq while chapter three provides literature review. The methodological aspect of this study are addressed in chapter four. Chapter five deals with data analysis and presentation of research findings while chapter six concludes the study by looking at policy implications and recommendations.

Chapter 2

SEISMICITY OF IRAQ

2.1 Introduction

There are numerous accounts of seismic activities that transpired in Iraq and their documentation spans from the period 1260BC to 1900AD (Alsinawi and Mosawi, 1988). The effects of these seismic activities vary in magnitude of impact. Alsinawi and Mosawi (1988) established that seismic activities in Iraq have followed a certain pattern which conformed to Iraq's major tectonic elements. The geographical location of Iraq lies within the Alpine belt which is situated at the northern part of the Arabian Plate. Moreover, the strength of seismic activities varied in strength and Alsinawi and Ghalib et al. (1975a) established that strong seismic activities were experienced in the Northern Region of Iraq compared to that which were experienced in the Southern Region. Studies undertaken in Northern Iraq about micro earthquakes revealed that more than 79 seismic activities were observed (Al-Mosawi, 1978).

2.2 Development of the Arabian Plate

It can be noted that seismicity events that transpire in Iraq are as a result of the Arabian plate Figure (2.1). This section therefore focuses on examining developments of the Arabian plate. The initial development of the Arabian plate was characterized by divisions that produced 5 terranes which later grew to 10 terranes. However, collision of the West and East Gondwana together with the expansion of the Nubio-Arabian Mozambique Ocean are contended to be the main factors that fostered the development of the Arabian plate. The formation of the Arabian plate followed three stages which

are oceanic accretion and subduction, orogenesis and extension (Jassim and Goff, 2006).

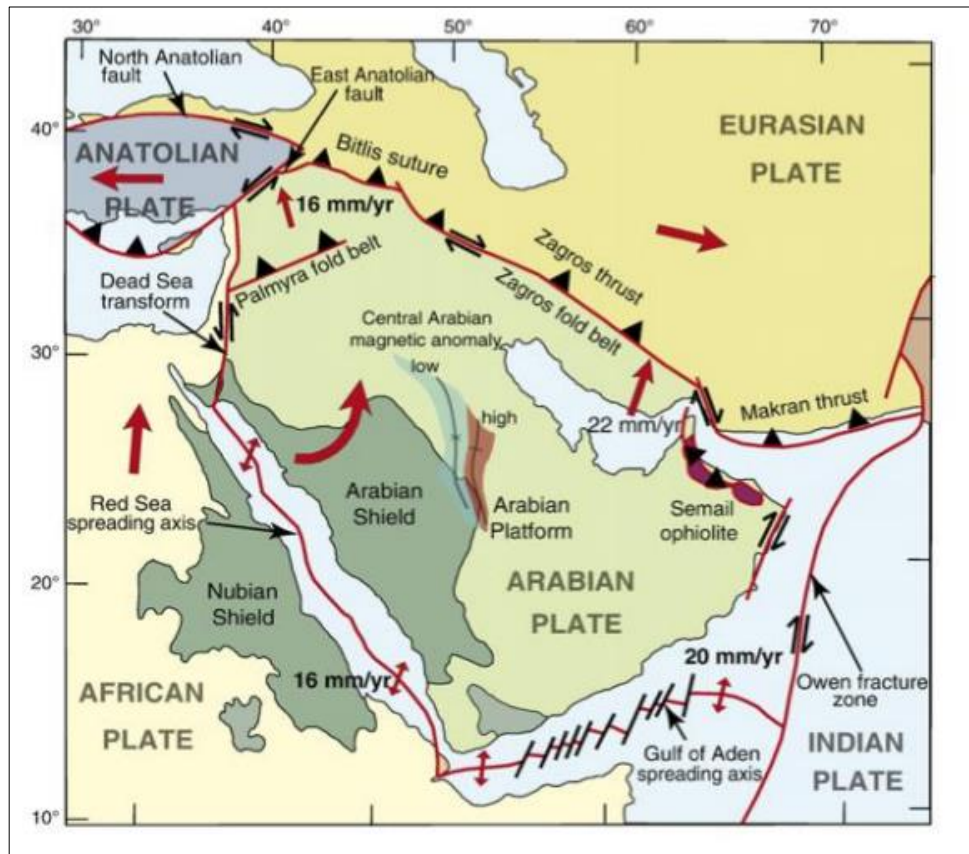


Figure 2.1: Movement of the Arabian Plate in relation to Africa (Johnson et al., 2003)

Figure 2.1 shown that the Arabian forms one of the biggest plates and Alsinawi (2001) asserts that movement of the Arabian Plate has been in relation to Aegean, Anatolian, Iranian, Somalian, African, and Eurasian plates. Movements of the Arabian Plate are however significantly related to those of the African plate. Arabian Plate's boundaries in the south and west are characterized by sea floors than span from the Red Sea to the Gulf of Eden. On the other hand, eastern and northern demarcations are distinguished with compressional suture zones. The Precambrian shield is located on the western part of the Arabian Plate. Formation of the Arabian Plates dates back to 25 to 30 million years and the Arabian Plate now constitutes Paleozoic intracratonic basins

(Alsinawi, 2001). According to Alsinawi (2001), neighboring plate boundaries that surround the Arabian plate are active and that it is subduced under the Iranian and Anatolian plates. The Zagros Region under which Iraq lies comprises of three zones namely: the zone of folding, imbricated belt and inner crystalline zone.

2.3 Seismic Tectonics and Seismicity of Iraq

Stratigraphic columns are a graphic description that provides lithology and age of the stratigraphy of a region which occurred during the Cenozoic and Mesozoic periods. This is usually structured in a manner that the younger age is placed at the bottom and the older at the top. A stratigraphic column is shown in Figure 2.2.

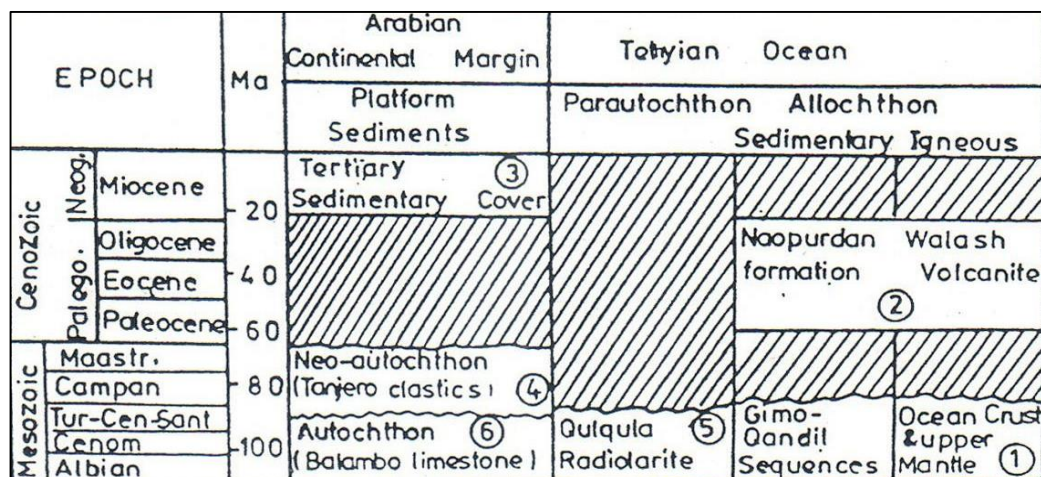


Figure 2.2: The stratigraphic column of Kurdistan Region of Iraq (Karim, 2009)

Various studies have also been undertaken to further heighten the available understanding about the Seismic technics and seismicity of North Iraq. Thus deductions by Ghalib et al. (1985) were based on the assertion that intraplate and interpolate seismicity have different implications and magnitudes of impacts on seismicity. This can be illustrated by Figure 2.3.

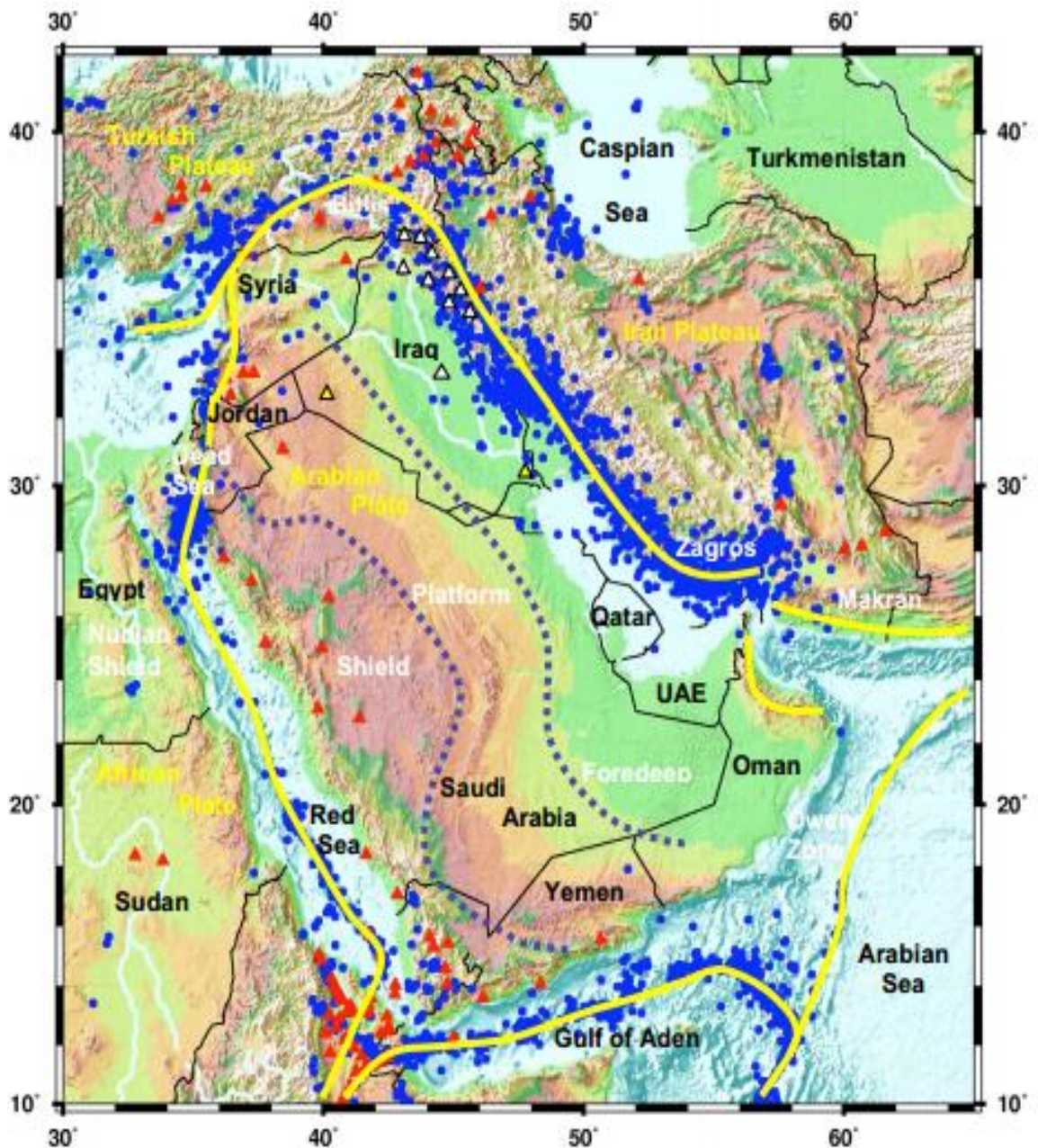


Figure 2.3: Intraplate and interplate Seismicity (Ghalib et al., 1985)

Interaction between the Arabian, Eurasian, African, and Indian plates is the primary force defining the present-day Seismotectonic framework of the Middle East. Figure 2.3 shown that interplate seismicity is significantly more important than intraplate activity. The plate margin seismicity is associated with a variety of boundaries that include spreading zones in the Gulf of Aden and the Red Sea, the transform fault along the Dead Sea rift and East Anatolia, the Bitlis suture in eastern Turkey, the northwest-

southeast trending Zagros thrust zone, the Makran east-west trending continental margin and subduction zone, and the Owen fracture zone in the Arabian Sea. The apparently aseismic Arabian plate interior features an exposed young shield, a deformed platform and a fore deep that consists of extra ordinarily thick layers of sediments and evaporates. Structural faults and folds cross these major tectonic regions.

The yellow lines denote plate boundaries while red triangles and blue circles represent volcanoes and earthquakes respectively. White triangles represent the 10 stations that compose the North Iraq Seismological Network (NISN). The yellow triangles reflect the location of some Iraq Seismological Network (ISN) stations, currently not operational.

This ISN network was composed of stations BHD, SLY, MSL, RTB, and BSR outside the cities of Baghdad, Sulaimaniyah, Mosul, Al Rutba, and Basra, respectively. The instrumentation at these five stations included short-, intermediate-, and long-period analog as well as some digital systems procured from various vendors and manufacturers.

2.3.1 Regional Seismicity

There are numerous seismicity events of diverse magnitudes that transpired in the Arabian Plate. Alsinawi (2001) posits that the number of seismicity events that transpired in the Arabian Plate surpasses 7000 and that three quarters of these 7000 seismicity events had a magnitude which spanned from 4.0 to 5.5. Investigations were undertaken to model the regional seismicity of Iraq and the results revealed the

existence of 10 area and 25 line sources (Jassim and Goff, 2006). Figure 2.4 shown the historical seismicity in Iraq and Figure 2.5 shown the borehole locations.

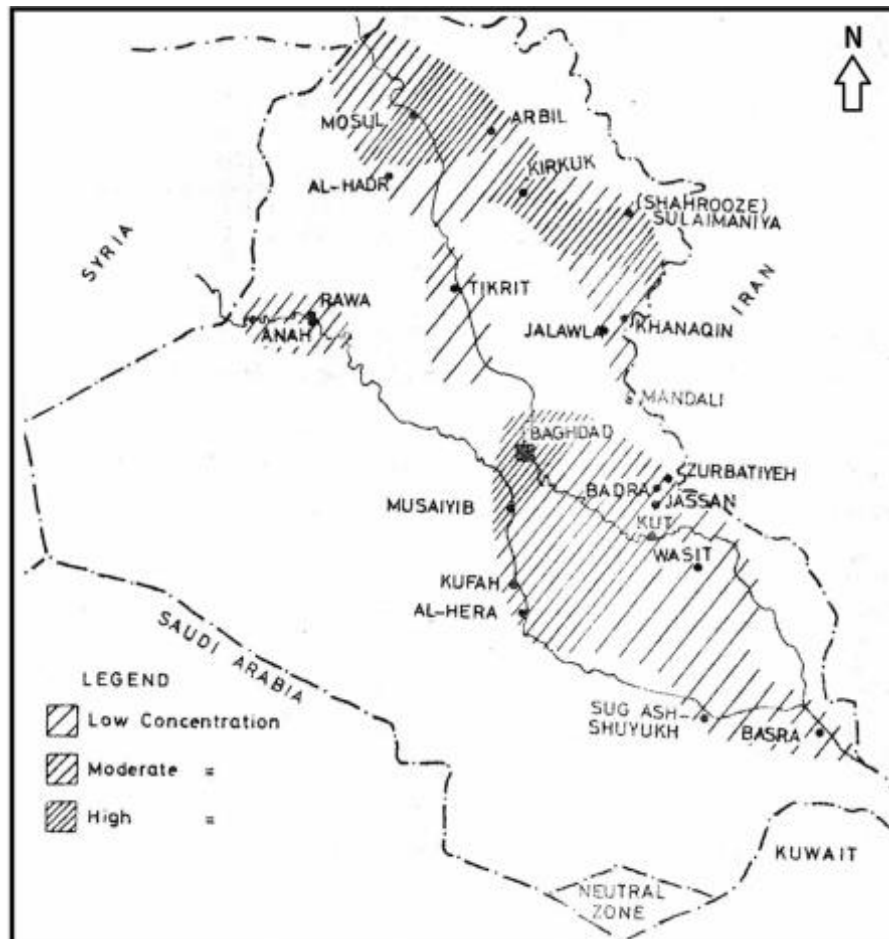


Figure 2.4: Historical Seismic map of Iraq, (Alsinawi and Ghalib, 1975a).



Figure 2.5: Borehole locations for study area

2.3.2 Macro and Microseismicity of Iraq

The nature of Macroseismicity of Iraq is considered not be homogenous and much of the activities are dominant in the Balambo-Tanjero and high Folded Zones (Jassim and Goff, 2006). However, characteristics of the Iraq's seismicity are considered to be of medium nature and of low focal depth. Figure 2.5 provides a graphical illustration of Iraq's seismicity.

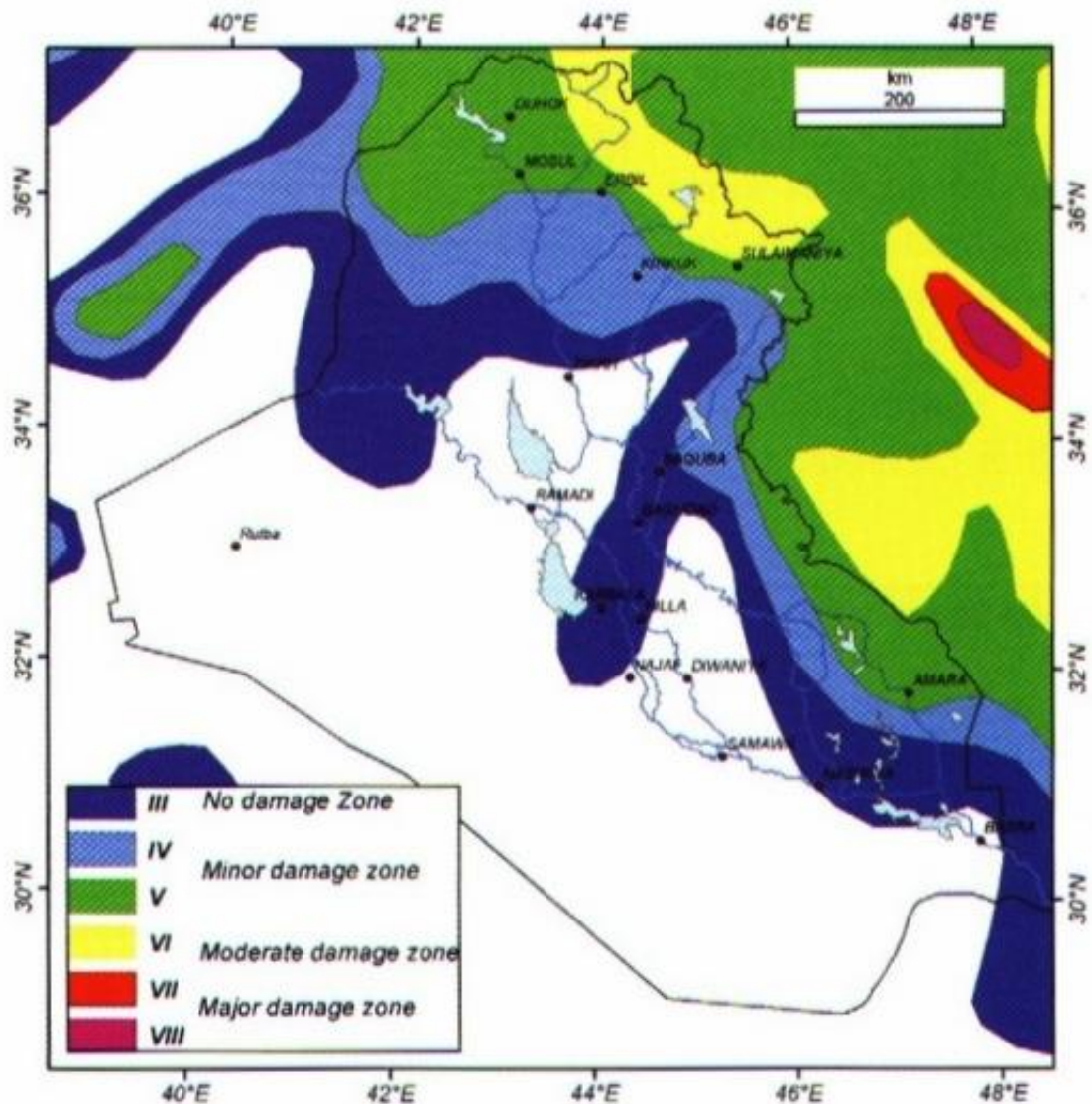


Figure 2.6: Seismicity of Iraq Zone (Alsinaawi and Qasrani, 2003)

The causes of seismicity between the fold and the stable shelf are attributed to different factors. Assertions by Jassim and Goff (2006) exhibited that seismicity of the later is caused by forces that are generated by shifts in the Arabian Plate while that of the former is attributed to local deformations. However, forces in the plate boundaries that are behind the formation of geological structures are active. These forces are the resultant cause of deformations and strain accumulation which is further causes stress. The Zagros and Taurus are the chief element behind the seismicity that is experienced

in Iraq as neotectonic takes effect. This can be showed by an isointensity map as shown in Figure 2.5 above.

Seismic activities are mainly concentrated in the Balamboo-Tanjero and High Folded zones and the tectonising of the Arabian Plate occurs within these areas. The tectonising of the Arabian Plate cause it to subdue under the Sanandaj-Sirjan Plate. Seismic activities are more concentrated around the transversal faults as compared to the northern parts of Iraq. Insights provided by Jassim and Goff (2006) showed that much of the seismic activities that occur in Iraq are of intermediate-shallow focus.

2.4 Seismic Hazard Analysis

Though indication of future seismic activities are very low, the potential of earthquakes occurring is very high and probable damages are also foreseen to be high (Jassim and Goff, 2006). Possible causes have pointed to the prevalence of liquefaction in the Mesopotamian Plain. The presence of quaternary sediments that are subject to liquefaction is the main element that is propagating future increase in earthquakes notably in East Iraq.

Seismic hazard analysis may encompass seismic zoning. This involves categorizing zones according to probable damages that may be experienced. Alsinawi and Qasrani (2003) produced a four zone seismic map. Such zones were zone of no damage, zone of minor damage, zone of moderate damage and zone of high damage. The differences in the zones was attributed to differences in magnitudes of damages. The seismicity index map produced by Alsinawi and Qasrani (2003) was shown in Figure 2.5.

Figure 2.6 shows the peak ground acceleration (PGA) values of Iraq. It can be noticed that PGA is about 0.1g to 0.2g for the city of Basra considered in this micro-zonation study. Also in this study it is taken approximately as 0.2g.

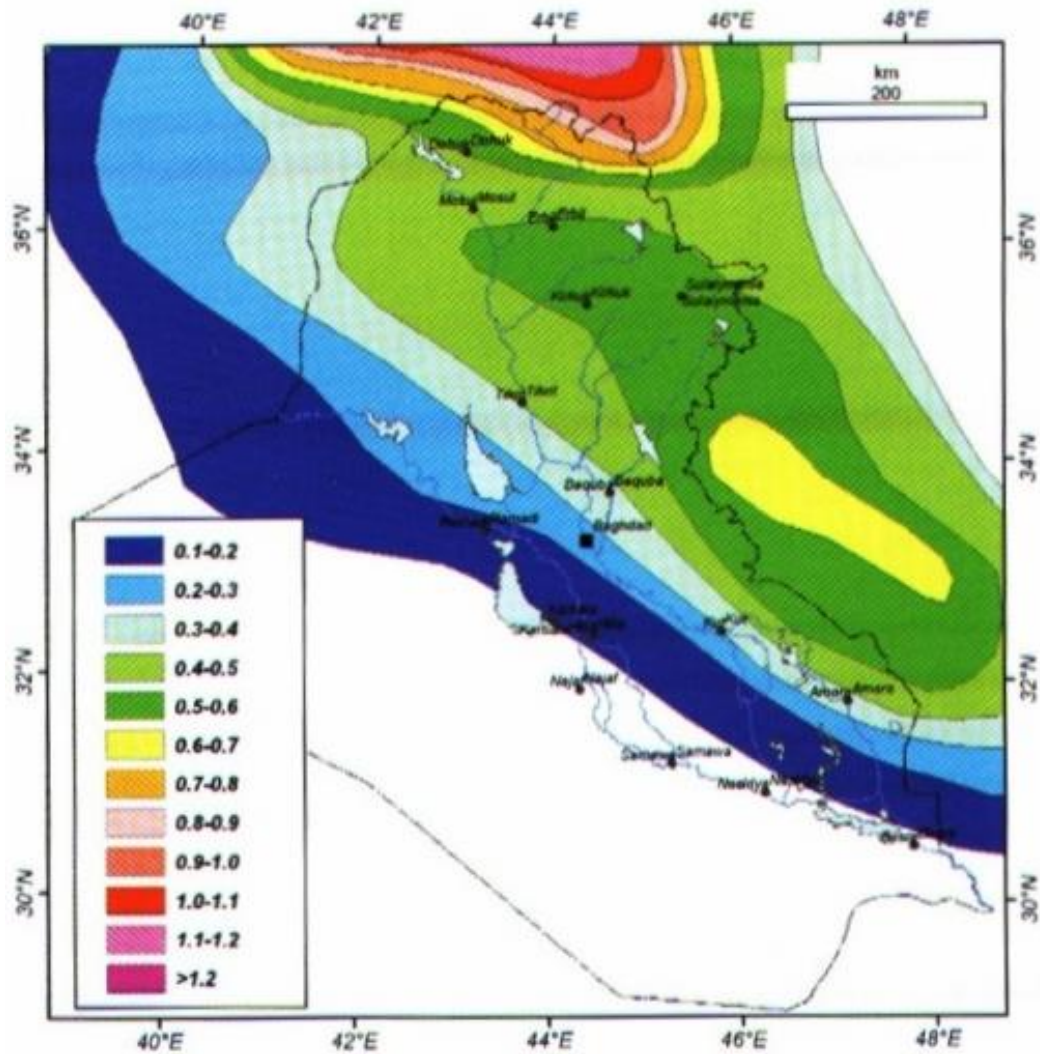


Figure 2.7: Seismic acceleration map with design period of 100 years (Geology of Iraq, 2006)

Chapter 3

LITERATURE REVIEW

3.1 Introduction

The prevalence of liquefaction has been followed by extensive studies that sought to provide a deeper assessment of the underlying causes and effects. Initial frameworks of the liquefaction studies were undertaken by Wang in 1979. Other studies such as the one undertaken by Seed et al. (1983) also emerged on the frontline by incorporating new ideas such as natural water content, clay fraction and liquid limit.

A series of studies also emerged to as new factors were being incorporated into the analysis but most of them are an extension of the study by Wang (1979). For instance, Youd (1998) adopted soil classification, liquid index and natural water content as the core determinants of liquefaction. The study by Youd et al. (2001) garnered strong support from Durgunoglu et al. (2004) who deployed a systematic cyclic triaxial approach in the analysis of the sensitivity of soft clay in Turkey.

The results concurred with the study results by Youd et al. (2001), has reported similar results. Perlea (2000) further concluded that liquefaction is bound to affect all soil types irrespective of cohesiveness and sensitivity but hinged on the nature of shaking. Thus the amount of energy to cause liquefaction is said to be different with fine-grained soils being contended to require more energy than sand.

Conclusions drawn from these studies showed that for fine grained soils have to be susceptible to Richter impacts above 7.2 for liquefaction to take effect. The prevalence of liquefaction follows areas that are prone to earthquakes and where the soil is saturated and loose. In this case, saturation aggravates excess pore water pressure (Mitchell, 1993).

A soil is said to be over consolidated when great static pressure was once applied in the past. Over consolidated soils are generally characterized by high rearrangement resistance and therefore tend to negatively impact liquefaction. Stability wise, over consolidated soils are regarded to be more stable as resistance is positively related with subjected pressure and soil. Studies by Seed (1979) have shown that soil samples whose depth is below 15 meters are more liquefied. Pressure and depth are key elements of liquefaction whereas soil composition, shape and size are essential elements of soil's susceptibility to liquefy (Seed et al., 1979).

Significant weight is also placed towards the role of soil composition and liquefaction. For example, Ishihara (1999) argues that there is a bilateral association between soil composition and liquefaction. Ishihara (1999) centered his argument on the fact that clay has a relatively high plasticity and hence restricts the movement of particles as pore water pressure is diminished. Conclusions in this aspect can therefore be drawn and argued that the lower the level of plasticity within a given soil sample the higher the chances of the soil to liquefy.

On the other hand, liquefaction is a function of soil permeability because soil permeability determines the extent to pore water movement within the soil. Thus low

soil permeability restricts water movement and this causes water pressures to increase as cyclic loading occurs. Permeability is also associated with water drainage capacity and this is best illustrated by clay which can hamper the absorption of pore water pressure. Liquefaction therefore requires that the soil have poor drainage capacity so as to retain and promote an increase in pore water pressure. Gravel can be observed to be possessing high permeability features and hence is lowly susceptible to liquefaction.

The nature and magnitude of liquefaction effects is endogenously determined by static shear and shear strength that is being applied to the soil deposit. Loss of stability occurs when shear load outweighs the reduction in shear strength (Ishihara, 1999). Alternatively, loss in soil stability emanates from flow slides or ground failures. Shear deformations take effect when shear strength but the absence of shear stresses can result in the formation of soil boils as pore water is driven out to the surface. Settlements will be formed when the soil deposits are vented but damages are less prevalent because of the resulting in the formation of settlements. According to Robertson et al. (1992) ground failures can broadly classified into deformation failure and flow failures.

Deformation failure occurs when the liquefied soil gains a significant amount of shear resistance without affecting the stability of the soil thereby causing the formation of limited deformations. On the other hand, flow failure occurs when liquefaction resultantly causes the formation of significantly large deformations. Despite the differences in the definition of the respective terms, their resultant effect is still termed liquefaction.

3.2 Fundamentals of Liquefaction

Despite the variety and a significant number of liquefaction definitions that have been used in the literature; the concept of liquefaction still remains a mystery to many countries around the world. It is a profound issue that the occurrence and effects of liquefaction are still leaving many individuals puzzled especially when the effects have caused a significant amount of adverse effects. Coduto (1999) defined liquefaction as an outcome that occurs when soils are subjected to progressive load which causes them to become saturated and in the process lose their coherence strength. Gallagher et al. (2007) defined it as a continuous and systematic decline in soil rigidity and strength caused by earthquakes.

Irrespective of the adopted definition, it can be noted that earthquakes propel a surge in water pressure between the pores and thus further causing more saturation and disintegration of the soil particles. This notion was reinforced by López and Blázquez (2006) who asserts that the absence of shear strength causes the soil particles to become saturated and assume a liquid form.

López and Blázquez (2006) further contended that a balance between pore water pressure and total stress will cause effective stress to decline to zero thereby causing liquefaction. On the other hand, it is imposed that the effects of liquefaction are somehow determined by the type of liquefaction (Elgamal et al., 2003). Thus the magnitude and nature of liquefaction tend to vary with the type of liquefaction. Coduto (1999) established that liquefaction can be in two forms and these are cyclic mobility and flow liquefaction.

3.2.1 Cyclic Mobility

Cyclic mobility is a form of liquefaction that occurs in intermediate and impenetrable sands that are saturated. When compared with flow liquefaction, shear movements produced under cyclic mobility are relatively less intensive (Gratchev, 2007). In an experiment conducted by Craig (1997) it was revealed that when shear is applied to a soil sample without cohesion, the resultant outcome is that there is contraction of the soil. The volume of the soil particles also increased in the process as the inherent force within the soil declined. A complicated liquefaction ensues when the contraction process comes to a complete end. Liquefaction of dense sand also goes through a path and this can be expressed diagrammatically as shown in figure 3.1.

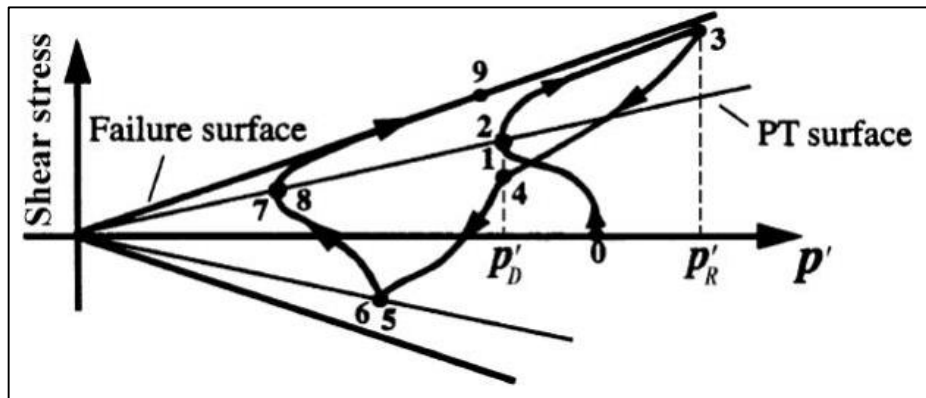


Figure 3.1: Stress path to failure for dense saturated sand (Elgamal et al., 2003)

The initial process commences at point 0 when and goes to the first phase (1) as shear stress is applied. During the initial stages there will be a lot of contractions which cause an increase in pore water pressure and thereby subsequently causing effective stress to decline. Contractions will decline in magnitude as the phase approaches the transformation phase (PT Surface). Point 2 and 3 are surrounded with acts of dilation in contraction forces. The strength of the soil changes as it is subjected to loading and

unloading. Loading causes the soil to gain strength while unloading causes to lose its strength. The gaining and losing of soil strength is what is termed cyclic mobility.

3.2.2 Flow Liquefaction

Dynamic loading and shear pressure have an effect of causing the volume of the loose sands to shrink. Craig (1997) advocates that the shrinkage of the volume of the particles results in an increase in pore water pressure and that decrease in effect stress. Figure 3.2 denotes that cyclic failure is not instant phenomenon but rather follows certain processes after the liquefaction stage. Thus the flow liquefaction contends that the associated stress follows a certain path which leads to cyclic failure.

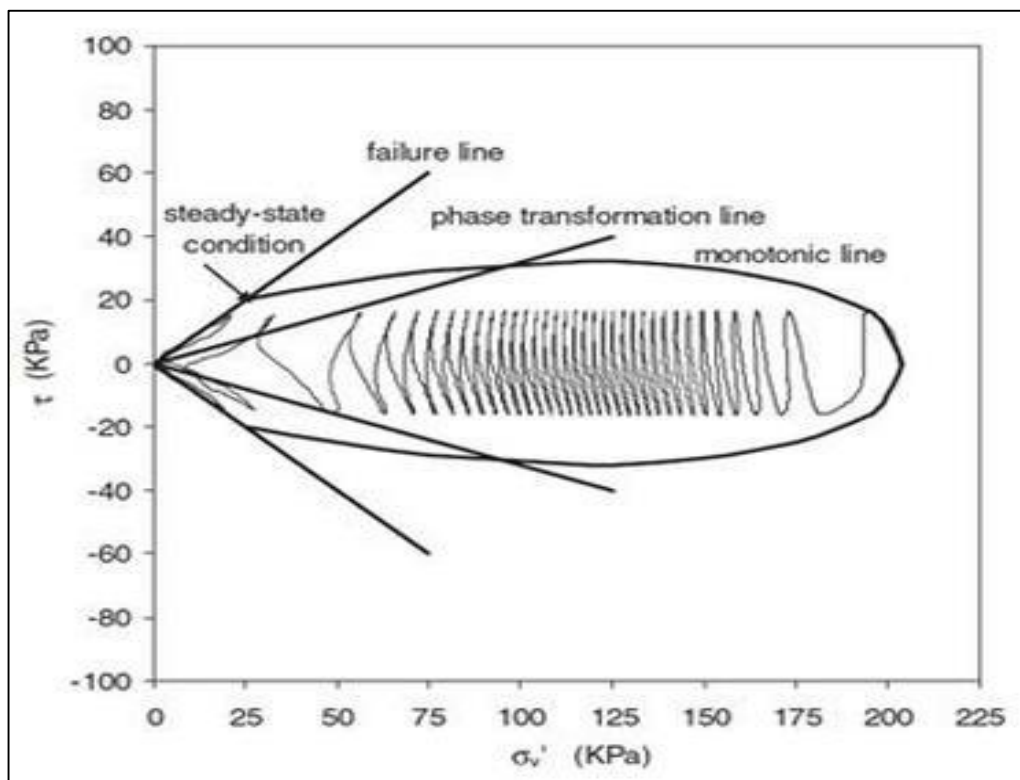


Figure 3.2: Flow liquefaction (Lopez and Blazquez, 2006)

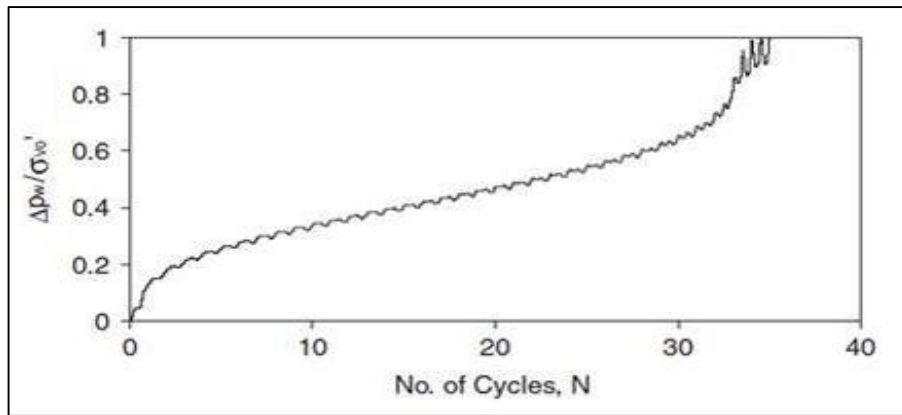


Figure 3.3: Adjustment path of flow liquefaction. (Lopez and Blazquez, 2006)

It is evident in Figure 3.2 and 3.3 that the intensity of shear strength declines at every stage as the pore water pressure increases with the subsequent level. The process commences with an initial ratio of shear stress to initial effective confining stress (CSR) of 0.08 and 200kPa of effective stress. Contraction increases as the soil is placed under a load and the same applies to water pressure between the soil pores. Under flow liquefaction, the initial stages does not cause a loss of water because the load is being applied at relatively high rate and hence the soil loses considerable strength. Water pressure between the soils pores increases at each stage as the magnitude of shear strength declines until the level of shear resistance is less than that of the associated stress. When such a condition is prevalent, failure is said to have occurred and this process is termed flow liquefaction (Madabhushi, 2007).

3.3 Effects of Liquefaction

Liquefaction has been and is still taken as a major cause behind the destruction in property. For instance, liquefaction tends to compromise the strength of a building's foundation. Thus the capacity of the soil to uphold the entire building is diminished causing the building to collapse or overturn. This incidence is similar to the Niigita incidence of 1964 where significant amount of buildings were destroyed as a result of

an earthquake. A similar description of the incidence can be shown in figure 3.4 and 3.5.



Figure 3.4: Destruction in buildings as a result of liquefaction (Madabhushi, 2007)



Figure 3.5: Loss of property due to liquefaction (USA Geological Survey)

The increases water pressure as a result of liquefaction can initiate landslides such as the San Fernando earthquake of 1971 where a dam collapsed and flooded nearby areas. The collapse of the dam was attributed to excess pore water pressure which was out of

the dam wall' restraining ability. This was also further heightened by underwater slides which destroyed the foundations of the dam walls.

3.4 Remedies of Liquefaction

There are several remedies that can be undertaken to alleviate or deal with the problem of liquefaction. It must however, be noted that there are also several cases of liquefaction that cannot be dealt with especially when the area is developed (Gallagher and Mitchell, 2002). According to Coduto (1999) there are basically five ways of dealing with liquefaction these are;

3.4.1 Soil Replacement

This approach involves replacing soil which is susceptible to liquefaction with soil that is highly compact. Such a process however requires that the liquefaction area be excavated and may be of considerable expenditure which officials may be reluctant to spend (Coduto, 1999).

3.4.2 Water Pumping

Water pumping is a draining process that involves the removal of water from the liquefaction area. This stems from the concept that saturation is the prime cause of liquefaction. Henceforth in doing so the amount of ground water declines thereby lowering the probability of another liquefaction event. Water pumping is more advantageous in lowering liquefaction but the associated tend to be exorbitant as far as the long term time frame is concerned (Coduto, 1999).

3.4.3 Solidification

With solidification, the liquefaction soil is solidified using grout and this is done at relatively high pressure. Gallgher et al., (2007) argue that grouting is barely effective. The reason suggested that differences in viscosity is a major hindrance as it impedes an even distribution of the grout.

3.4.4 Gravel Drains

Gravel drains are a way of reducing water pressure from the pores which occurs as the soil is subjected to constant loading. Das (1983) strongly asserts that gravel drainages are a fast way of removing the excess water from the soil.

3.4.5 Enhancing Resistance to Liquefaction

This method requires the adoption of in-situ techniques. Such methods include methods that can improve or enhance soil particles' coherence (contact). An increase in soil contact of the particles help in absorbing of shear impacts even in the event of an earthquake (Madabhushi, 2007).

3.4.6 Resistant Structures

The most significant effect is to position structures in areas that are less prone to liquefaction and must be coupled with structures that are resistant to liquefaction. However, the ability to build structures in areas that are not prone to liquefaction is hampered by availability of space, acquisition costs and land restrictions (Madabhushi, 2007).

3.5 Liquefaction and Nanoparticles

Nanoparticles are a microscopic particles with at least one dimension less than 100 nm (Science Daily) and can either be non-engineered or engineered. The difference being that non-engineered nanoparticles are produced by naturally while engineered nanoparticles are specifically designed to conform to certain attributes so that they can be able to serve the required uses. Engineered nanoparticles can serve as good remedial strategy towards the problem of liquefaction. This is because they can be tailor made to deal with saturation either by absorbing the water or by improving the soil's coherence (Huang and Wang, 2016). Huang and Wang (2016) identified three basic nanoparticles that can be utilised to deal with liquefaction and these are;

1. Silica
2. Bentonite
3. Laponite

Díaz-Rodríguez et al. (2008) undertook a study on the remedies of liquefaction by employing colloidal silica which comprises of silica nanoparticles. The results revealed that both viscosity and density of the solution initially commence at low levels but the solution later changes to a viscous solution of high density. The solution bonds together loose soil particles thereby reducing potential liquefaction effects. Mollamahmutoglu et al. (2010) strongly supported the use of colloidal silica citing that it is cost effective.

Some studies have shown strong support for the use of bentonite (Gratchev et al., 2007 and Mongondry et al., 2004). The adoption of bentonite as a remedy stems from the idea that bentonite helps in increasing soil resistance to liquefaction. The level of cyclic load resistance is relatively high as compared to colloidal silica and is estimated to be at least 7% more than that of colloidal silica (Mongondry et al., 2004).

Other studies indicated favor towards laponite. For instance, Bonn et al. (1999) and Mouchid et al. (1994) examined the application of laponite in liquefaction as a remedial strategy towards liquefaction. Advantages of the use of laponite outweigh those of other nanoparticles in the sense that laponite always a high viscosity irrespective of the concentration level.

3.6 Structural Designs and Liquefaction

A significant number of studies have been criticized on the basis of failing to offer a concrete description of what transpires as the soil-piles go through liquefaction (Olson and Stark, 2002). The study by Mitchell (2006) offered significant insights in response to those criticism. The study by Mitchell (2006) strongly contended that soil-piles undergo four-stages of liquefaction. It is shown in Figure 3.6.

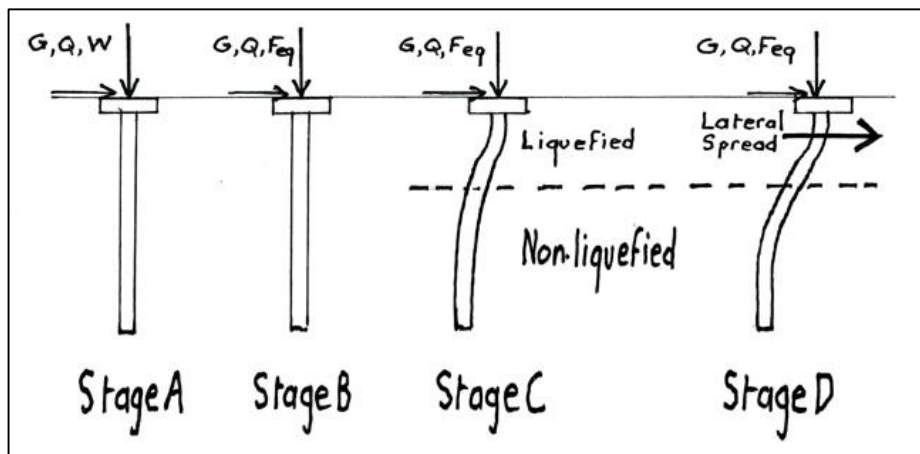


Figure 3.6: Liquefaction effects on pile designs Mitchell, (2006)

The occurrence of an earthquake is therefore viewed as imposing effects on the wind load (W), factored live load (Q) and the dead load (G). Thus under normal circumstances (stage A) these three loads are the only prevailing loads that are being subjected to the soil piles.

In stage B, the occurrence of an earthquake will impose a new load (F_{eq}) on the soil pile. It can be noted that at stage B there is a combination of three different loads (G, Q, F_{eq}). The additional load (F_{eq}) serves as a threatening element towards liquefaction. In the event that liquefaction occurs, the soil may fail to uphold the pile and if liquefaction does not occur then stability of the pile is guaranteed.

It is observed that a considerable earthquake intensity can induce liquefaction causing the soil to lose a relatively small amount of support offered to the pile (Olson & Stark, 2002). Thus stage C is associated with a decline in the soil's shear strength which causes it to lose support. Bending and horizontal displacement will become evident as shaft resistance dwindles.

3.7 Soil Susceptibility and Liquefaction

Soil susceptibility is a major force to reckon with when examining the concept of liquefaction. The extent to which liquefaction occurs greatly hinges on soil susceptibility. For instance, Erhan (2009) outlined that sand soils are more prone to liquefaction in the event of an earthquake. Liquefaction tends to vary especially between sensitive clays, cohesive clays and loose sand. The interaction between soil susceptibility and liquefaction is also influenced by the magnitude of the earthquake. This implies that earthquakes of high magnitude can exert a significant amount of force which can heighten the degree of liquefaction. Further insights by Erhan (2009) revealed that non-plastic silts require more energy in order for liquefaction to ensue as compared to fine grained soils. Thus deductions can be made that liquefaction will be more prevalent in fine grained soils as compared to non-plastic silts. This can be reinforced by observations that were made after the occurrence of the Taiwan and Adapazari, Turkey earthquakes.

Different studies were undertaken to determine the role of soil size on liquefaction. It was deduced that the cyclic triaxial test was a poor indicator of soil susceptibility to liquefaction (Bray et al., 2004). Revelations by Bray et al., were based on comparisons between the Chinese and Adapazari soil sample comparison test. Propositions were therefore made citing that the soil volume provided a misleading indicator of

liquefaction susceptibility and soil response. Therefore other profound measures of liquefaction susceptibility and soil response are recommended. Contrasting studies were made by Durgunnoglu et al. (2004) that huge strains can also be found in high plasticity clays. The occurrence of such strains is conditional to the Cyclic Stress Ratio value or the magnitude of an earthquake. Soil susceptibility can also be determined using strain stress behavior. It can thus be deduced that a proper selection of suitable conditions under which soil susceptibility is determined is a crucial element to consider. Different susceptibility approaches can cause significant differences in results and hence consensus drawn. Moreover, cyclic and monotonic loading tests exhibited that there are smooth changes in plasticity indices from soil samples exhibiting sand like features to soils with high clay characteristics. Plasticity index for clay soils equal or less than 7.

Boulangier and Idris (2004) postulated that empirical analysis, laboratory tests and in situ methods can be employed to examine the soils cyclic strength. However, most techniques for determining cyclic strengths are more applicable to soil samplers exhibiting clay like features with fine grains. Conclusions can therefore be made that silts and clay soil samples have relatively low cyclic strengths which can decrease when exposed to earthquakes of high magnitude. It is also of paramount importance that soil susceptibility differs between soils samples and tends to be high in fine grained soil require high energy for liquefaction to take effect. Therefore the level of liquefaction tends to increase with the nature and extent of finesse of the soil grains.

3.8 Detection of Liquefaction

The most commonly used method that can be used to determine the possibilities of liquefaction is the one adopted by Youd et al. (2001). The determination of

liquefaction requires that liquefaction resistance and earthquake loading (determined by the shear stress ratio-CSR) be incorporated into the estimation process (Youd et al., 2001).

The above expression exhibits that there is a unilateral association between the CSR ratio and the total vertical overburden stress. This entails that an increase in the total vertical overburden stress will result in a decrease in the CSR ratio. The opposite is true but a contrasting effect is observed between CSR ratio and the effective total vertical overburden stress.

Youd et al. (2001) based their study on the analysis of earthquakes whose magnitude was around 7.5 moment magnitude (M_w). The respective CSR ratios of each earthquake were then related with the soil properties using obtained CPT and SPT estimates. The SPT comprised of normalized value N_{60} with an associated 100 kPa of overburden stress and an energy ratio of 60%. On the other hand, CPT had a normalized dimensionless figure Q_{cIN} . Using these factors, Youd et al. (2001) proceeded to estimate the cyclic resistance ratio (CRR).

The combination of CSR and CRR is what is used to determine the possibilities of liquefaction. The computation by Youd et al. (2001) gives what is known as the Factor of Safety (FS).

Factor of safety is based on the rule of thumb that a value of less than 1 implies that the probability of liquefaction occurring is very high while a value greater than 1

implies liquefaction will not occur. The model expression by Youd et al. (2001) is relatively significant in areas which are prone to earthquakes.

3.8.1 Standard Penetration Test (SPT)

The formulation of the Standard Penetration Test (SPT) follows the aftermath of the Niigata earthquake that rocked Japan in 1966. Kishida (1966) asserts that the main thrust behind the SST was to demarcate comparable differences between non-liquefiable and liquefiable conditions. The SPT is however based on the CSR and CRR estimation. Figure 3.7 provides a diagrammatic expression of the SPT test.

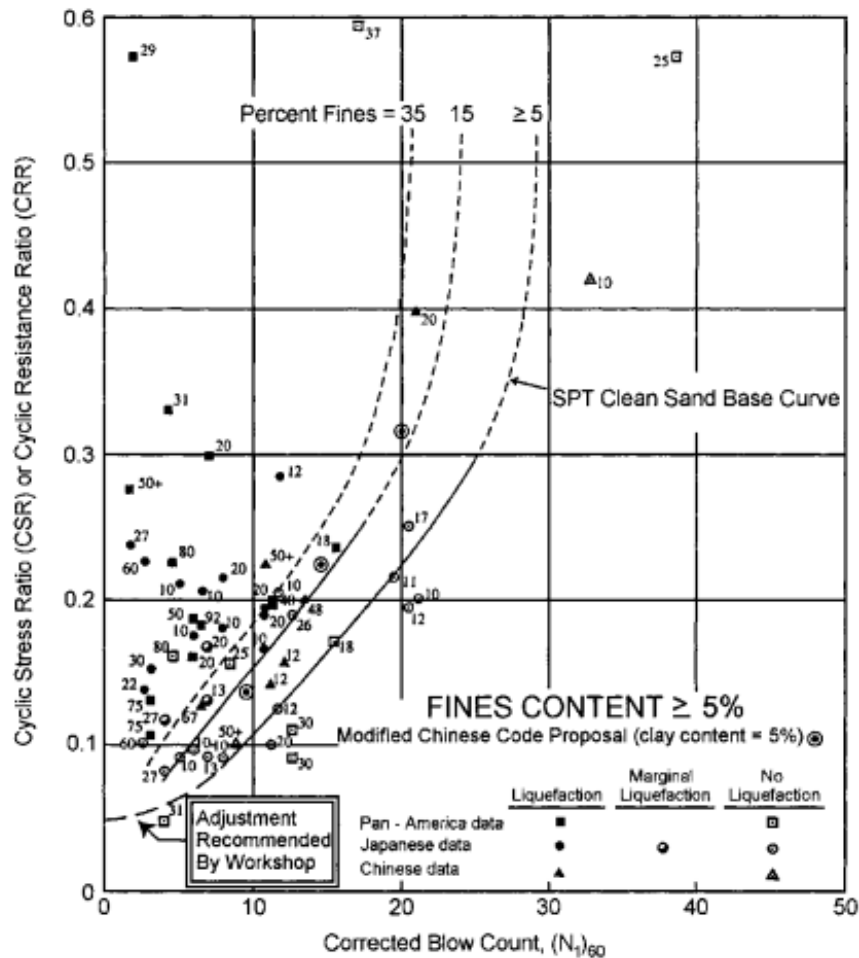


Figure 3.7: SPT clean-sand base curves for earthquake magnitudes of 7.5 (Youd et al. 2001)

The formulation of the SPT follows the determination of liquefaction induced cyclic stress ratio (CSR). The above figure provides a description liquefaction occurrence potential based on the non-occurrence and occurrence of earthquakes. Thus data is collected from both sites which have witnessed an occurrence of an earthquake and those that have not witnessed earthquake events. Figure 3.7 is therefore appropriate for earthquakes whose magnitudes is approximately 7.5 and if the magnitude of the earthquakes exceeds 7.5 then the Magnitude Scaling Factor is used. SPT results can however vary with the number of non-liquefaction and liquefaction events. For instance, Cetin et al. (2000) examined a total of 67 combined non-liquefaction and liquefaction and the results showed that 12 cases had fines contents $FC \leq 5\%$ and that 32 cases had $34\% \geq FC \leq 6\%$. Contrasting results were obtained by Seed et al. (2003) and they revealed that 14 cases had $FC \geq 35\%$, 46 cases had $34\% \geq FC \geq 6\%$ while 65 cases had $FC \leq 5\%$.

3.8.2 Cone Penetration Test (CPT)

The cone penetration test (CPT) is the widely used in situ indicator and has been utilized to examine liquefaction resistance. CPT is considered to provide reliable estimates of liquefaction resistance of potentially liquefiable soils (Stark and Olson, 1995). Youd et al. (2001) established that the use of CPT yields profound results and this follows a study of 19 different study site areas. The results by Youd et al. (2001) accurately reveals both the non-occurrence and occurrence of liquefaction with an 85% probability of accuracy. This gained enormous support from various scholars who strongly favored the use of CPT (Juang et al. 2003; Seed et al. 1983; and Boulanger and Idriss 2004). The use of CPT is a refinement of other measures such as CRR and SPT and the proposition of the CPT is diagrammatically exhibited in Figure 3.8.

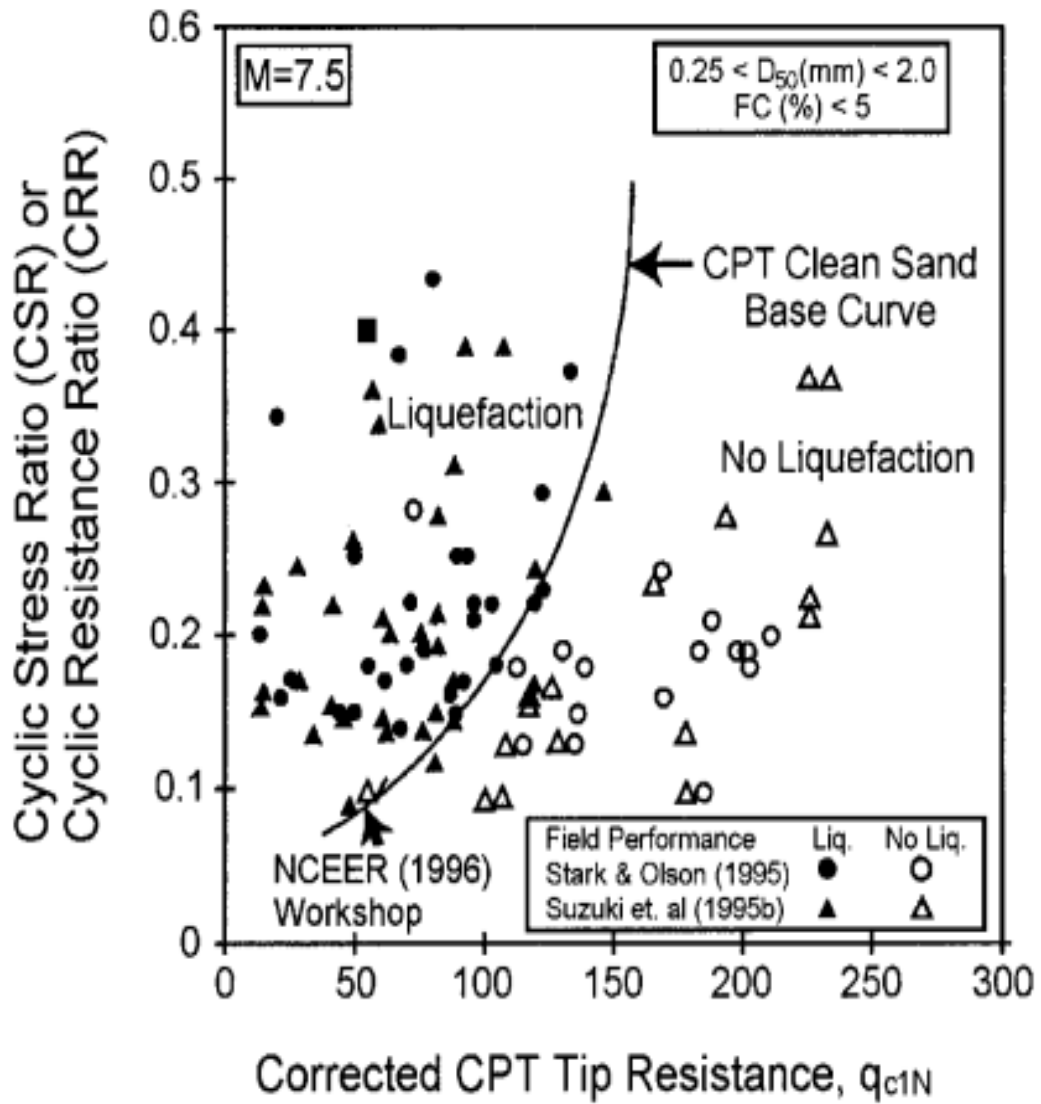


Figure 3.8: Estimate CRR by CPT Data (Youd et al., 2001)

Figure 3.8 offers ways of determining the CRR in clean sands with an FC of 5 %.

Figure 3.8 shows the graphical relationship between normalized CPT tip resistance q_{c1N} and CRR of the two different soil samples. The CRR curve demarcates the difference between soils in which liquefaction was present and were it was absent.

Chapter 4

METHODOLOGY

4.1 Introduction

In the field of geotechnical engineering, resolving soil liquefaction potential is a very important aspect (Youd et al., 2001). Today, all around the world, the standard penetration test, SPT is generally and mostly employed in order to achieve on site specific estimate of liquefaction potential.

In the case of the Basra soil, its estimate of soil liquefaction potential and the relationships of the parameters involved can be done by using the in-situ standard penetration test, SPT. The correlation between the SPT and the undrained shear strength can be used and the liquefaction potential of the soil can be evaluated. In the present study, the site investigation included 20 boreholes with SPT N value measurement. The liquefaction potential calculations were basically based on Seed and Idriss (1971) simplified procedure using the SPT values. In this study, all the field and laboratory test results were obtained from ANDREA Company. Appendix A and B show the result for all the data and borehole details used in this study.

4.2 Liquefaction Evaluation Based on Index Properties

In the past, under big earthquakes, the liquefaction potential of sandy and silty sand's had been examined widely (Durgunoglu et al., 2007). There is still a further need to study and examine the liquefaction potential of fine grained soils such as silt and silty clays. Physical properties such as Atterberg limits: Liquid and Plastic limits and water

content are utilized in order to evaluate the liquefaction potential of fine-grained soils. Likewise, in this work, physical properties of fine-grained soils were also used in order to calculate the liquefaction potential. The following five criteria based on the index properties and water content were considered to evaluate the liquefaction potential of fine-grained soils:

4.2.1 The Polito and Martin (2001) Criteria

Polito and Martin (2001) suggested that fine-grained soils with the plasticity index (PI) below 7 and the liquid limit (LL) below 25, are considered to be liquefiable. Fine-grained soils with PI between 7 and 10 and LL between 25 and 30, are taken to be potentially liquefiable as shown in Figure 4.1.

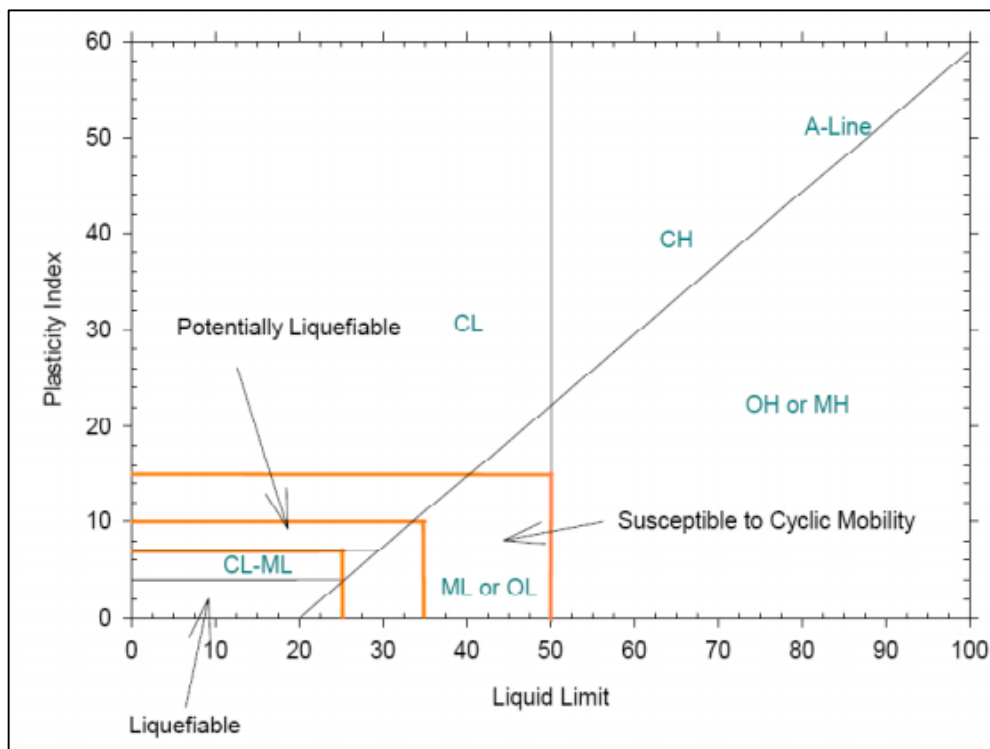


Figure 4.1: Recommendations of Polito and Martin (2001) for the assessment of liquefaction potential of fine grained soils.

4.2.2 The Seed et al. (2003) Criteria

Figure 4.2 shows the Seed et al. (2003) criteria for assessing the liquefaction potential of fine grained soils. According to this criteria, soils with sufficient fines content can liquefy depending on its water content and LL.

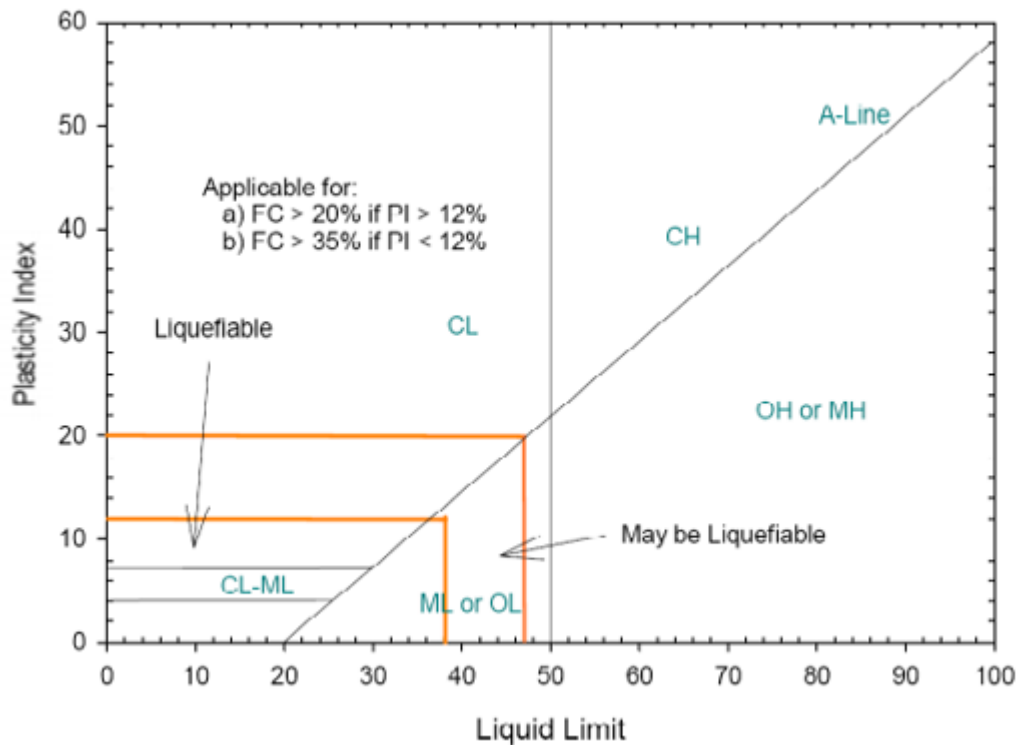


Figure 4.2: Seed et al. (2003) criteria for the assessment of liquefaction potential of fine-grained soils.

4.2.3 The Chinese Criteria (1982)

The Modified Chinese Criteria, which is the most broadly used criteria to distinguish potentially liquefiable soils was assessed by Wang (1979) and Seed and Idriss (1982). According to this criteria, fine or cohesive soils are thought to be of potentially liquefiable if:

- Liquid Limit (LL) is below or equivalent to 35%.
- Natural water content is above or equivalent to 90% of liquid limit

4.2.4 The Bray and Sancio (2004) Criteria

According to Bray et al. (2004) criteria shown in Figure 4.3, a deposit of soil is thought to be vulnerable to liquefaction or cyclic mobility if the soil plasticity index is less than or equal 12 ($PI < 12$) and the ratio of natural water content to liquid limit is equal or greater than 0.85 ($w_c/LL \geq 0.85$). Then again, a soil deposit modestly susceptible to liquefaction or cyclic mobility, if the ratio of natural water content to liquid limit is equal or greater than 0.80 ($w_c/LL \geq 0.80$) and the plasticity index is between twelve and twenty ($12 < PI \leq 20$). Then again, according to by Bray et al. (2004), soils with plasticity index bigger than 20 ($PI > 20$) are considered excessively clayey, making it impossible to liquefy.

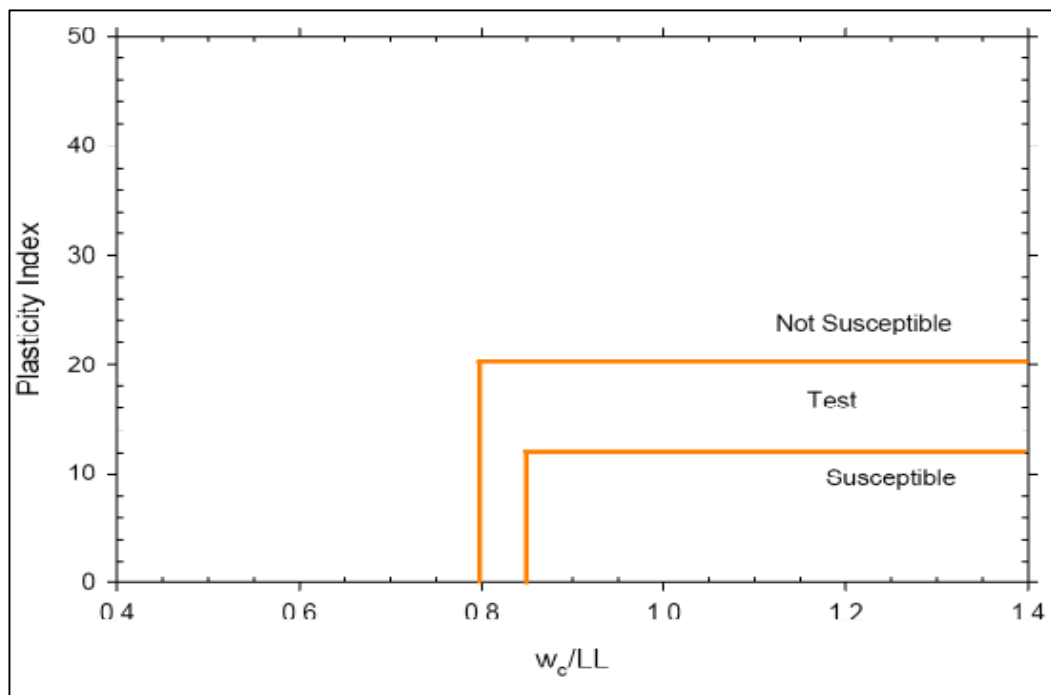


Figure 4.3: Bray and Sancio (2004) criteria for liquefaction susceptibility of fine grained soils.

4.2.5 Boulanger and Idriss (2004 and 2006) Criteria

According to Boulanger and Idriss (2004 and 2006) criteria, the soil sample should be sorted into "clay like" and "sand-like". Fine-grained soils can confidently be expected

to display clay- like characteristic if they possess a plasticity index equal or bigger than seven ($PI \geq 7$) and not be susceptible to liquefaction. Soil considered sand- like if plasticity index smaller than 7 ($PI < 7$) and susceptible to liquefaction. Figure 4.4 shows the condition in this criteria.

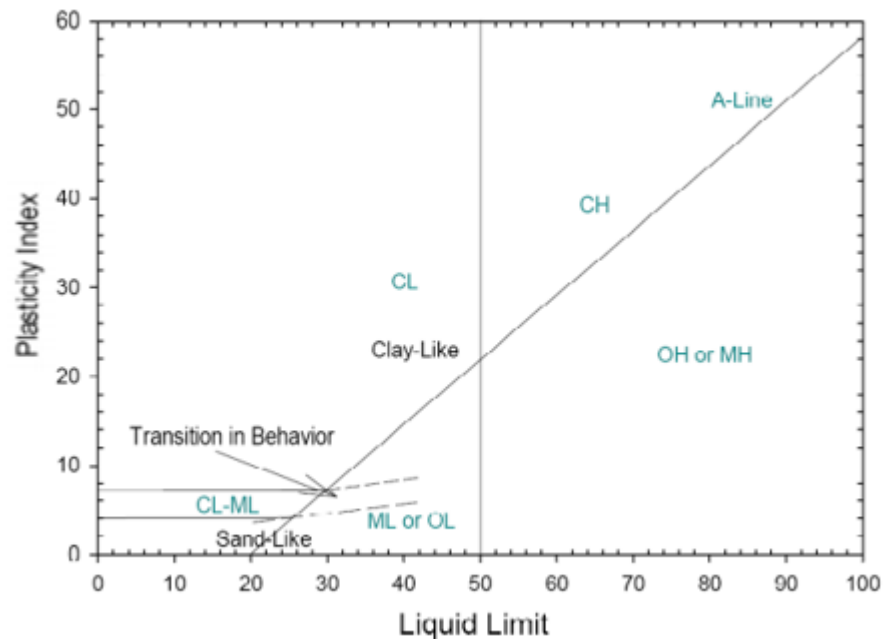


Figure 4.4: Boulanger and Idriss (2004-2006) criteria for the assessment of liquefaction potential.

4.3 Soil Parameters Obtained from Field Tests

4.3.1 The Standard Penetration Test (SPT)

Some of the data used in this study was obtained from an in-situ dynamic penetration test which is also known as the standard penetration test, SPT. The objective of the SPT is to determine the SPT N-value, which is an indication of the soil strength parameters especially in granular soils. The SPT N value can be correlated with soil properties for geotechnical engineering design. This value can also be used for predicting the susceptibility of the soils to liquefaction.

The recovery of disturbed samples is also possible during this operation. The ASTM D1586-99 was followed as a guide line in performing the test. The test includes recording the quantity of blows of 63.5 kg standard hammer with a 76 cm drop to drive the 50.8 mm width standard split spoon sampler into the soil sample at a separate distance of 30.5 cm.

4.4 Soil Parameters Obtained from Laboratory Test

4.4.1 The Unconfined Compression Test

An ASTM (ASTM D-2166) test standard was applied on undisturbed soil sample for conducting the unconfined compressive strength test (UCS).

4.4.1.1 Sensitivity

As shown in Equation 4.1, the ratio of undisturbed strength to remoulded strength is utilized as a quantitative measure of sensitivity. Table 4.1 shows one of the several classifications of sensitivity being proposed.

$$S_t = \frac{\text{Undisturbed strength}}{\text{Remolded strength}} \quad (4.1)$$

Table 4.1: Classifications of sensitivity (Rosenqvist, 1953)

Sensitivity	S_t
Insensitive	~ 1.0
Slightly Sensitive Clays	1-2
Medium Sensitive Clays	2-4
Very Sensitive Clays	4-8
Slightly Quick Clays	8-16
Medium Quick Clays	16-32
Very Quick Clays	32-64
Extra Quick Clays	> 64

The sensitivity of fine grained soil has appeared to give good correlation with liquidity index (LI) which is given in Equation 4.2. LI depends on water content (W_c), LL and PL of the soil.

$$LI = \frac{W_c - PL}{PI} \quad (4.2)$$

A typical relationship between the undrained shear strength of the remoulded clay and the liquidity index has been suggested by Mitchell (1993) as described in Equation 4.3.

$$S_u = \frac{1}{(LI - 0.21)^2} \quad (4.3)$$

where,

S_u = Remoulded undrained shear strength

4.4.2 Atterberg Limits

In the present study, Atterberg limits such as Liquid Limit (LL), and Plastic Limit (PL) tests were performed on disturbed samples by ASTM Standards (ASTM D-4318).

Liquid limit (LL) is defined as the moisture content at which soil begins to behave as a liquid material and begins to flow.

Plastic limit (PL) is defined as the moisture content at which soil begins to behave as a plastic material.

Plasticity index (PI) indicates the degree of plasticity of a soil. The greater the difference between liquid and plastic limits, the greater is the plasticity of the soil.

LL and PI values are used as basis for grouping the fine-grained soils in engineering soil classification systems.

4.5 Soil Liquefaction Potential Assessment

In this study, three techniques were used to estimate the liquefaction potential of the soils using:

- The liquefaction potential index (LPI),
- The probability of liquefaction (P_{Liq}), and
- The factor of safety against liquefaction (FS).

Two estimation variables were vital in order to evaluate the liquefaction potential of soils. These are:

- The capacity of soil to resist liquefaction described as cyclic resistance ratio (CRR).
- The seismic demand on a soil layer described as cyclic stress ratio (CSR),

The possibility to liquefaction can be estimated by comparing the cyclic resistance ratio (CRR) with the earthquake loading (CSR). This is stated as a factor of safety against liquefaction. If the CSR exceeds the CRR, liquefaction is expected to occur.

4.5.1 Evaluation of Cyclic Stress Ratio, CSR

The equation proposed by Seed and Idriss (1971) shown below was used to estimate the cyclic stress ratio

$$CSR = 0.65 \cdot \frac{a_{max}}{g} \cdot \frac{\sigma_{vo}}{\sigma'_{vo}} \cdot r_d \quad (4.4)$$

where;

a_{max} = represents the peak horizontal acceleration at the ground surface generated by the earthquake

g = represents acceleration due to gravity

σ_{vo} = total vertical overburden stress (kN/m²)

σ'_{vo} = effective vertical overburden stress (kN/m²)

r_d = stress reduction coefficient.

The r_d value was computed using the below equations (Liao and Whitman 1986-b):

$$r_d = 1.0 - 0.00765z \quad \text{for } z \leq 9.15 \text{ m} \quad (4.5-a)$$

$$r_d = 1.174 - 0.0267z \quad \text{for } 9.15 \text{ m} < z \leq 23 \text{ m} \quad (4.5-b)$$

$$r_d = 0.744 - 0.008z \quad \text{for } 23 \text{ m} < z \leq 30 \text{ m} \quad (4.5-c)$$

$$r_d = 0.5 \quad \text{for } z > 30 \quad (4.5d)$$

where,

z is the depth below the ground surface.

4.5.2 Evaluation of Liquefaction Resistance (CRR)

Both laboratory and field test results can be used to determine CRR value. In this study, field results of standard penetration test (SPT) was used in determining the CRR values.

4.5.2.1 SPT N value correction

In the SPT, the amount of energy transmitted to the drill rods and the overburden pressure have a significant effect on the SPT N value. The applied energy may vary from 30 to 90% of the theoretical value. For that reason, SPT blow counts must be normalized to a standard energy value, and also to an overburden pressure of around 100 kPa before its results are employed for use in liquefaction analysis. For instance, the United States standard uses N_{60} , which compares to 60% of the potential energy of the sledge coming to the SPT sampler. These standardization factors are examined later in this segment.

4.5.2.1.1 Influence of Fines Content on liquefaction potential

Robertson et al. (1996) stated that an apparent increment of CRR was observed with increased fines content. For the approximate corrections of the influence of fines content (FC) on CRR, the equations below were recommended by Boulanger and Idriss (2006) for use.

$$(N_1)_{60cs} = (N_1)_{60} + \Delta (N_1)_{60} \quad (4.6)$$

The equations created by Boulanger and Idriss were for the correction of $(N_1)_{60}$ to an equal clean sand value, $(N_1)_{60cs}$.

where:

$(N_1)_{60cs}$ = an equivalent clean sand standard penetration resistance value.

$\Delta (N_1)_{60}$ = correction factor for fines content.

The correction factor $\Delta (N_1)_{60}$ is shown in Figure 4.5 and calculated with the linear function:

- For $FC \leq 5\%$: $\Delta (N_1)_{60} = 0.0$ (4.7a)

- For $5 < FC < 35\%$: $\Delta (N_1)_{60} = 7 \cdot (FC - 5) / 30$ (4.7b)

- For $FC \geq 35\%$: $\Delta (N_1)_{60} = 7.0$ (4.7c)

where:

FC represents the fines content (percent finer than 0.075 mm).

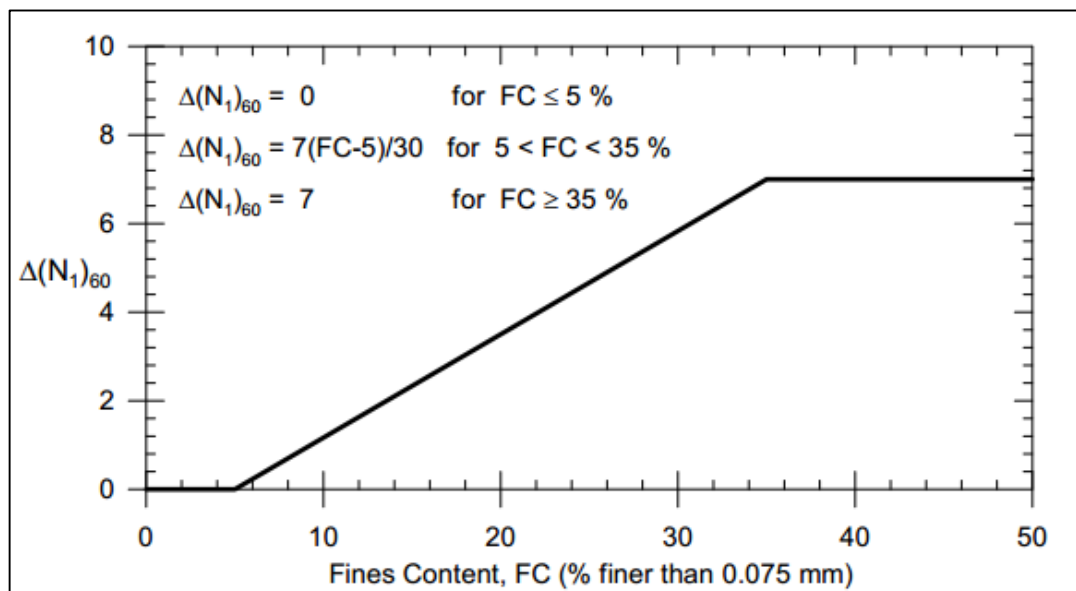


Figure 4.5: The correction factor $\Delta (N_1)_{60}$ for fines content (Boulanger and Idriss 2006).

Equation 4.8 can be used to determine $(N_1)_{60}$

$$(N_1)_{60} = N_{60} \cdot C_N \tag{4.8}$$

where

N_{60} = The corrected SPT N value

C_N = the overburden correction factor to normalize N_m to a common reference effective overburden stress.

N_m = standard penetration resistance.

As the N values for SPT rise with an increase in effective overburden stress (Seed and Idriss, 1982), the overburden stress correction factor is carried out. The following equation which is suggested by Liao and Whitman (1986a) is normally used in order to determine this C_N factor:

$$C_N = \left(\frac{P_a}{\sigma'_{vo}} \right)^{0.5} \quad (4.9)$$

where C_N represents the normalised Nm to an effective overburden pressure σ'_{vo} of around 100 kPa (1 atm), p_a , atmospheric pressure.

C_N ought not to surpass an estimated value of 1.7 as expressed by Youd et al. (2001). CRR was obtained from the below equations as suggested by Youd et al. (2001) by taking into account the corrected blow counts. Rauch (1998) developed this equation.

$$CRR_{7.5} = \frac{1}{34 - (N_1)_{60cs}} + \frac{(N_1)_{60cs}}{135} + \frac{50}{(10 \cdot (N_1)_{60cs} + 45)^2} - \frac{1}{200} \quad (4.10)$$

where;

$CRR_{7.5}$ = the cyclic resistance ratio for (M_w 7.5)

4.6 Calculation of Factor of Safety (FS) Against Liquefaction

By considering the earthquake loading (CSR) and the liquefaction resistance (CRR), the liquefaction potential can be evaluated. This is typically shown as a factor of safety against liquefaction, which is;

$$FS = \frac{CRR}{CSR} \quad (4.11)$$

Liquefaction is normally expected to happen if $FS \leq 1$ for traditional deterministic approach or method. In this study, the factor of safety values will be determined for earthquake magnitudes of $M_w = 6.0, 6.5, 7.0$ and 7.5 .

4.6.1 Magnitude Scaling Factor, MSF

Only earthquakes of magnitude 7.5 are subjected to the CRR given in equation 4.10.

A magnitude scaling factor is used for an earthquake magnitude other than 7.5. The magnitude scaling factors, MSF for SPT-based criteria defined by various researchers are given in Table 4.2. According to Bouglanger and Idriss (2004), the below equations can be used to find the MSF:

$$MSF = 6.9 \exp \left[\frac{-M}{4} \right] - 0.058 \leq 1.8 \quad (4.12)$$

where

M= earthquake magnitude

Subsequently, the factor of safety against liquefaction was computed as shown below:

$$FS = \left(\frac{CRR_{7.5}}{CSR} \right) \cdot MSF \quad (4.13)$$

Table 4.2: MSF value defined by various researchers (Youd and Noble 1997a)

Magnitude, M	Seed and Idriss (1982)	Idriss ^a	Ambraseys (1988)	Arango (1996)		Andrus and Stokoe (1997)	Youd and Noble (1997b)		
				Distance Based	Energy based		$P_L < 20\%$	$P_L < 32\%$	$P_L < 50\%$
5.5	1.43	2.20	2.86	3.00	2.20	2.8	2.86	3.42	4.44
6.0	1.32	1.76	2.20	2.00	1.65	2.1	1.93	2.35	2.92
6.5	1.19	1.44	1.69	1.60	1.40	1.6	1.34	1.66	1.99
7.0	1.08	1.19	1.30	1.25	1.10	1.25	1.00	1.20	1.39
7.5	1.00	1.00	1.00	1.00	1.00	1.00	—	—	1.00
8.0	0.94	0.84	0.67	0.75	0.85	0.8?	—	—	0.73?
8.5	0.89	0.72	0.44	—	—	0.65?	—	—	0.56?

4.7 The Liquefaction Potential Index (LPI)

In order to properly assess and quantify the risk of liquefaction, liquefaction potential index, LPI was proposed by Sonmez (2003) as in Table 4.3.

According to Lenz (2007), LPI was produced to incorporate liquefaction potential over depth and get an evaluation of liquefaction-related surface damage for a boring area or location.

According to the method by Iwasaki et al. (1982), the LPI can be defined as:

$$LPI = \int_0^{20} F_L(z) \cdot w(z) \cdot dz \quad (4.14)$$

$$FL = 0 \quad \text{for } FS \geq 1 \quad (4.15-a)$$

$$FL = 1 - FS \quad \text{for } FS < 1 \quad (4.15-b)$$

$$w(z) = 10 - 0.5z \quad \text{for } z < 20\text{m} \quad (4.16-a)$$

$$w(z) = 0 \quad \text{for } z > 20\text{m} \quad (4.16-b)$$

where

z represents depth in meters

dz represents the differential increment of depth

In this study, LPI was determined by using Table 4.3 proposed by Sonmez (2003). The LPI values were determined from the computed factor of safety values obtained from SPT.

Table 4.3: Classification of liquefaction potential index (Sonmez, 2003).

Liquefaction Potential Index (LPI)	Liquefaction Potential Classification
0	Non-liquefiable
$0 < \text{LPI} \leq 2$	Low
$2 < \text{LPI} \leq 5$	Moderate
$5 < \text{LPI} \leq 15$	High
$\text{LPI} > 15$	Very High

4.8 Probability of Liquefaction

Any deterministic method or technique should be calibrated so that the meaning of the computed FS is well known in terms of the liquefaction probability (Chen and Juang, 2000). Juang (2000) have included the Robertson and Wride (1998) method and brought out the below mapping function to evaluate probability of liquefaction;

$$P_{\text{Liq}} = \frac{1}{\left(1 + \frac{\text{FS}^B}{A}\right)} \quad (4.17)$$

where

P_{Liq} : Liquefaction probability

FS: Factor of safety against liquefaction

The coefficient of A is equal to 1.0 and B is equal 3.3.

Lee et al. (2003) assessed another method after Iwasaki et al. (1982), by taking into consideration the probability function proposed by Juang et al. (2003).

The $F(z)$ term of the LPI suggested by Iwasaki et al. (1982) was substituted by P_{Liq} and LPI and renamed liquefaction risk index (I_r) in the new method.

$$I_r = \int_0^{20} PLiq(z) \cdot w(z) \cdot dz \quad (4.18)$$

where,

P_{Liq} = Probability of liquefaction.

z = depth in meter.

$w(z)$ = the weighting factor.

dz = the differential increment of depth.

A rather new method was suggested by Sonmez and Gokceoglu (2005) using the Lee et al. (2003) approach. The term liquefaction severity index, LS was used rather than liquefaction index risk, IR. This is the main distinction of this new method.

$$L_s = \int_0^{20} PL(z) \cdot w(z) \cdot dz \quad (4.19)$$

where

L_s = Liquefaction severity index.

$PLiq$ = Probability of liquefaction

$$P_{Liq} = \frac{1}{(1+FS)^{3.3}} \quad (4.21-a)$$

$$PLiq \text{ represents } 0 \quad \text{for } FS \geq 1.411 \quad (4.21-b)$$

FS = Factor of safety against liquefaction.

z = depth in meters.

dz = the differential increment of depth.

$$w_{(z)} \text{ represents } 10-0.5z \quad \text{for } z < 20m \quad (4.20-a)$$

$$w_{(z)} \text{ represents } 0 \quad \text{for } z > 20m \quad (4.20-b)$$

The classification of liquefaction severity index, L_s and liquefaction severity suggested by Sonmez and Gokceoglu (2005) are given in Table 4.4. In this study, this suggested correlation will be applied to predict the risk of liquefaction.

Table 4.4: The Liquefaction severity classification (Sonmez and Gokceoglu, 2005)

Liquefaction Severity Index (L_s)	Liquefaction Severity Classification
$85 \leq L_s < 100$	Very High
$65 \leq L_s < 85$	High
$35 \leq L_s < 65$	Moderate
$15 \leq L_s < 35$	Low
$0 < L_s < 15$	Very Low
$L_s=0$	Non-liquefied

4.9 Coefficient of Determination, R^2 : SPT versus LL, PI, Shear Strength Parameters

In this study, the best fitting among the calculated and the predicted results suggested by various researchers is plotted and the correlation coefficient represented as R^2 is determined. The R^2 coefficient of determination is a statistical measure of how well the regression line approximates the actual data points (Taylor, 1990). As indicated by the estimations of R^2 , the relationship between any two parameters can be grouped as:

$R^2 < 0.30$ considered to have no connection,

R^2 of 0.30 to 0.499 are thought to be a mild relationship,

R^2 of 0.50 to 0.699 are thought to be a moderate relationship and,

R^2 of 0.70 to 1.0 are regarded to be a strong relationship (Mostafa, 2003).

In the present study, numerous figures have been plotted so as to analyses and also show the relationship between field and experimented results which include the measured SPT number (N_{60}), depth of test sample (D) from the ground surface, the shear strength parameters (C and ϕ) and the Atterberg limits.

4.10 Predicting q_c from the SPT N Number

SPT is one of the common oldest in situ test used for soil investigation. On the other hand, cone penetration test, CPT is one of the best investigation tool in the field. These tests represent soil resistance to penetration. CPT is quasi-static and SPT is dynamic (Fauzi, 2015). In previous studies, several correlations between SPT and CPT values were done (Robertson et al., 2010). In the present study, the measured CPT values are missing so the measured SPT values will be used to predict the CPT values in the field. The following equations (Equations 4.22 to 4.24) proposed by Abbas et al. (2014), kara et al. (2010), and Fauzi et al. (2015) will be used respectively to predict the CPT values from SPT results:

$$q_c = 0.274N^{1.015} \quad (4.22)$$

$$q_c = 0.2152N^{0.8252} \quad (4.23)$$

$$q_c = 0.95N^{0.64} \quad (4.24)$$

where

q_c = cone penetration resistance

N= Measured SPT N value

4.11 Estimating the Undrained Shear Strength (S_u) by SPT N Value

SPT is one of the common tests to evaluate the undrained shear strength parameters of fine grained soils in the field.

Undrained shear strength, S_u of the fine grained soils can be determined either by the unconsolidated undrained triaxial test (UU) or the unconfined compression test (UC). In this study, UC test was used to determine unconfined compressive strength (q_u) of the fine grained soils. The correlation proposed by Terzaghi & Peck (1967) shown in Table 4.5 was used to determine the relationship between q_u and SPT.

Table 4.5: Correlation between q_u and SPT by Terzaghi and Peck (1967)

Consistency	SPT-N	q_u (kPa)
Very Soft	< 2	< 25
Soft	2 - 4	25 - 50
Medium	4 – 8	50 - 100
Stiff	8 - 15	100 - 200
Very Stiff	15 – 30	200 - 400
Hard	> 30	> 400

In the present study, the comparison between the measured and the predicted S_u values according to Sanglerat 1972, Nixon 1982 and Decourt 1990 methods were given and the results were discussed. Equations given below (Equations 4.25-4.27) are suggested by Sanglerat (1972), Nixon (1982) and Decourt (1990), respectively.

$$S_u = 10N \quad (4.25)$$

$$S_u = 12N \quad (4.26)$$

$$S_u = 12.5N \quad (4.27)$$

Chapter 5

RESULTS AND DISCUSSIONS

5.1 Soil Classification in Boreholes

In this study, as aforementioned, 20 boreholes from Basra in Iraq were taken and from the samples obtained in these boreholes, particle size, hydrometer and Atterberg limits test results were used to classify these soils in the boreholes. Soil types of Basra region were identified according to Unified Soil Classification System (USCS) as listed in Tables 5.1 to 5.20.

Table 5.1: Value SPT, Atterberg limits and soil classification for Borehole 1

SPT	Depth (m)	LL (%)	PL (%)	PI (%)	Soil Type
1	3.0-3.5	41	22	19	CL
1	6.0-6.5	51	24	27	CH
1	10.5-11.0	54	27	27	CH
4	13.5-14.0	47	23	24	CL
4	15.0-15.5	44	21	23	CL
17	21.0-21.5	47	21	26	CL
11	24.0-24.5	56	26	30	CH
97	27.0-27.5				SM

In Borehole 1 depths between 27.0 m to 27.5 m, the Atterberg limits could not be obtained because of the non-plastic properties of the soil in these depths.

Table 5.2: Value SPT, Atterberg limits and soil classification for Borehole 2

SPT	Depth (m)	LL (%)	PL (%)	PI (%)	Soil Type
1	3.0-3.5	46	22	24	CL
1	6.0-6.5	50	23	27	CH
1	7.5-8.0	52	24	28	CH
1	10.5-11.0	47	21	26	CL
3	15.0-15.5	43	19	24	CL
23	22.5-23.0	50	22	28	CH
97	27.0-27.5	40	22	18	CL

Table 5.3: Value of SPT, Atterberg limits and soil classification for Borehole 3

SPT	Depth (m)	LL (%)	PL (%)	PI (%)	Soil Type
22	3.0-3.5	35	18	17	CL
14	4.5-5.0	40	18	22	CL
12	9.0-9.5	46	20	26	CL
17	12.0-12.5	48	23	25	CL
29	15.0-15.5	52	25	27	CH
36	19.5-20.0	56	25	31	CH
41	24.0-24.5	55	23	32	CH
44	27.0-27.5	51	22	29	CH

Table 5.4: Value of SPT, Atterberg limits and soil classification for Borehole 4

SPT	Depth (m)	LL (%)	PL (%)	PI (%)	Soil Type
24	1.5-2.0	39	18	21	CL
23	4.5-5.0	33	15	18	CL
15	7.5-8.0	31	13	18	ML-OL
12	12.0-12.5	38	17	21	CL
22	16.5-17.0	37	18	19	CL
51	27.0-27.5	54	22	32	CH
61	30.0-30.5	55	21	34	CH

Table 5.5: Value of SPT, Atterberg limits and soil classification for Borehole 5

SPT	Depth (m)	LL (%)	PL (%)	PI (%)	Soil Type
1	0.0-0.5	48	21	27	CL
1	6.0-6.5	51	22	29	CH
1	8.0-8.5	53	23	30	CH
2	12.0-12.5	41	18	23	CL
4	18.0-18.5	43	19	24	CL
25	24.0-24.5	43	20	23	CL
39	27.0-27.5	45	21	24	CL
100	34.0-34.5	49	20	29	CL
100	42.0-42.5	47	22	25	CL
100	46.0-46.5				SM
100	50.0-50.5				SM
100	60.0-60.5				SM

Table 5.6: Value of SPT, Atterberg limits and soil classification for Borehole 6

SPT	Depth (m)	LL (%)	PL (%)	PI (%)	Soil Type
1	0.0-0.5	54	23	31	CH
1	4.0-4.5	52	23	29	CH
1	8.0-8.5	54	24	30	CH
1	12.0-12.5	47	21	26	CL
5	18.0-18.5	38	18	20	CL
21	24.0-24.5	44	19	25	CL
60	27.0-27.5	46	22	24	CL
72	38.0-38.5	38	21	17	CL
79	42.0-42.5	42	23	19	CL
80	46.0-46.5				SM
100	60.0-60.5				SM

In Boreholes 5 and 6 soils below 46.0 m depth are non-plastic. Therefore Atterberg limits was not obtained. In some boreholes (Borehole 1, 2, 3, 4, 5, 6, 9, 10, 11, 12,

etc.), the SPT values within the depth approximately 12 m are very low indicating a very soft clay.

Table 5.7: Value of SPT, Atterberg limits and soil classification for Borehole 7

SPT	Depth (m)	LL (%)	PL (%)	PI (%)	Soil Type
3	3.0-3.5	45	21	24	CL
4	7.0-7.5	44	23	21	CL
31	16.5-17.0	46	22	24	CL
49	18.5-19.0	37	21	16	CL
69	24.0-24.5				SM
83	30.0-30.5				SM

Table 5.8: Value of SPT, Atterberg limits and soil classification for Borehole 8

SPT	Depth (m)	LL (%)	PL (%)	PI (%)	Soil Type
4	1.5-2.0	53	24	29	CH
6	7.0-7.5	59	28	31	CH
9	14.0-14.5	50	23	27	CH
27	15.5-16.0	56	20	26	CH
82	21.0-21.5	36	19	17	CL
100	27.0-27.5				SM

Table 5.9: Value of SPT, Atterberg limits and soil classification for Borehole 9

SPT	Depth (m)	LL (%)	PL (%)	PI (%)	Soil Type
1	1.5-2.0	58	25	33	CH
1	6.0-6.5	54	26	28	CH
4	9.0-9.5	44	20	24	CL
25	15.0-15.5	42	19	23	CL
70	21.0-21.5	45	21	24	CL
75	27.0-27.5				SM
72	30.0-30.5	48	22	26	CL

Table 5.10: Value of SPT, Atterberg limits and soil classification for Borehole 10

SPT	Depth (m)	LL (%)	PL (%)	PI (%)	Soil Type
1	0.0-0.5	53	25	28	CH
1	4.0-4.5	56	26	30	CH
3	8.0-8.5	45	22	23	CL
19	12.0-12.5	49	23	26	CL
51	15.0-15.5				SM
50	21.0-21.5	51	23	28	CH
75	24.0-24.5				SM
69	30.0-30.5	42	20	22	CL

Table 5.11: Value of SPT, Atterberg limits and soil classification for Borehole 11

SPT	Depth (m)	LL (%)	PL (%)	PI (%)	Soil Type
2	4.5-5.0	41	21	20	CL
1	7.5-8.0	49	24	25	CL
6	11.0-11.5	46	22	24	CL
4	13.0-13.5	33	18	15	CL
23	17.0-17.5	37	18	19	CL
21	19.0-19.5	34	18	16	CL
20	21.0-21.5	43	20	23	CL
72	25.0-25.5	47	23	24	CL

Table 5.12: Value of SPT, Atterberg limits and soil classification for Borehole 12

SPT	Depth (m)	LL (%)	PL (%)	PI (%)	Soil Type
2	3.0-3.5	48	24	24	CL
1	6.0-6.5	45	22	23	CL
2	7.5-8.0	43	21	22	CL
7	11.0-11.5	44	23	21	CL
11	13.0-13.5	47	22	25	CL
25	17.0-17.5	45	21	24	CL
20	19.0-19.5	59	26	33	CH
41	21.0-21.5	48	23	25	CL

Table 5.13: Value of SPT, Atterberg limits and soil classification for Borehole 13

SPT	Depth (m)	LL (%)	PL (%)	PI (%)	Soil Type
12	1.5-2.0	48	22	26	CL
11	4.5-5.0	56	23	33	CH
16	7.5-8.0	54	20	34	CH
19	15.0-15.5	39	23	16	CL
72	19.0-19.5				SM
40	27.0-27.5				SM

Table 5.14: Value of SPT, Atterberg limits and soil classification for Borehole 14

SPT	Depth (m)	LL (%)	PL (%)	PI (%)	Soil Type
12	3.0-3.5	56	25	31	CH
8	7.5-8.0	50	21	29	CH
25	11.0-11.5	54	23	31	CH
32	13.0-13.5	38	21	17	CL
39	21.0-21.5	51	22	29	CH

Table 5.15: Value of SPT, Atterberg limits and soil classification for Borehole 15

SPT	Depth (m)	LL (%)	PL (%)	PI (%)	Soil Type
7	1.5-2.0	54	23	31	CH
4	4.5-5.0	57	24	33	CH
9	7.5-8.0	52	25	27	CH
	15.0-15.5				SM
	21.0-21.5				SM
41	24.0-24.5	66	29	37	CH
58	35.0-35.5	61	26	35	CH

Table 5.16: Value of SPT, Atterberg limits and soil classification for Borehole 16

SPT	Depth (m)	LL (%)	PL (%)	PI (%)	Soil Type
8	0.5-1.0	50	24	26	CH
10	4.5-5.0	41	19	22	CL
5	7.5-8.0	39	18	21	CL
	15.0-15.5				SM
26	21.0-21.5	47	22	25	CL
26	27.0-27.5	49	23	26	CL
25	30.0-30.5	67	26	41	CH

Table 5.17: Value of SPT, Atterberg limits and soil classification for Borehole 17

SPT	Depth (m)	LL (%)	PL (%)	PI (%)	Soil Type
3	2.5-3.0	40	28	12	CL
3	7.5-8.0	42	20	22	CL
4	15.0-15.5	34	16	18	CL
	17.5-18.0	36	17	19	CL
42	20.0-20.5	45	24	21	CL
	22.5-23.0	49	25	24	CL
14	30.0-30.5	37	25	12	CL

Table 5.18: Value of SPT, Atterberg limits and soil classification for Borehole 18

SPT	Depth (m)	LL (%)	PL (%)	PI (%)	Soil Type
2	2.5-3.0	45	20	25	CL
	7.5-8.0	38	17	21	CL
	12.5-13.0	42	19	23	CL
26	17.5-18.0	40	18	22	CL
44	25.0-25.5	51	23	28	CH
	27.5-28.0	35	16	19	CL
59	32.0-32.5	37	20	17	CL

Table 5.19: Value of SPT, Atterberg limits and soil classification for Borehole 19

SPT	Depth (m)	LL (%)	PL (%)	PI (%)	Soil Type
10	0.5-1.0	52	24	28	CH
7	4.5-5.0	56	23	33	CH
	9.0-9.5	45	19	26	CL
10	12.0-12.5	48	22	26	CL
26	18.0-18.5	32	15	17	CH
76	24.0-24.5	34	16	18	CL
37	35.0-35.5	43	20	23	CL

Table 5.20: Value of SPT, Atterberg limits and soil classification for Borehole 20

SPT	Depth (m)	LL (%)	PL (%)	PI (%)	Soil Type
4	1.5-2.0	46	21	25	CL
9	4.5-5.0	48	22	26	CL
11	7.5-8.0	47	26	21	CL
4	12.0-12.5	49	22	27	CL
2	15.0-15.5	51	22	29	CH
21	24.0-24.5	57	24	33	CH
24	30.0-30.5	46	22	24	CL
38	35.0-35.5	38	21	17	CL

Overview of these Tables (5.1-5.20) indicate that most of the soils in these boreholes can be categorized in two groups of clay with low plasticity CL and clay with high plasticity CH. In some boreholes, non-plastic silty sands, SM type soils were recorded after around 25 m depth.

5.2 Assessment of Liquefaction by Index Properties

Based on physical properties of soils aforementioned in Chapter 4, five criteria suggested by different researchers will be used to assess the liquefaction susceptibility of Basra soils in Iraq.

5.2.1 The Polito and Martin (2001) Criteria

Figure 5.1 shows the effect of plasticity index in predicting the liquefaction potential of fine grained soils suggested by Polito and Martin (2001). Figure 5.1 shows the Atterberg limit test results of Basra soil determined experimentally. The figure indicates that all the obtained plasticity index and the liquid limit values of Basra soil are above 10 and 35 respectively, indicating the soils to have a cyclic mobility failure rather than liquefaction failure.

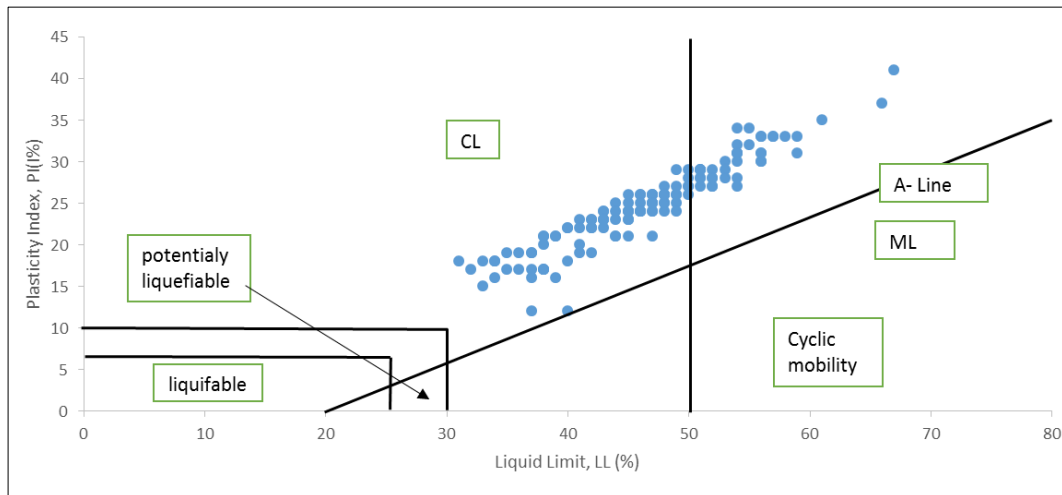


Figure 5.1: Liquefaction behaviour of Basra soils based on Polito and Martin (2001) criteria

5.2.2 Seed et al. (2003) Criteria

Figure 5.2 shows the liquefaction potential of Basra soil according to Seed et al. (2003). According to the values obtained for Basra soil, there are no points existing in Zone A. From the figure, it can be seen that, some points fall in Zone B indicating that these soils are moderately susceptible to liquefaction and need further testing.

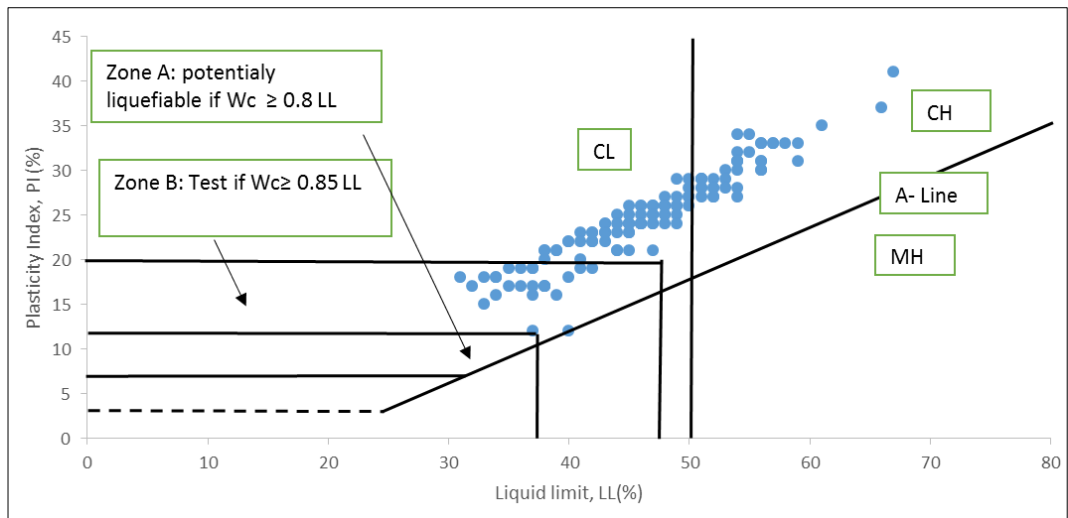


Figure 5.2: Liquefaction behaviour of Basra soils based on Seed et al. (2001).

5.2.3 Chinese Criteria (1982)

According to Chinese criteria as shown in Figure 5.3, a few points of Basra soils lie in liquefaction susceptible zone. According to the Chinese criteria, soils are susceptible to liquefaction if $5\mu\text{m} \leq 15\%$.

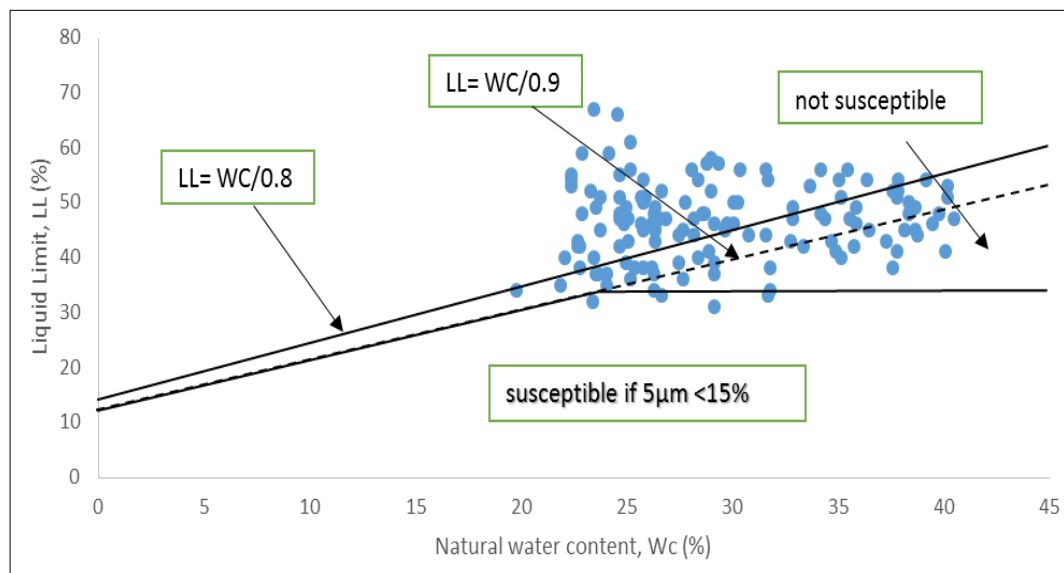


Figure 5.3: Basra soils susceptible to liquefaction according to Chinese criteria (1982).

5.2.1 Bray and Sancio (2004) Criteria

According to Bray et al. (2004) criteria, only one point is susceptible to liquefaction and few points are moderately susceptible to liquefaction (Figure 5.4). The other points fall outside the risky zone.

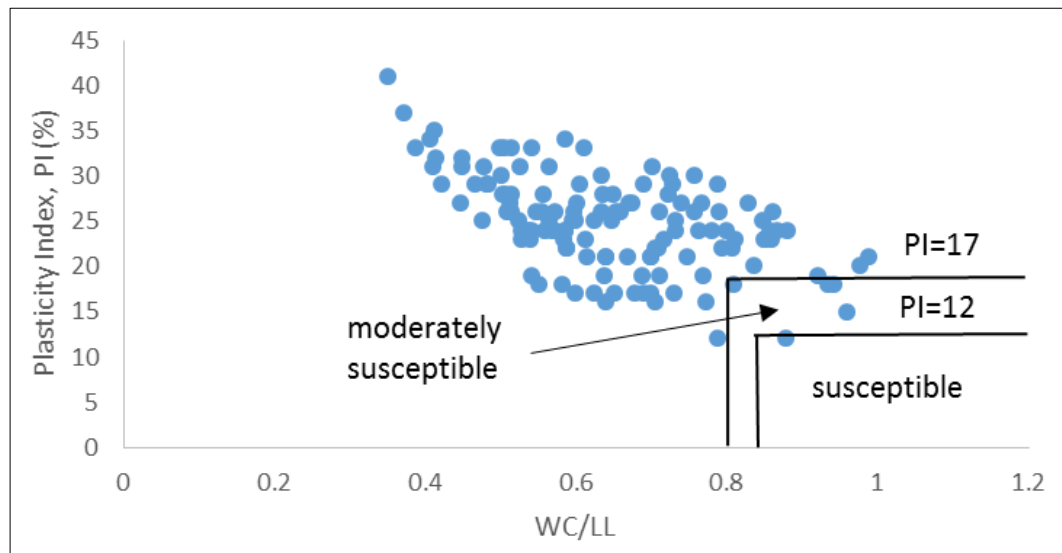


Figure 5.4: Basra soils susceptible to liquefaction according to Bray and Sancio (2004)

5.2.2 Boulanger and Idriss (2004 and 2006) Criteria

According to Boulanger and Idriss (2004 - 2006), Basra soils shown in Figure 5.5 are clay-like soils and not susceptible to liquefaction which are defined as fine-grained soils which undergo cyclic mobility rather than cyclic liquefaction (Boulanger and Idriss, 2006). They recommended to use the term “liquefaction” for sand-like soils if $PI < 7$ and “cyclic failure” for clay-like soils.

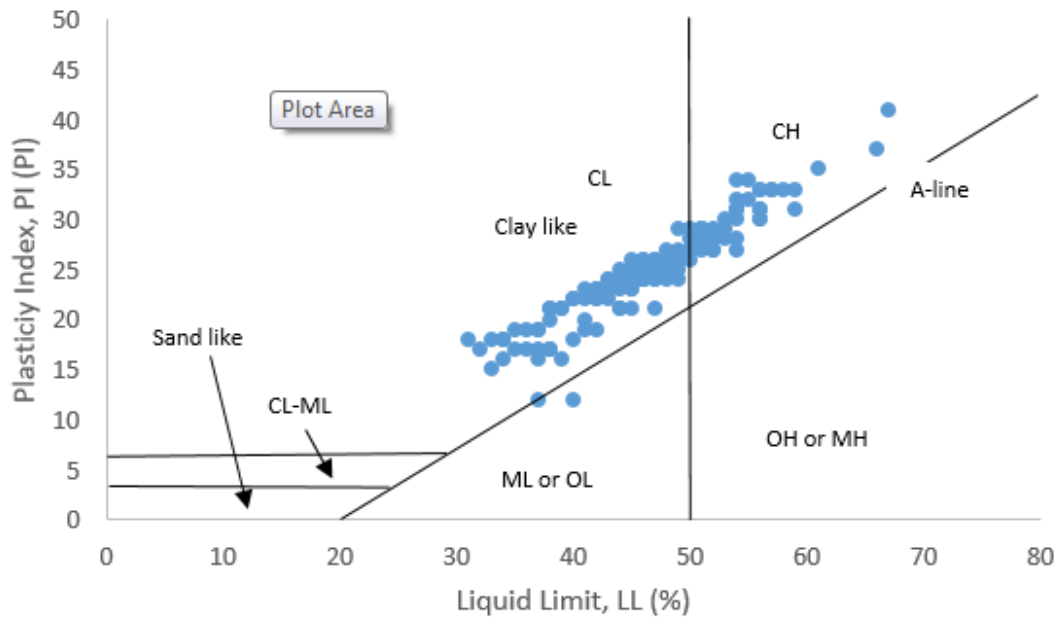


Figure 5.5 Basra soils susceptible to liquefaction according to Boulanger and Idriss (2004 and 2006)

The liquefaction susceptibility of Basra soils was evaluated by using the five criteria based on LL, PL, and natural water content. The comparison of the liquefaction susceptibility results indicated that two of the criteria suggested by Seed et al. (2003) and Bray et al. (2004) seem to give similar susceptibility to liquefaction prediction for Basra soils.

5.3 In-situ and Laboratory Tests Results Used for Predicting the Liquefaction Susceptibility of Basra Soils

5.3.1 Sensitivity

The ratio of the undisturbed undrained shear strength to remolded undrained shear strength of fine grained soils was used to determine the sensitivity of Basra soils. The undisturbed undrained shear strength of the soils were obtained from the laboratory unconfined compression tests whereas the remolded undrained shear strength was calculated from the liquidity index formula. Table 5.21 shows the result of sensitivity values obtained for Basra soils at the different depths.

Table 5.21: Result of sensitivity values of Basra soil

Borehole	Depth (m)	Liquidity index, LI %	Undisturbed shear strength (kPa)	Remolded shear strength (kPa)	Sensitivity, S_t
1	6.0-6.5	0.62	28	11.03	2.54
2	3.0-3.5	0.73	22	3.71	5.93
5	6.0-6.5	0.63	14	5.73	2.44
6	4.0-6.0	0.51	17	10.48	1.57
7	16.5-17.0	0.10	108	82.64	1.31
8	15.5-16.0	0.39	148	31.40	4.71
9	9.0-9.5	0.78	29	3.04	9.53
10	8.0-8.5	0.73	27	3.75	7.19
11	5.5-5.0	0.96	6	1.80	14.43
12	11.0-11.5	0.56	44	8.30	5.3
13	7.5-8.0	0.54	63	55.59	1.13
14	7.5-8.0	0.32	52	81.62	0.64
15	7.5-8.0	0.06	89	46.25	1.92
16	7.5-8.0	0.43	34	9.57	3.55
17	15.0-15.5	0.88	38	2.24	16.95
18	12.5-13.0	0.73	33	3.69	8.94
19	9.0-9.5	0.41	40	24.62	1.62
20	12.0-12.5	0.40	58	26.25	2.18

The values in the table indicate that the sensitivities of Basra soil is high. This means that if the soils are susceptible to cyclic loading, they may develop excessive deformations and loose strength during earthquake. Table 5.22 shows the classification of sensitivity of Basra soils according to Rosenqvist (1953).

Table 5.22: Sensitivity classification of Basra soils according to Rosenqvist (1953).

Borehole	Depth (m)	S_t	S_t Class
1	6.0-6.5	2.54	Medium sensitive
2	3.0-3.5	5.93	Very sensitive
5	6.0-6.5	2.44	Medium sensitive
6	4.0-6.0	1.57	Slightly sensitive
7	16.5-17.0	1.31	Slightly sensitive
8	15.5-16.0	4.71	Very Sensitive
9	9.0-9.5	9.53	Slightly Quick
10	8.0-8.5	7.19	Very Sensitive
11	5.5-5.0	14.43	Slightly Quick
12	11.0-11.5	5.3	Very Sensitive
13	7.5-8.0	1.13	Slightly Sensitive
14	7.5-8.0	0.64	Insensitive
15	7.5-8.0	1.92	Slightly Sensitive
16	7.5-8.0	3.55	Medium Sensitive
17	15.0-15.5	16.95	Medium Quick
18	12.5-13.0	8.94	Slightly Quick
19	9.0-9.5	1.62	Slightly Sensitive
20	12.0-12.5	2.18	Medium Sensitive

5.3.2 Factor of Safety Determination Based on SPT N Value

Detail and procedures for calculating $CRR_{7.5}$ by using $(N_1)_{60cs}$ was explained in Chapter 4. As aforementioned, Seed and Idriss (1971) equation was used to determined CSR. Peak Ground Acceleration, PGA for Basra soil was considered to be as 0.2g. Using $CRR_{7.5}$ and CSR values, factor of safety ($FS_{7.5}$) against liquefaction for M_w 7.5 was detected. Magnitude Scaling Factor, MSF was used to determine the FS values for 6, 6.5, and 7 earthquake magnitudes. MSF was calculated by using Equation 4.12 given in Chapter 4 and MSF values were found to be 1.48, 1.30, and 1.14 for earthquake magnitudes of 6.0, 6.5, and 7.0 respectively. Then, with the calculated values of MSF, the factor of safety values were determined at these earthquake magnitudes: 6.0, 6.5,

7.0, and 7.5. Table 5.23 shows the calculated CRR, CSR and factor of safety values at different earthquake magnitudes and depths.

Table 5.23: Calculated factor of safeties against liquefaction using SPT $(N_1)_{60cs}$ values

Borehole	Depth	$(N_1)_{60}$	$(N_1)_{60cs}$	CRR _{7.5}	CSR	FS ₆	FS _{6.5}	FS ₇	FS _{7.5}
1	1.5	1.70	8.70	0.10	0.13	1.17	1.03	0.90	0.79
	19.5	10.18	17.18	0.18	0.18	1.53	1.34	1.18	1.03
2	3.0	1.70	8.70	0.10	0.18	0.82	0.72	0.63	0.55
	19.5	5.38	12.38	0.13	0.17	1.15	1.01	0.89	0.78
3	4.5	19.03	26.03	0.31	0.16	2.91	2.56	2.24	1.97
	13.5	25.84	30.84	0.54	0.19	4.2	3.69	3.23	2.83
4	7.5	16.48	23.48	0.26	0.17	2.36	2.07	1.82	1.59
	15.0	13.96	20.48	0.23	0.16	1.98	1.54	1.52	1.34
5	10.0	1.14	8.14	0.10	0.27	0.54	0.47	0.41	0.36
	18.0	3.44	10.44	0.12	0.21	0.84	0.73	0.64	0.56
6	10.0	2.21	9.21	0.11	0.26	0.61	0.53	0.47	0.41
	18.0	4.18	11.18	0.12	0.21	0.91	0.80	0.70	0.61
7	7.0	4.70	11.70	0.13	0.22	0.86	0.75	0.66	0.58
	18.5	36.38	43.38	0.21	0.17	1.51	1.59	1.40	1.22
8	7.0	5.44	12.44	0.14	0.21	0.95	0.83	0.73	0.64
	14.0	7.66	14.66	0.16	0.20	1.17	1.03	0.90	0.79
9	9.0	4.63	11.63	0.13	0.22	0.87	0.77	0.67	0.59
	13.0	18.54	25.54	0.30	0.21	2.16	1.90	1.66	1.46
10	4.0	1.7	8.7	0.10	0.13	1.2	1.05	0.92	0.81
	12.0	19.37	26.37	0.32	0.20	2.37	2.08	1.81	1.60
11	1.5	17	24	0.27	0.13	3.15	2.77	2.43	2.13
	7.5	1.28	8.28	0.10	0.24	0.61	0.53	0.47	0.41
12	1.5	3.4	10.4	0.12	0.13	1.35	1.18	1.04	0.91
	13.0	10.86	17.86	0.19	0.23	1.25	1.10	0.96	0.84
13	7.5	18.77	25.77	0.31	0.22	2.06	1.81	1.58	1.39
	15.0	16.19	23.19	0.36	0.20	1.95	1.71	1.50	1.32
14	4.5	10.18	17.18	0.18	0.20	1.33	1.17	1.02	0.9
	9.0	19.33	26.33	0.32	0.22	2.12	1.87	1.64	1.43
15	1.5	11.90	18.90	0.20	0.13	2.31	2.03	1.78	1.57
	7.5	10.34	17.34	0.18	0.22	1.26	1.10	0.97	0.85
16	1.5	5.10	12.10	0.13	0.13	1.52	1.34	1.17	1.03
	7.5	5.57	12.57	0.14	0.22	0.94	0.82	0.72	0.63
17	5.0	4.53	11.53	0.13	0.13	1.5	1.32	1.16	1.01
	15.0	3.50	10.50	0.12	0.18	0.99	0.87	0.76	0.67
18	5.0	3.28	10.28	0.12	0.13	1.37	1.20	1.05	0.92
	15.0	11.96	18.96	0.20	0.18	1.63	1.43	1.26	1.10
19	4.5	10.77	17.77	0.19	0.24	1.16	1.02	0.89	0.78
	18.0	20.47	27.47	0.35	0.19	2.8	2.46	2.16	1.89
20	4.5	13.04	20.04	0.22	0.20	1.58	1.38	1.21	1.06
	12.0	3.74	10.74	0.12	0.21	0.84	0.74	0.65	0.57

According to the calculated FS values in Table 5.23 based on $(N_1)_{60cs}$, the liquefaction potential of Basra soils was found to be high in almost most of the boreholes.

5.3.3 Liquefaction Potential Index, LPI Based on SPT

LPI for Basra regions were estimated for four different earthquake magnitudes ($M_w=6.0, 6.5, 7.0, 7.5$) and a_{max} was taken to be $= 0.2g$. Tables 5.24 to 5.27 show the results and the classification of LPI for Basra soils according to Sönmez (2003). The result indicated that at the earthquake magnitude, $M_w= 7.5$, Basra soil has a high LPI. At 7.0 and 6.5 earthquake magnitudes, Basra soil had a moderate LPI, whereas at earthquake magnitude of 6.0, Basra soil had a low LPI value.

Table 5.24: SPT based Liquefaction Potential Index, LPI classification at $M_w= 6.0$

Borehole	LPI	LPI classification
1	0	Non-liquefiable
2	2.39	Moderate
3	0	Non-liquefiable
4	0	Non-liquefiable
5	5.96	High
6	4.79	Moderate
7	1.97	Low
8	0	Non-liquefiable
9	2.35	Moderate
10	0	Non-liquefiable
11	8.29	High
12	0	Non-liquefiable
13	0	Non-liquefiable
14	0	Non-liquefiable
15	0	Non-liquefiable
16	1.27	Low
17	0.2	Low
18	0	Non-liquefiable
19	0	Non-liquefiable
20	3.68	Moderate

Table 5.25: SPT based Liquefaction Potential Index, LPI classification at Mw= 6.5

Borehole	LPI	LPI classification
1	0	Non-liquefiable
2	3.73	Moderate
3	0	Non-liquefiable
4	0	Non-liquefiable
5	7.21	High
6	6.19	High
7	3.44	Moderate
8	1.47	Low
9	4.35	Moderate
10	0	Non-liquefiable
11	9.84	High
12	0	Non-liquefiable
13	0	Non-liquefiable
14	0	Non-liquefiable
15	0	Non-liquefiable
16	3.68	Moderate
17	2.46	Moderate
18	0	Non-liquefiable
19	0	Non-liquefiable
20	6.05	High

Table 5.26: SPT based Liquefaction Potential Index, LPI classification at Mw= 7.0

Borehole	LPI	LPI classification
1	1.38	Low
2	5.24	High
3	0	Non-liquefiable
4	0	Non-liquefiable
5	8.32	High
6	7.42	High
7	5.53	High
8	4.85	Moderate
9	6.12	High
10	2.8	Moderate
11	11.41	High
12	0.3	Low
13	0	Non-liquefiable
14	0	Non-liquefiable
15	0.7	Low
16	5.81	High
17	4.46	Moderate
18	0	Non-liquefiable
19	2.76	Moderate
20	8.13	High

Table 5.27: SPT based Liquefaction Potential Index, LPI classification at $M_w = 7.5$

Borehole	LPI	LPI classification
1	3	Moderate
2	6.4	High
3	0	Non-liquefiable
4	0	Non-liquefiable
5	9.3	High
6	8.52	High
7	5.78	High
8	8.28	High
9	7.68	High
10	6.91	High
11	12.42	High
12	2.59	Moderate
13	0	Non-liquefiable
14	2.61	Moderate
15	3.21	Moderate
16	7.68	High
17	6.23	High
18	3.31	Moderate
19	5.57	High
20	9.98	High

5.3.4 Liquefaction Severity Index Based on SPT

Probability of liquefaction was calculated by using the factor of safety values determined from SPT sounding. Again, four different earthquake magnitudes (6.0, 6.5, 7.0, and 7.5) were used to determine the liquefaction severity, L_s .

Tables 5.28 to 5.31 show the L_s values and the classification of liquefaction severity according to Sonmez and Gokceoglu (2005). The results in these tables indicate that the liquefaction severity values for Basra soil fall in very low severity class. Unlike

the previous analysis in this study, the risk of liquefaction in Basra region was found to be very low according to Sonmez and Gokçeoglu (2005).

Table 5.28: SPT based liquefaction severity index and the classification at Mw= 6.0

Borehole	Ls	Liquefaction Severity Classification
1	1.11	Very Low
2	2.08	Very Low
3	0	Non-Liquefied
4	0	Non-Liquefied
5	3.37	Very Low
6	2.91	Very Low
7	1.81	Very Low
8	2.82	Very Low
9	2.36	Very Low
10	2.68	Very Low
11	4.4	Very Low
12	1.42	Very Low
13	0	Non-Liquefied
14	1.56	Very Low
15	1.43	Very Low
16	2.36	Very Low
17	4.06	Very Low
18	2.54	Very Low
19	2.01	Very Low
20	3.08	Very Low

Table 5.29: SPT based liquefaction severity index and the classification at Mw= 6.5

Borehole	Ls	Liquefaction Severity Classification
1	1.45	Very Low
2	2.69	Very Low
3	0	Non-Liquefied
4	0	Non-Liquefied
5	3.94	Very Low
6	3.44	Very Low
7	2.19	Very Low
8	3.51	Very Low
9	2.86	Very Low
10	3.36	Very Low
11	5.15	Very Low
12	1.80	Very Low
13	0	Non-Liquefied
14	1.99	Very Low
15	1.81	Very Low
16	2.89	Very Low
17	5.10	Very Low
18	3.23	Very Low
19	2.52	Very Low
20	5.17	Very Low

Table 5.30: SPT based liquefaction severity index and the classification at Mw= 7.0

Borehole	Ls	Liquefaction Severity Classification
1	1.79	Very Low
2	3.14	Very Low
3	0	Non-Liquefied
4	0	Non-Liquefied
5	4.53	Very Low
6	4.01	Very Low
7	2.62	Very Low
8	4.30	Very Low
9	3.43	Very Low
10	4.17	Very Low
11	5.94	Very Low
12	2.25	Very Low
13	0	Non-Liquefied
14	2.49	Very Low
15	2.25	Very Low
16	3.48	Very Low
17	6.35	Very Low
18	5.34	Very Low
19	3.11	Very Low
20	6.29	Very Low

Table 5.31: SPT based liquefaction severity index and the classification at Mw= 7.5

Borehole	Ls	Liquefaction Severity Classification
1	2.19	Very Low
2	3.56	Very Low
3	0	Non-Liquefied
4	0	Non-Liquefied
5	5.16	Very Low
6	4.62	Very Low
7	3.27	Very Low
8	5.21	Very Low
9	4.06	Very Low
10	5.1	Very Low
11	6.78	Very Low
12	2.76	Very Low
13	1.19	Very Low
14	3.08	Very Low
15	2.77	Very Low
16	5.15	Very Low
17	7.81	Very Low
18	6.67	Very Low
19	3.79	Very Low
20	7.58	Very Low

5.3 Correlations between SPT and Shear Strength Parameters

5.4.1 Measured Atterberg Limits and SPT N Values

Figures 5.6 to 5.9 show the LL, PL, PI, and corrected SPT N_{60} values with changing depths, respectively. From these Figures, it can be seen that there are no correlation between the Atterberg limits and soil depth since Atterberg limit values are dependent on the physical and mechanical properties of soil particles.

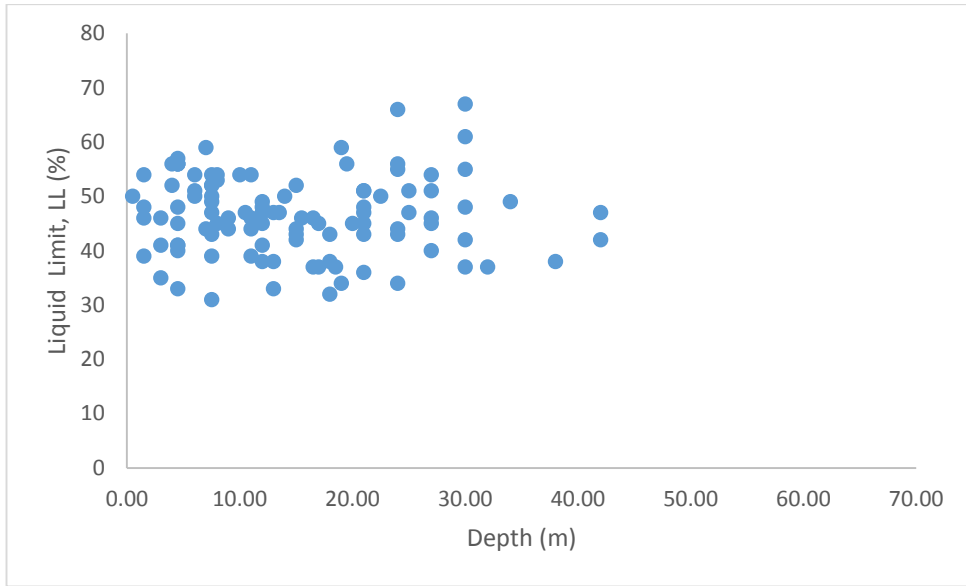


Figure 5.6: Liquid limit values with changing depth

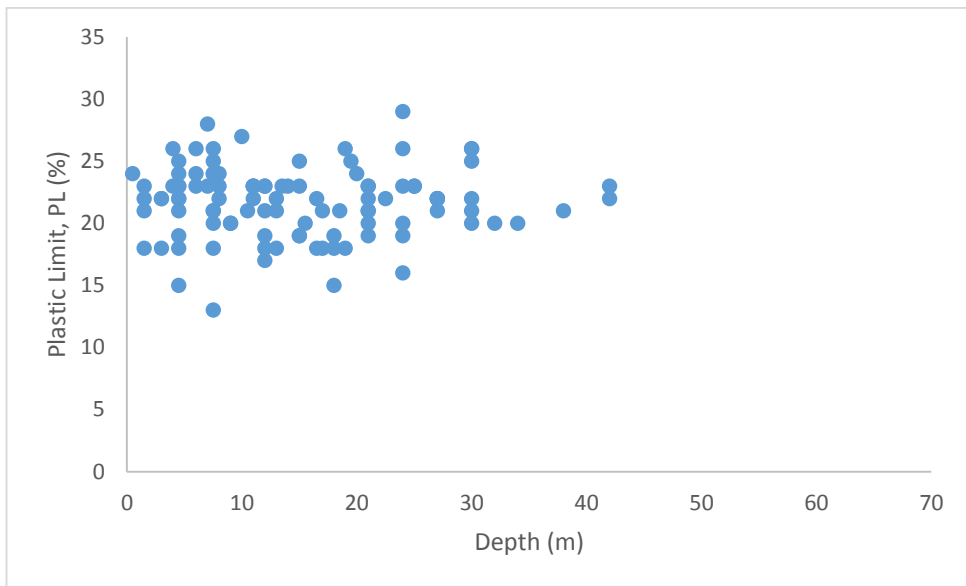


Figure 5.7: Plastic limit values with changing depth

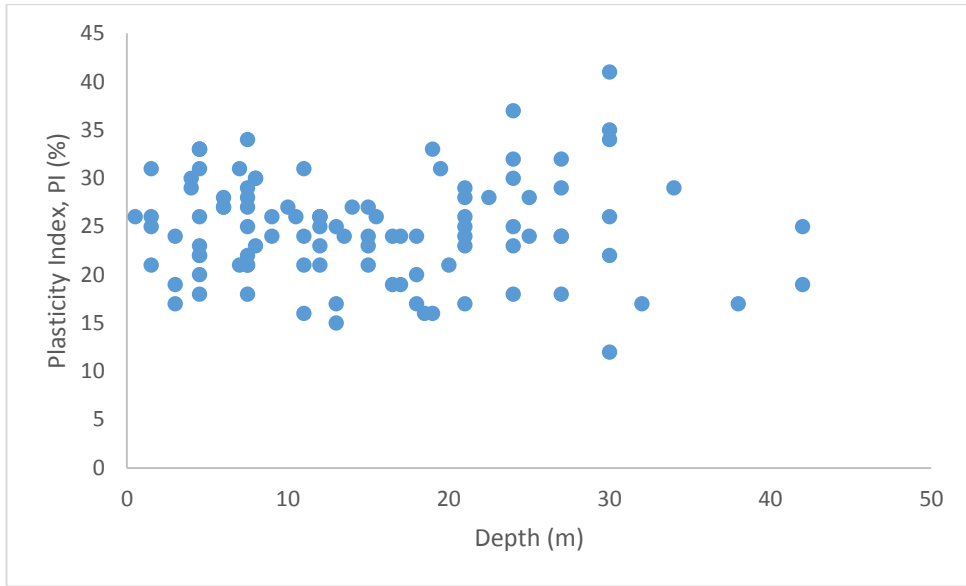


Figure 5.8: Plasticity index versus depth

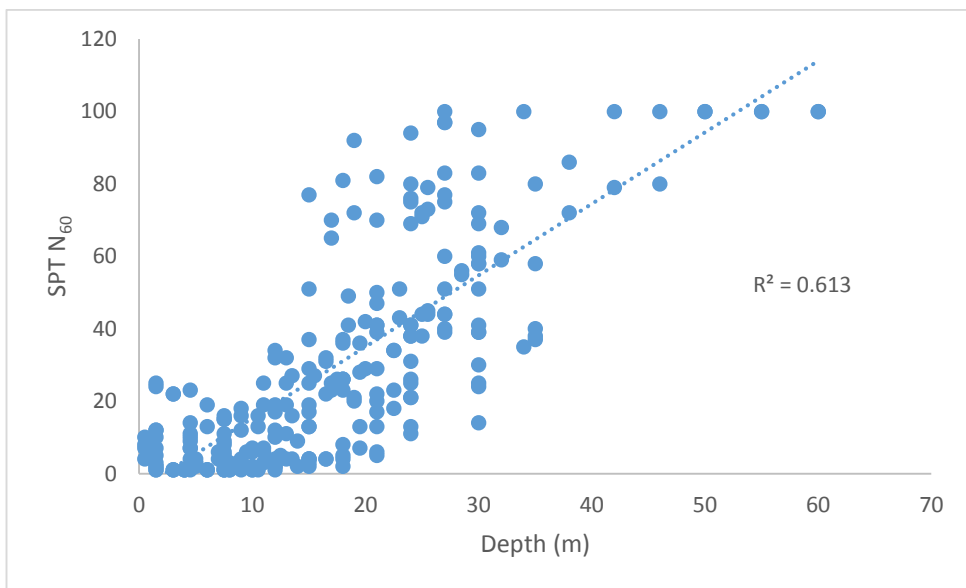


Figure 5.9: Depth versus corrected SPT N_{60} values

Figure 5.9 shows the values of corrected SPT N_{60} with depth for the boreholes. From the figure, it can be seen that with increasing depth, increase in the SPT values was observed. This can be explained due to the increase in the effective overburden pressure and a consequent increase in the relative density of deeper soil layers below ground surface. The value of R^2 coefficient obtained for Figure 5.9 is equal to 0.613 which shows a moderate relationships between depth and the corrected SPT N_{60} value.

5.4.2 Correlation between SPT, Atterberg Limits and the Shear Strength Parameters

The relationship between the corrected SPT N_{60} values and the Atterberg limit was shown in Figures 5.10 to 5.12, respectively. SPT number is mainly dependent on the relative density of soil layers. As the relative density increases, the SPT N value decreases. On the other hand, Atterberg limits depend on the chemistry and mineralogy of the soil particles. Because of this, it can be noticed that Atterberg limits did not have any effect on SPT N value. Also there is no good correlation between SPT and Atterberg limits.

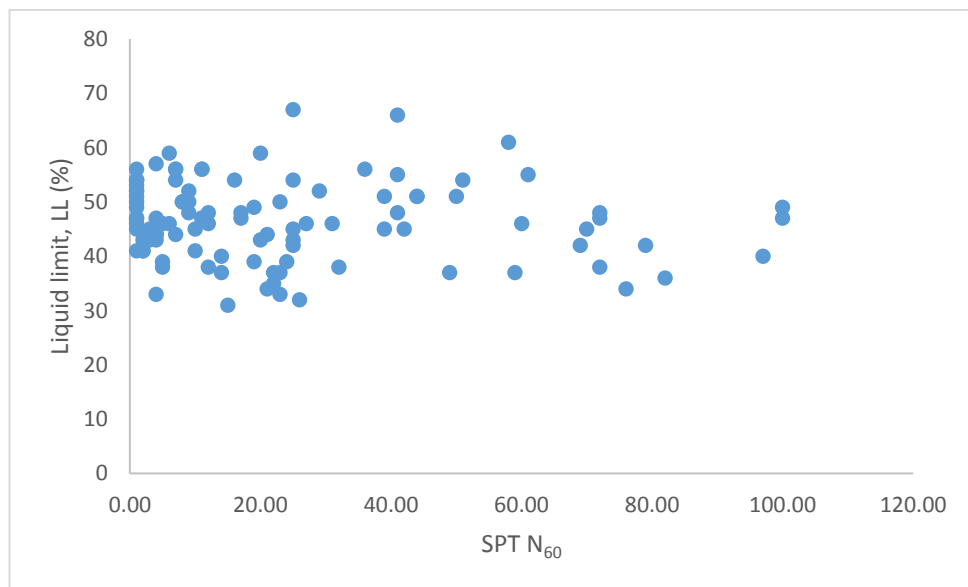


Figure 5.10: SPT N_{60} value versus liquid limit

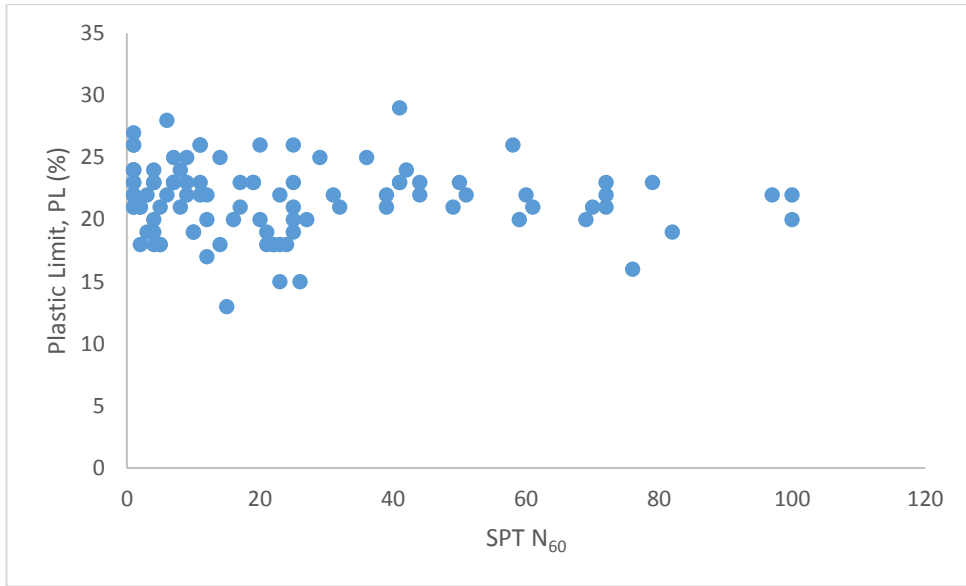


Figure 5.11: SPT N₆₀ value versus plastic limit

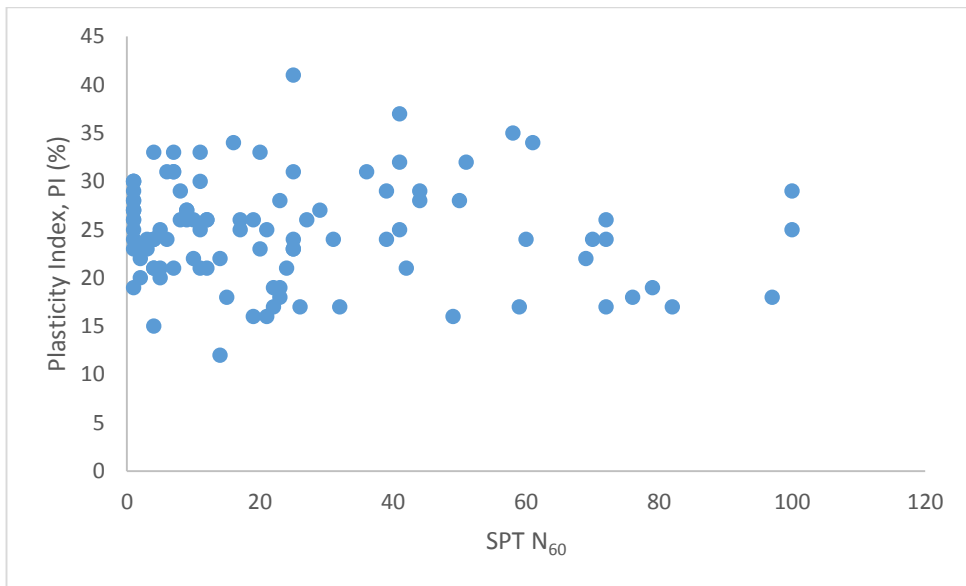


Figure 5.12: SPT N₆₀ value versus plasticity index

Figures 5.13 and 5.14 show the relationship between SPT and the shear strength parameters (c and ϕ) respectively. The figures indicated that increase in SPT numbers resulted in an increase in shear strength parameters of the soil. This is due to the increase in relative density which leads to an increase in the corrected SPT number and consequently increase in the shear strength parameters. In Figure 5.13 and Figure

5.14, the R^2 coefficient was found to be 0.8633 and 0.9553, respectively. This shows a good correlation between SPT number and the shear strength parameters.

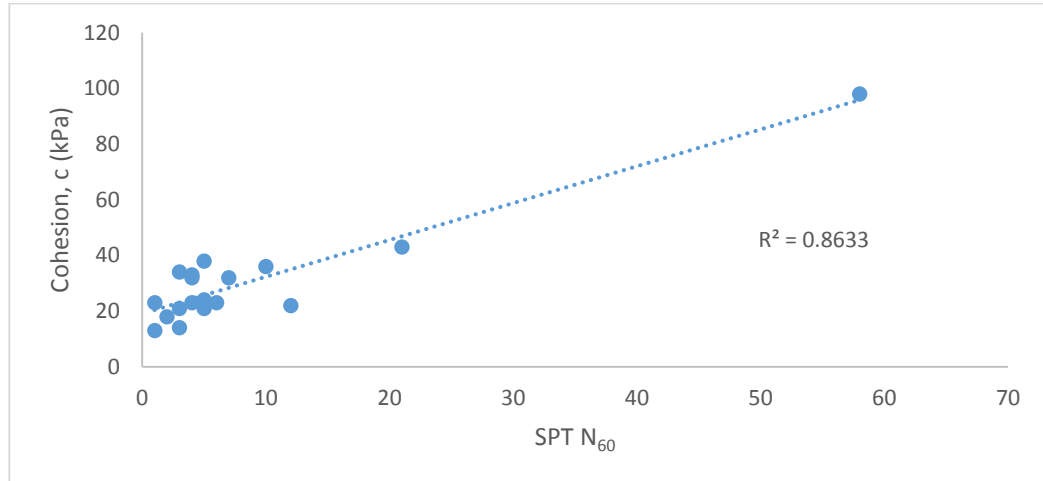


Figure 5.13: SPT N_{60} value versus cohesion

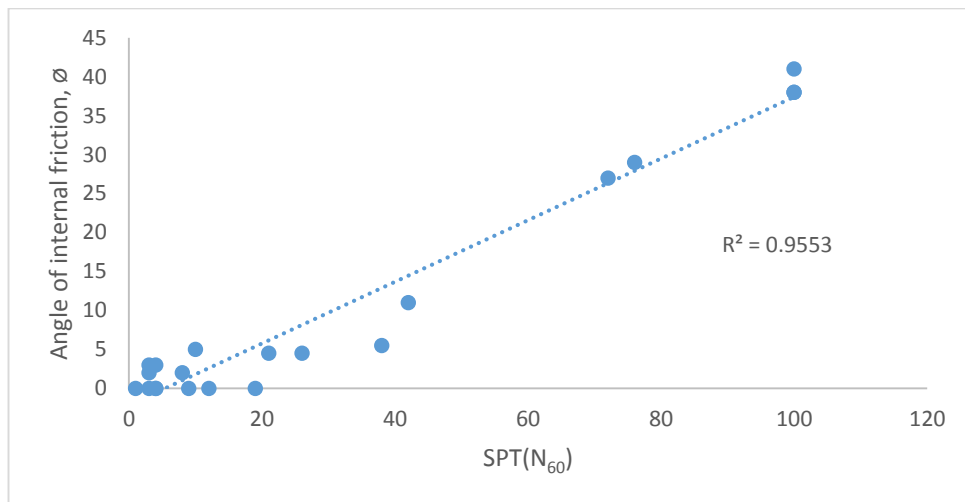


Figure 5.14: SPT N_{60} values versus angle of internal friction

The comparison of the internal friction angle values obtained from the measured SPT values and the values obtained from the equations suggested by Peck et al. (1974) and Hatanaka et al. (1996) are shown in Figure 5.15 and Figure 5.16.

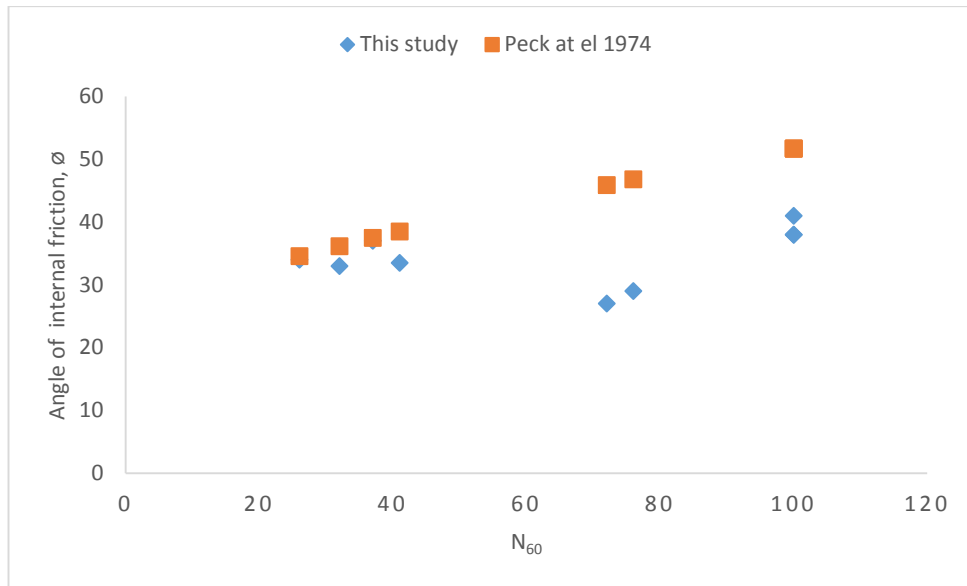


Figure 5.15: Correlation between N_{60} and the angle of internal friction for silty sand

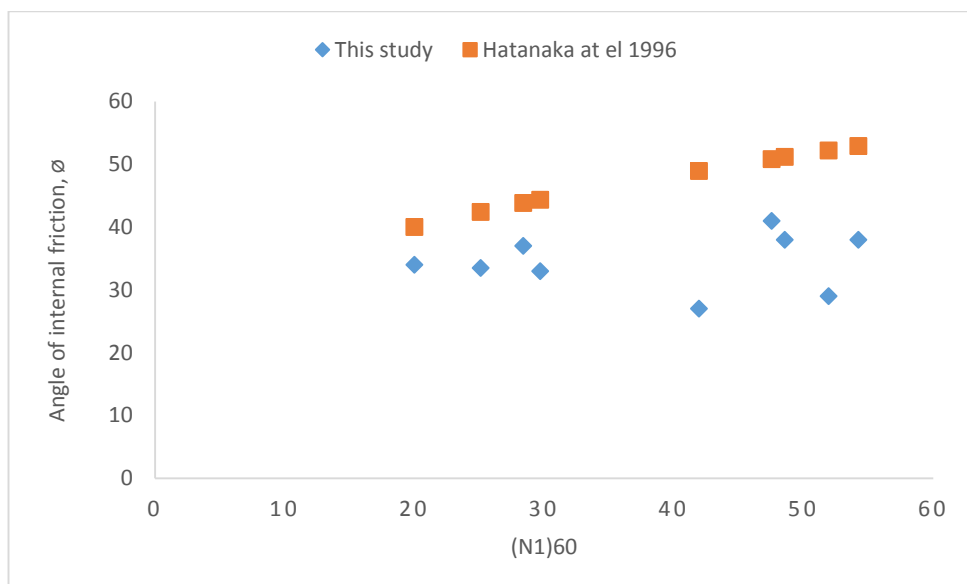


Figure 5.16: Correlation between $(N1)_{60}$ and angle of internal friction for silty sand

5.4.2 Predicting Cone Penetration Resistance q_c by Using SPT N Number

In the literature, there are lots of correlations between SPT, N value and CPT value Robertson et al. (2010). As known, these tests are in-situ soil tests and both of them represent soil resistance to penetration. CPT is quasi-static and SPT is dynamic (Fauzi, 2015). SPT is one of the common and oldest tests used throughout the world in soil investigation and foundation design. On the other hand, CPT is usually used to

determine the geotechnical properties of soil and soil stratigraphy (Abbas, 2014). In this study, SPT measurements were done but the CPT values were missing. For predicting the CPT values, the existing correlations between the SPT and CPT found by the other researchers, had been used and the CPT values were predicted.

Figure 5.17 indicated that the findings of these three researchers are not in a very good harmony. There are discrepancies among the findings of the q_c values. Kara (2010) method gives the more conservative prediction. Because of the variances among the predicted values, it seems that the predicting the q_c values from the SPT values is not very reliable.

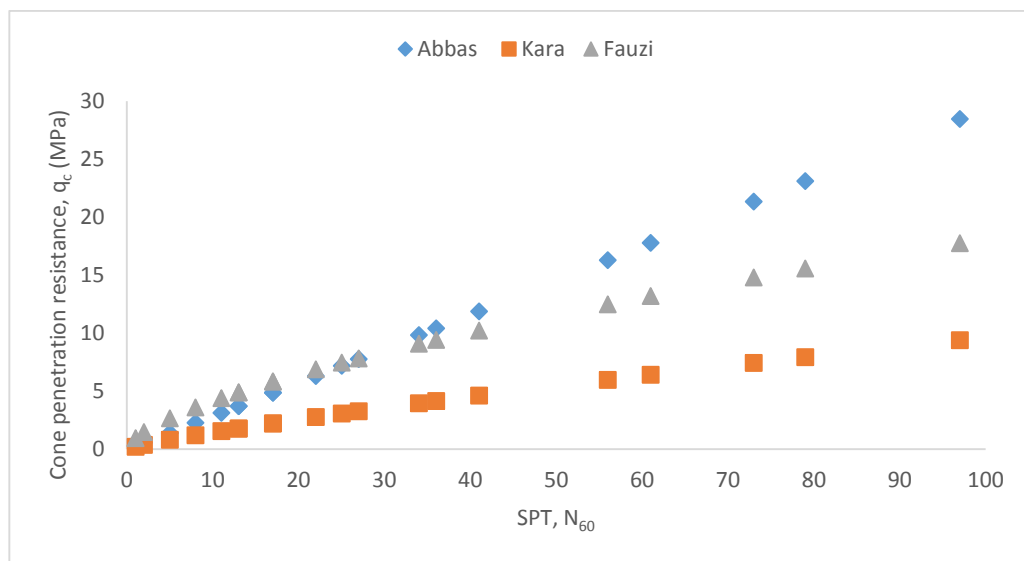


Figure 5.17: Correlation between SPT and the cone penetration resistance, q_c

5.4.3 Estimating Undrained Shear Strength (S_u) by SPT Value

Figure 5.18 shows the relationships between SPT value and undrained shear strength (S_u). The figure shows there is a strong relation between SPT value and S_u . The coefficient of R^2 was found to be 0.9336. Equation 5.1 presents the proposed correlation between SPT N_{60} number and undrained shear strength (S_u).

$$S_u = 1.3382 N_{60} + 12.294 \quad (5.1)$$

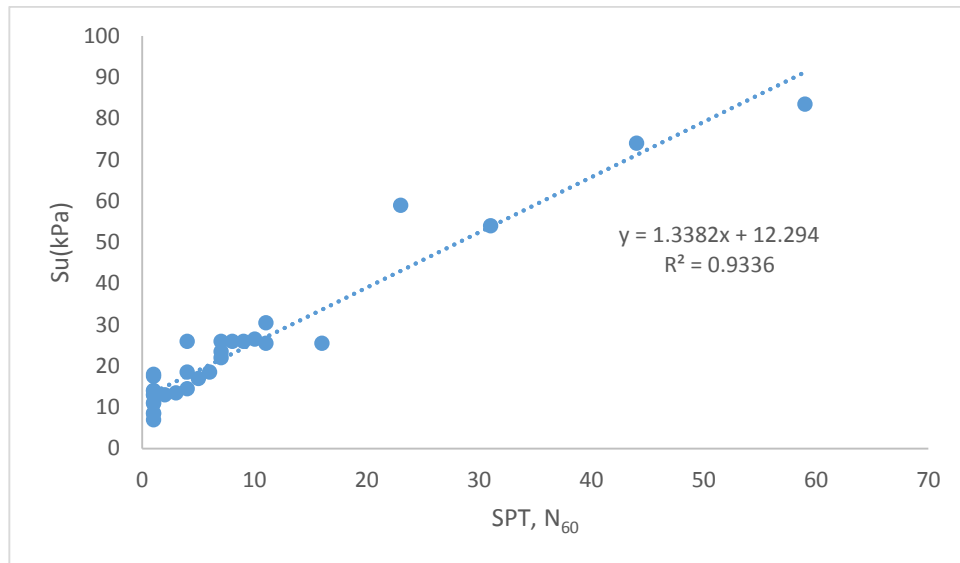


Figure 5.18: Relationships between SPT N_{60} and S_u

Figure 5.19 shows the correlation between SPT number and S_u obtained for Basra soil. In the same figure, the correlations proposed by other researchers (Sanglerat 1972; Nixon, 1982 and Decourt, 1990) were also presented. Figure 5.19 shows that the correlations proposed by Nixon (1982) and Decourt (1990) are in good harmony. The S_u results are very close to each other. Figure 5.19 indicated that the correlation proposed by Sanglerat (1972) and result of this study are not very close to Nixon (1982) and Decourt (1990). The correlation obtained in this study shows disagreement with the others.

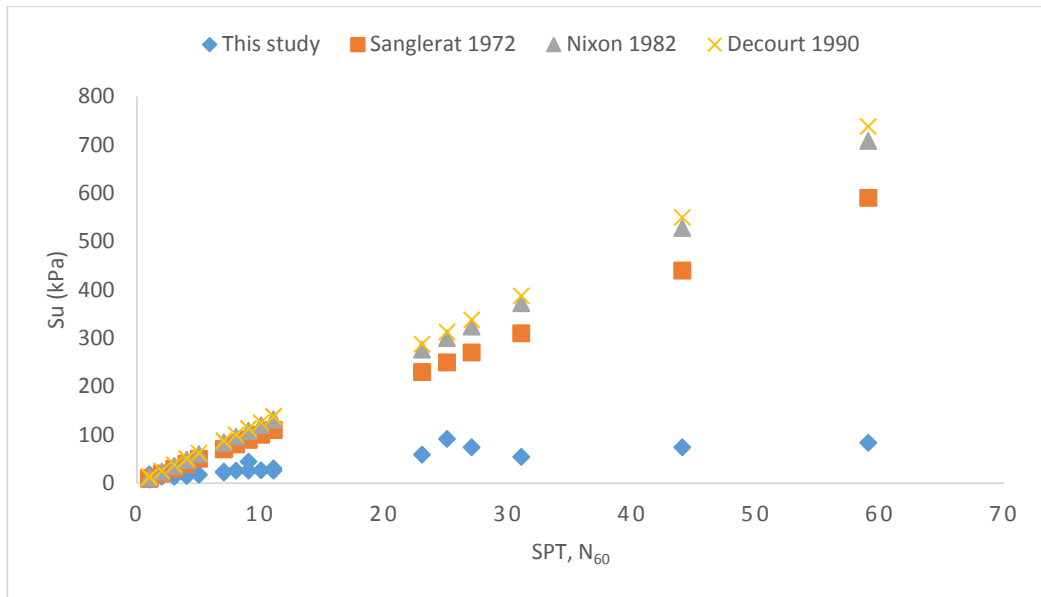


Figure 5.19: The SPT, N_{60} versus S_u proposed by some researchers

Chapter 6

CONCLUSION

Estimation of liquefaction susceptibility of fine-grained soils during earthquakes is a complicated problem in geotechnical engineering. According to the results of in-situ and laboratory tests, Basra region consists of sands, silty sand and clays.

In this study, in situ and laboratory tests were used to evaluate the liquefaction potential of sand and fine grained soils in Basra city, Iraq. Also, the reliability of using the SPT values in predicting the Atterberg limits, shear strength and the cone penetration resistance of fine grained soils was also evaluated. Based on the measured Atterberg limits, SPT N values and the correlations, the following conclusions can be made:

1. Atterberg limit test results and natural water content were used to evaluate the liquefaction potential of fine-grained soils based on the five criteria mentioned in Chapters 4 and 5. According to the results obtained, Seed et al. (2003) and Bray et al. (2004) criteria's were found to be the most applicable within the other criteria. Chinese criteria, Boulngar at el. (2006) and Polito (2001) criteria did not conform for the Basra soils.
2. Sensitivity value of Basra soils were estimated indirectly by using the unconfined compressive strength (q_u) and the liquidity index (LI). The result indicated that Basra soils are very sensitive and because of this, they can fail in lateral spreading and vertical deformation during earthquakes.

3. The measured SPT N values were used and the CSR and CRR were calculated in order to determine the factor of safety against liquefaction. According to the calculated FS values, Basra soils had a high liquefaction potential. The results of this analysis seemed to be contradicting because of the presence of the clay percentage in soils. Low FS value can also be due to the fact that SPT is more applicable to sandy soils not clays.
4. As suggested by Juang (2003), liquefaction severity index (Ls) and the liquefaction potential index (LPI) values for Basra soils were also calculated by using the SPT soundings. The calculated results indicated that the liquefaction severity index values for the study area fall in very low severity class. On the other hand, liquefaction potential index for $M_w = 7.5$ has a high liquefaction potential, whereas for $M_w 7.0$ and 6.5 the liquefaction potential is moderate. The liquefaction potential index for $M_w 6.0$ was found to be low. Since Basra soils consist of fine grained soils more than sands, it was expected not to have a high risk for liquefaction during earthquakes. But, in Basra region, both lateral spreadings and liquefaction made ground distortion could be the main problem during heavy earthquakes ($M_w \geq 6.5$).
5. The relationships between depth and SPT showed that the depth of soil below ground surface significantly affects the SPT N values. This is explained because of the increase in effective overburden pressure with the increase in confinement with depth below the ground surface. Conversely, because of the physical and mechanical nature and the mineralogy of the fine grained soils, no correlation between the Atterberg limits and SPT values was obtained.

6. Strong correlation between the shear strength parameters (c and ϕ) and the SPT values of Basra soil was obtained. The findings indicated that SPT values can be used for predicting the shear strength parameters of silty clays. The correlation obtained between SPT and the internal friction angle, ϕ in this study was compared with the findings of Peck et al. (1974) and Hatanaka et al. (1996). The results indicated that the correlation obtained in this study gave more conservative results than the other two studies.
7. Based on (Sanglerat, 1972; Nixon, 1982 and Decourt, 1990) and the findings in this study, there is no consistent correlation between the S_u values obtained in this study and the S_u values obtained in the others studies.
8. The prediction of cone penetration resistance q_c from the measured SPT values according to Abbas (2014), Kara (2010) and Fauzi (2015) gave contradictory results. The q_c values obtained for Basra soils by using the correlations suggested by these studies were inconsistent and not dependable. Therefore, the prediction of q_c from SPT is not promising and direct measurement of q_c is needed.

REFERENCES

- Abbas. S. A., Juhlin, C., & Malemir, A. (2014). A reliable correlation of SPT-CPT data for southwest of Sweden. *Electronic Journal of Geotechnical Engineering, 19*, 1013-1032.
- Al Moosawi, H. (1978). Seismic Zoning Considerations in Iraq. *Master Thesis*, University of Baghdad.
- Alsinawi, S. A. (2001). Seismological considerations of the Eastern Arab region. *In Proceedings of the Euro Mediterranean Seminar on Natural, Environmental and Technological Disasters*. Algeria.
- Alsinawi, S. A., & Al-Eqabi, G. (1978). Induced Microearthquake Activity in the Mishraq Sulphur Mine. Proc. 5th *Iraq Geology Congress*. Baghdad, In Press.
- Alsinawi, S. A., & Ghalib, H. A. (1975a). *Seismicity and Seismotectonic of Iraq*. *Bull. Coll. Sc.*, 16, 369-41.
- Alsinawi, S. A., & Qasrani, Z. A. (2003). Earthquake Hazard Considerations for Iraq. *Fourth International Conference of Earthquake Engineering and Seismology*, Republic of Iran.
- Alsinawi, S. L., & Mosawi, H. I. (1988). Seismic Zoning and other Seismic Parameters Consideration for Iraq. *British Stainless Steel Association*, 35, 185-192.

- Alsinawi, W., A., & Hamad, J. M. (1991). Seismicity of Al-Mashriq Area. *The conference on the Geodynamics development of the Arabian Lithosphere* ALYarmuk University- Erbid-Jordan.
- Bonn, D., Kellay, H., Tanaka, H., Wegdam, G., & Meunier, J. (1999). Laponite: What is the difference between a gel and a glass? *Langmuir*, 15(22), 7534-7536.
- Bray J. D., & Dashti S. (2004-a). Subsurface Characterization at Ground Failure Sites in Adapazari, Turkey. *Journal of Geotechnical and Geoenvironmental Engineering*, 130(7), 673-685.
- Bray, J. D., Sancio, R. B., Riemer, M. F., & Durgunoglu, T. (2004, January). Liquefaction susceptibility of fine-grained soils. In *Proc., 11th Int. Conf. on Soil Dynamics and Earthquake Engineering and 3rd Int. Conf. on Earthquake Geotechnical Engineering* (Vol. 1, pp. 655-662). Stallion Press, Singapore.
- Buday, T., & Jasim S. Z. (1987). The Regional Geology of Iraq, Tectonism, Magmatism and Metamorphism Vol 2. *Iraqi Geological Survey and Mineral Investigation Press*, Baghdad, 352.
- Buday, T. (1980). Regional Geology of Iraq: Vol.1, Stratigraphy and Palaeogeography. *GEOSURV*. Baghdad. 445.

- Cetin, K. O., Seed, R. B., Moss, R. E., Der Kiureghian, A., Tokimatsu, K., Harder Jr, L. F., & Kayen, R. E. (2000). Field case histories for SPT-based in situ liquefaction potential evaluation. *Journal of Geotechnical and Geoenvironmental Engineering Research Report*. University of California.
- Chen, C. J., & Juang, C. H. (2000). Calibration of SPT-and CPT-based liquefaction evaluation methods. *Geotechnical Special Publication*, 49-64.
- Coduto, D. P. D. P. (1999). *Geotechnical engineering: principles and practices* (No. Sirsi) i9780135763803).
- Craig, R. F. (1997). *Soil Mechanics*. E & FN SPON. London, UK.
- Das Braja, M. (1983). *Fundamentals of Soil Dynamics*.
- Das, B. M. (2010). *Geotechnical Engineering Handbook*. J. Ross Publishing.
- Diaz, D., Patakfalvi, R., Velasco-Arias, D., Rodriguez-Gattorno, G., & Santiago-Jacinto, P. (2008). Synthesis and direct interactions of silver colloidal nanoparticles with pollutant gases. *Colloid and Polymer Science*, 286(1), 67-77.
- Dixit, J., Dewaikar, D. M., & Jangid, R. S. (2012). Assessment of liquefaction potential index for Mumbai city. *Natural Hazards and Earth System Sciences*, 12(9), 2759-2768.

- Durgunoglu, H. T., & Bilsel, H. (2007). A Microzonation Study Based On Liquefaction and Cyclic Failure Potential of Fine-Grained Soils. *Fourth International Conference on Earthquake Geotechnical Engineering*, Greece.
- Durgunoglu, H. T., Yilmaz, O., Kalafat, M., Karadayilar, T., & Eser, M. (2004). An Integrated Approach for Characterization and Modeling of Soft Clays under Seismic Loading; A Case Study. *Proceeding 11th ICSD and 3th ICEGE*, 7-9.
- Elgamal, A., Yang, Z., Parra, E., & Ragheb, A. (2003). Modeling of cyclic mobility in saturated cohesionless soils. *International Journal of Plasticity*, 19(6), 883-905.
- Gallagher, P. M., & Mitchell, J. K. (2002). Influence of colloidal silica grout on liquefaction potential and cyclic undrained behavior of loose sand. *Soil Dynamics and Earthquake Engineering*, 22(9), 1017-1026.
- Gallagher, P. M., Conlee, C. T., & Rollins, K. M. (2007). Full-scale field testing of colloidal silica grouting for mitigation of liquefaction risk. *Journal of Geotechnical and Geoenvironmental Engineering*, 133(2), 186-196.
- Ghalib, H. A. A., Russell, D. R., & Kijiko, A. (1985). Optimal design of a seismological network for the Arabia ncountries, *Pure Appl. Geophys.* 122: 694–712.

- Goknur, E. (2009). Assessment of Liquefaction/Cyclic Failure Potential of Tuzla Soils. *Master of Science Thesis in civil Engineering, Eastern Mediterranean University, North Cyprus.*
- Gopal Madabhushi, S. P. (2007). Ground improvement methods for liquefaction remediation. *Proceedings of the Institution of Civil Engineers-Ground Improvement, 11(4)*, 195-206.
- Gratchev, I. B., Sassa, K., Osipov, V. I., Fukuoka, H., & Wang, G. (2007). Undrained cyclic behavior of bentonite–sand mixtures and factors affecting it. *Geotechnical and Geological Engineering, 25(3)*, 349-367.
- Hamada, M., Isoyama, R., & Wakamatsu, K. (1995). The Hyogoken-Nambu (Kobe) Earthquake, Liquefaction, Ground Displacement and Soil Condition in Hanshin Area. *Monograph Association for Development of Earthquake Prediction, School of Science and Engineering, Waseda University and Japan Engineering Consultants, Ltd., 194p.*
- Huang, Y., & Wang, L. (2016). Experimental studies on nanomaterials for soil improvement: a review. *Environmental Earth Sciences, 75(6)*, 1-10.
- Idriss, I. M., & Boulanger, R. W. (2006). Semi-empirical procedures for evaluating liquefaction potential during earthquakes. *Soil Dynamics and Earthquake Engineering, 26(2)*, 115-130.

- Ishihara, K. (1996). *Soil behaviour in earthquake geotechnics*. Clarendon Press; Oxford University Press.
- Ishihara, K. (1999). Terzaghi oration: Geotechnical aspects of the 1995 Kobe earthquake. In *Proceedings of* (Vol. 14, pp. 2047-2073).
- Iwasaki, T., Tokida, K., Tatsuoka, F., Watanabe, S., Yasuda, S., & Sato, H. (1982). Microzonation for soil liquefaction potential using simplified methods. In *Proceedings of the 3rd international conference on microzonation, Seattle* (Vol. 3, pp. 1310-1330).
- Jarushi, F., & AlKaabi, S. M. (2015). A New Correlation between SPT and CPT for Various Soils. *International Journal of Environmental, Ecological, Geological and Geophysical Engineering*, 9(2), 101-107.
- Jassim, S. Z., & Goff, J. C. (2006). *Geology of Iraq*. Dolin, Prague and Moravian Museum. Brno.
- Jennifer, D. L. (2007). *The liquefaction susceptibility, resistance, and response of silty and clayey soils*. ProQuest.
- Johnson, P. R., & Woldehaimanot, B. (2003). Development of the Arabian-Nubian Shield: perspectives on accretion and deformation in the northern East African Orogen and the assembly of Gondwana. *Geological Society, London, Special Publications*, 206(1), 289-325.

- Kara, O., & Gündüz, Z. (2010). Correlation between CPT and SPT in Adapazari, Turkey. *Sakarya Public Works and Settlement Directorate*, Sakarya, Turkey.
- Karim, K. H., Habib, H., & Raza, S. (2009). The lithology of the lower part of Qulqula Radiolarian Formation (Early Cretaceous), Kurdistan Region, NE Iraq. *Iraqi Bulletin of Geology and Mining*, 5, 9-24.
- Kishida, H. (1966). Damage to reinforced concrete buildings in Niigata city with special reference to foundation engineering. *Soils and Foundations*, 6(1), 71-88.
- Lee, D. H., Ku, C. S., & Yuan, H. (2004). A study of the liquefaction risk potential at Yuanlin, Taiwan. *Engineering Geology*, 71(1), 97-117.
- Lenz, J. A. (2007). *Statistical and Spatial Variability of Liquefaction Potential in Regional Mapping Using CPT, SPT and V (s) Data from the Oakland and Monterey Bay Areas, California*. ProQuest.
- Liao, S. S. C., Whitman, R. V. (1986-b). Catalogue of Liquefaction and Nonliquefaction Occurrences during Earthquakes, Res. Rep. Dept. of Civ. Eng., *Massachusetts Institute of Technology*, and Cambridge, Mass.
- López-Querol, S., & Blázquez, R. (2006). Liquefaction and cyclic mobility model for saturated granular media. *International journal for numerical and analytical methods in geomechanics*, 30(5), 413-439.

- Mitchell, J. K. (1993). *Fundamentals of Soil Behavior*. Second Edition, University Of California, Berkeley.
- Mitchell, R. A., & Kramer, S. L. (2006). Ground motion intensity measures for liquefaction hazard evaluation. *Earthquake Spectra*, 22(2), 413-438.
- Mollamahmutoglu, M., & Yilmaz, Y. (2010). Pre-and post-cyclic loading strength of silica-grouted sand. *Proceedings of the Institution of Civil Engineers-Geotechnical Engineering*, 163(6), 343-348.
- Mongondry, P., Tassin, J. F., & Nicolai, T. (2005). Revised state diagram of Laponite dispersions. *Journal of Colloid and Interface Science*, 283(2), 397-405.
- Mostafa, M. A. A. N. (2013). Reliability of using standard penetration test (SPT) in predicting properties of silty clay with sand soil. *International Journal of Civil and Structural Engineering*, 3(3), 545.
- Mourchid, A., Delville, A., Lambard, J., Lecolier, E., & Levitz, P. (1995). Phase diagram of colloidal dispersions of anisotropic charged particles: equilibrium properties, structure, and rheology of laponite suspensions. *Langmuir*, 11(6), 1942-1950.
- Nassaji, F., & Kalantari, B. (2011). SPT capability to estimate undrained shear strength of fine-grained soils of Tehran, Iran. *The Electronic Journal of Geotechnical Engineering*, 16.

- Nehlig, P., Fréour, G., Goër, A. , Huguet, D., Leyrit, H., Maroncle, J. L., Roger, J., Roig, J. Y., Surmely, F., Thiéblemont, D., & Vidal, N. (2002b) Geological map of Murat, explanatory Notes. *U.S Geology Survey*. In press.
- Olson, S. M., & Stark, T. D. (2002). Liquefied strength ratio from liquefaction flow failure case histories. *Canadian Geotechnical Journal*, 39(3), 629-647.
- Perlea, V. G., Pak, R. Y. S., & Yamamura, J. (2000). Liquefaction of cohesive soils. In Soil dynamics and liquefaction. *Proceedings of sessions of Geo-Denver American Society of Civil Engineers*, 107, 58-76.
- Polito C. (2001). Plasticity Based Liquefaction Criteria. *Proceedings of 4th IC on Recent Advances in Geotechnical Earthquake Engineering and Soil Dynamics*, Univ. of Missouri-Rolla, Rolla, Mo., 133.
- Rauch, A. F. (1998). An Empirical Method for Predicting Surface Displacements Due to Liquefaction-Induced Lateral Spreading in Earthquakes. *PhD Thesis*, Virginia Polytechnic Institute and State University.
- Robertson, P. K. (1990). Soil classification using the cone penetration test. *Canadian Geotechnical Journal*, 27(1), 151-158.
- Robertson, P. K. (2004). Evaluating soil liquefaction and post-earthquake deformations using the CPT. in *Proc. 2nd Int. Conf. on Site Characterization ISC* (Vol. 2, pp. 233-249).

- Robertson, P. K. (2009). Evaluation of flow liquefaction and liquefied strength using the cone penetration test. *Journal of Geotechnical and Geoenvironmental Engineering*, 136(6), 842-853.
- Robertson, P. K., & Fear, C. E. (1996). Soil liquefaction and its evaluation based on SPT and CPT. In *Proc. NCEER Workshop on Evaluation of Liquefaction Resistance*.
- Robertson, P. K., & Wride, C. E. (1998). Evaluating cyclic liquefaction potential using the cone penetration test. *Canadian Geotechnical Journal*, 35(3), 442-459.
- Rosenqvist, I. T. (1953). Considerations on the sensitivity of Norwegian quick clays. *Geotechnique*, 3(5), 195-200.
- Sancio, R. B., Bray, J. D., Stewart, J. P., Youd, T. L., Durgunoğlu, H. T., Önalp, A., & Karadayılar, T. (2002). Correlation between ground failure and soil conditions in Adapazari, Turkey. *Soil Dynamics and Earthquake Engineering*, 22(9), 1093-1102.
- Science Daily Nanoparticles. (2016, January 13). Retrieved from: <https://www.sciencedaily.com/terms/nanoparticle.htm>
- Seed, B. (1979). Soil Liquefaction and Cyclic Mobility Evaluation for Level Ground during Earthquakes. *Journal of Geotechnical and Geoenvironmental Engineering*, 105(ASCE 14380).

- Seed, H. B., & Idriss, I. M. (1971). Simplified procedure for evaluating soil liquefaction potential. *Journal of Soil Mechanics & Foundations Div.*, 97(9), 1249–1273.
- Seed, H. B., & Idriss, I. M. (1982). *Ground motions and soil liquefaction during earthquakes* (Vol. 5). Earthquake Engineering Research Institute.
- Seed, H. B., Idriss, I. M., & Arango, I. (1983). Evaluation of liquefaction potential using field performance data. *Journal of Geotechnical Engineering*, 109(3), 458-482.
- Seed, R. B., Cetin, K. O., Moss, R. E., Kammerer, A. M., Wu, J., Pestana, J. M., ... & Faris, A. (2003). Recent advances in soil liquefaction engineering: a unified and consistent framework. In *Proceedings of the 26th Annual ASCE Los Angeles Geotechnical Spring Seminar: Long Beach, CA*.
- Sladen, J. A., D'hollander, R. D., & Krahn, J. (1985). The liquefaction of sands, a collapse surface approach. *Canadian Geotechnical Journal*, 22(4), 564-578.
- Sonmez, H. (2003). Modification of the liquefaction potential index and liquefaction susceptibility mapping for a liquefaction-prone area (Inegol, Turkey). *Environmental Geology*, 44(7), 862-871.
- Sonmez, H., & Gokceoglu, C. (2005). A liquefaction severity index suggested for engineering practice. *Environmental Geology*, 48(1), 81-91.

- Taylor, R. (1990). Interpretation of the correlation coefficient: a basic review. *Journal of diagnostic medical sonography*, 6(1), 35-39.
- Terzaghi, K., & Peck, R. B. (1967). *Soil mechanics in engineering practice* (No. 624.151 T47 1967).
- U.S Geological Survey Science for a changing World. (2016, January 8). Retrieved from: <http://usgs.gov/earthquake/eqinthnews.htm>
- Wang, W. (1979). *Some findings in soil liquefaction*. Earthquake Engineering Department, Water Conservancy and Hydroelectric Power Scientific Research Institute. Beijing, China.
- Youd, T. L., & Perkins, D. M. (1978). Mapping liquefaction-induced ground failure potential. *Journal of the Soil Mechanics and Foundations Division*, 104(4), 433-446.
- Youd, T. L. (1998). *Screening guide for rapid assessment of liquefaction hazard at highway bridge sites*. Buffalo, New York: Multidisciplinary Center for Earthquake Engineering Research.

Youd, T. L., Idriss, I. M., Andrus, R. D., Arango, I., Castro, G., Christian, J. T., Dobry, R., Liam Finn, W. D., Harder, L. F., Hynes, M. E., Ishihara, K., Koester, J. P., Liao, S. S. C., Marcuson, W. F., Martin, G. R., Mitchell, J. K., Moriwaki, Y., Power, M. S., Robertson, P. K., Seed, R. B., & Stokoe, K. H. (2001). Liquefaction resistance of soils: summary report from the 1996 NCEER and 1998 NCEER/NSF workshops on evaluation of liquefaction resistance of soils. *Journal of Geotechnical and Geoenvironmental Engineering*, 127(10), 817-833.

APPENDICES

Appendix A: Laboratory Test Result



ANDREA
ENGINEERING TESTS LABORATORY
Website: www.andrealab.com Email: azadi@andrealab.com

SUMMARY OF TEST RESULTS

Borehole (1)

Site Western Breakwater/ Al-Faw Grand Port

Sheet 1 of 3

Borehole No. 1

Date July, 2014

Location of Specimen			Index Properties			Natural Water Content %	Dry Density KN/m ³	Specific Gravity	Strength Tests			Consolidation Test				Swelling Pressure kPa	Sieve Analysis % Passing No. 200	Chemical Test						
B.H. No.	Sample No.	Depth (m)	Sample Type	LL %	PL %				PI %	Unconfined Compression kPa	Triaxial Compression Cohesion kPa	Friction Angle	e ₀	P _c	C _c			C _r	SO ₃ %	TSS %	Cl %	OM %	PH	
1	1	1.5-2.0	DS												91.2	0.16	1.92	Nil	2.89	7.8				
	2	3.0-3.5	DS	41	22	19																		
	3	4.0-4.5	US				37.8	12.2	2.69	28				1.054	100	0.31	0.035	4		0.15	2.01	Nil	2.49	7.9
	4	6.0-6.5	DS	51	24	27																		
	5	7.5-8.0	DS																					
	6	8.0-8.5	US				36.4	13.0	2.70		13	0°	1.141	110	0.34	0.037								
	7	10.5-11.0	DS	54	27	27																		
	8	12.0-12.5	DS																					
	9	12.5-13.0	US				34.4	13.6	2.68	31				0.982	125	0.29	0.028							
	10	13.5-14.0	DS	47	23	24																		
	11	15.0-15.5	DS	44	21	23	31.6																	
	13	18.0-18.5	DS						2.70															
	15	21.0-21.5	DS	47	21	26	26.9																	
	17	24.0-24.5	DS	56	26	30	28.1																	



ANDREA
ENGINEERING TESTS LABORATORY
Website: www.andrealab.com Email: azadi@andrealab.com

		26.5-28.0	DS						2.66																
	19	27.0-27.5	DS	Non-Plastic																					



SUMMARY OF TEST RESULTS(2)

Borehole (2)

Site Western Breakwater/ Al-Faw Grand Port
Borehole No. 2

Sheet 2 of 3
Date July, 2014

Location of Specimen			Index Properties			Natural Water Content %	Dry Density KN/m ³	Specific Gravity	Strength Tests			Consolidation Test				Swelling Pressure kPa	Sieve Analysis % Passing No. 200	Chemical Test				
B.H. No.	Sample No.	Depth (m)	Sample Type	LL %	PL %				PI %	Unconfined Compression kPa	Triaxial Compression Cohesion kPa	Friction Angle	e ₀	P _c	C _c			C _r	SO ₃ %	TSS %	Cl %	OM %
2	1	1.5-2.0	DS												97.8							
	2	3.0-3.5	DS	46	22	24	39.5									0.15	1.64	Nil	1.78	7.8		
	3	4.5-5.0	US				38.4	13.9	2.70	22				1.087	95	0.34	0.055	7	92.1			
	4	6.0-6.5	DS	50	23	27																
	5	7.5-8.0	DS	52	24	28	37.6									0.17	2.04	Nil	2.99	8.0		
	6	9.0-9.5	DS						2.70							97.0						
	7	10.5-11.0	DS	47	21	26																
	8	12.0-12.5	US				40.5	12.6	2.69	19				0.964	110	0.29	0.047					
	9	13.5-14.0	DS													56.6						
	10	15.0-15.5	DS	43	19	24																
	12	18.0-18.5	US				37.3	13.8	2.70		21	0°	0.941	120	0.27	0.034						
	14	21.0-21.5	DS													96.2						
	15	22.5-23.0	DS	50	22	28	25.8															
	16	24.0-24.5	DS						2.68							55.3						



	17	26.5-26.0	DS													48.2				
	18	27.0-27.5	DS	40	22	18	22.1													



SUMMARY OF TEST RESULTS

Borehole (3)

Site WQ II - Mishrif Cl-13
Borehole No. 5

Sheet 5 of 6
Date April, 2014

Location of Specimen			Index Properties			Natural Water Content %	Dry Density KN/m ³	Specific Gravity	Strength Tests			Consolidation Test				Swelling Pressure kPa	Sieve Analysis % Passing No. 200	Chemical Test				
B.H. No.	Sample No.	Depth (m)	Sample Type	LL %	PL %				PI %	Unconfined Compression kPa	Triaxial Compression Cohesion kPa	Friction Angle	e ₀	P _c	C _c			C _r	SO ₃ %	TSS %	Cl %	OM %
5	1	1.5-2.0	DS				21.9								92.8	0.24	1.46		1.96	8.6		
	2	3.0-3.5	DS	35	18	17					0.982	100	0.33	0.035								
	3	4.5-5.0	DS	40	18	22	23.5	2.69							70.2							
	4	6.0-6.5	DS				29.2								95.1							
	6	9.0-9.5	DS	46	20	26																
	7	10.5-11.0	DS				28.6															
	8	12.0-12.5	DS	48	23	25		2.70			1.106	125	0.39	0.054						94.4		
	10	15.0-15.5	DS	52	25	27	23.3															
	12	18.0-18.5	DS												92.6							
	13	19.5-20.0	DS	56	25	31	25.2				0.805	145	0.27	0.048								
	15	22.5-23.0	DS												82.5							
	16	24.0-24.5	DS	55	23	32	24.7								93.0							
	18	27.0-27.5	DS	51	22	29																
	20	30.0-30.5	DS					2.72							91.2							

SUMMARY OF TEST RESULTS

Borehole (4)

Site WQ II - Mishrif CI-13

Borehole No. 6

Sheet 6 of 6

Date April 2014

Location of Specimen				Index Properties			Natural Water Content %	Dry Density KN/m ³	Specific Gravity	Strength Tests			Consolidation Test				Swelling Pressure kPa	Sieve Analysis % Passing No. 200	Chemical Test				
B.H. No.	Sample No.	Depth (m)	Sample Type	LL %	PL %	PI %				Unconfined Compression kPa	Triaxial Compression Cohesion kPa	Friction Angle	e ₀	P _c	C _c	C _r			SO ₃ %	TSS %	Cl %	OM %	PH
6	1	1.5-2.0	DS	39	18	21																	
	2	3.0-3.5	DS				25.0																
	3	4.5-5.0	DS	33	15	18		2.70															
	4	6.0-6.5	DS				26.7																
	5	7.5-8.0	DS	31	13	18				0.912	115	0.31	0.042										
	7	10.5-11.0	DS				29.2																
	8	12.0-12.5	DS	38	17	21																	
	10	15.0-15.5	DS					2.70															
	11	16.5-17.0	DS	37	18	19	25.4																
	13	19.5-20.0	DS							0.763	140	0.29	0.047										
	15	25.5-26.0	DS				23.6																
	17	27.0-27.5	DS	54	22	32																	
	18	30.0-30.5	DS					2.72															
	20	30.0-30.5	DS	55	21	34	22.4																

SUMMARY OF TEST RESULTS

Borehole(5)

Site New Transformer/Fao Station

Borehole No. 2

Sheet 2 of 3

Date June, 2014

Location of Specimen				Index Properties			Natural Water Content %	Dry Density KN/m ³	Specific Gravity	Strength Tests			Consolidation Test				Swelling Pressure kPa	Sieve Analysis % Passing No. 200	Chemical Test				
B.H. No.	Sample No.	Depth (m)	Sample Type	LL %	PL %	PI %				Unconfined Compression kPa	Triaxial Compression Cohesion kPa	Friction Angle	e ₀	P _c	C _c	C _r			SO ₃ %	TSS %	Cl %	OM %	PH
2	1	0.0-0.5	DS	48	21	27																	
	2	2.0-2.5	US				39.8	11.9	2.70	11	0°	1.134	95	0.31	0.047	0	98.2	0.28	5.61	0.62	2.43	8.0	
	3	4.0-4.5	DS														96.9						
	4	6.0-6.5	US	51	22	29	40.2	11.6	2.71	14		1.282	100	0.36	0.056	0		0.24	5.88	0.76	2.07	8.1	
	5	8.0-8.5	DS	53	23	30																	
	6	10.0-10.5	DS														95.7						
	7	12.0-12.5	DS	41	18	23	34.9																
	8	15.0-15.5	DS					2.70									98						
	9	18.0-18.5	DS	43	19	24	32.8																
	10	21.0-21.5	DS														90.3						
	11	24.0-24.5	DS	43	20	23											92.8						
	12	27.0-27.5	DS	45	21	24	26.4																
	13	30.0-30.5	DS					2.71									97.1						
	14	34.0-34.5	DS	49	20	29	23.6																
	15	38.0-38.5	DS														96.8						
	16	42.0-42.5	DS	47	22	25	24.7										73.4						
	17	46.0-46.5	DS	Non Plastic			20.6	15.8		0	38°*						16.3						
	18	50.0-50.5	DS	Non Plastic				2.67															

* Remolded Sample

SUMMARY OF TEST RESULTS

	19	55.0-55.5	DS														79.2					
	20	60.0-60.5	DS	Non Plastic			21.4	15.5		0	41°*											

SUMMARY OF TEST RESULTS

Borehole (6)

Site New Transformer/Fao Station
Borehole No. 3

Sheet 3 of 3
Date June 2014

Location of Specimen			Index Properties			Natural Water Content %	Dry Density KN/m ³	Specific Gravity	Strength Tests			Consolidation Test				Swelling Pressure kPa	Sieve Analysis % Passing No. 200	Chemical Test				
B.H. No.	Sample No.	Depth (m)	Sample Type	LL %	PL %				PI %	Unconfined Compression kPa	Triaxial Compression Cohesion kPa	Friction Angle	e ₀	P _c	C _c			C _r	SO ₃ %	TSS %	Cl %	OM %
3	1	0.0-0.5	DS	54	23	31																
	2	2.0-2.5	US				37.9	12.3	2.71	12	0°	0.993	90	0.44	0.067	0	96.3	0.33	7.81	0.53	5.63	8.2
	3	4.0-4.5	DS	52	23	29																
	4	6.0-6.5	US				39.2	11.8	2.70	17		1.194	100	0.40	0.059	0	98.1					
	5	8.0-8.5	DS	54	24	30											0.21	6.24	0.69	2.71	8.0	
	6	10.0-10.5	DS														56.3					
	7	12.0-12.5	DS	47	21	26	35.6															
	8	15.0-15.5	DS														52.4					
	9	18.0-18.5	DS	38	18	20	31.8															
	10	21.0-21.5	DS						2.70								95.3					
	11	24.0-24.5	DS	44	19	25	27.5										96.0					
	12	27.0-27.5	DS	46	22	24																
	13	30.0-30.5	DS				24.9										89.6					
	14	34.0-34.5	DS						2.67								49.2					
	15	38.0-38.5	DS	38	21	17	22.8	15.4		8	27°*											
	16	42.0-42.5	DS	42	23	19											64.3					
	17	46.0-46.5	DS	Non Plastic					2.66													
	18	50.0-50.5	DS														25.8					

* Remolded Sample

SUMMARY OF TEST RESULTS

	19	55.0-	DS	Non Plastic			19.8	15.9			0	38°*										
	20	60.0-60.5	DS						2.65								18.7					

SUMMARY OF TEST RESULTS

Borehole (7)

Site Borehole Al Basra Governorate Building
No. 2

Sheet 2 of 4
Date August 2013

Location of Specimen			Index Properties			Natural Water Content %	Dry Density KN/m ³	Specific Gravity	Strength Tests			Consolidation Test				Swelling Pressure kPa	Sieve Analysis % Passing No. 200	Chemical Test				
B.H. No.	Sample No.	Depth (m)	Sample Type	LL %	PL %				PI %	Unconfined Compression kPa	Triaxial Compression Cohesion kPa	Friction Angle	e ₀	P _c	C _c			C _r	SO ₃ %	TSS %	Cl %	OM %
2	1	1.0-1.5	US				21.9	15.1		34	3°					94.8						
	2	3.0-3.5	US	45	21	24	23.8	14.5	2.70	46		0.762	80	0.22	0.034	17	1.22	7.92	1.09	5.37	8.2	
	3	5.0-5.5	DS													96.2						
	4	7.0-7.5	DS	44	23	21																
	5	9.5-1.0	US				30.8	13.8	2.69	21	0°	0.932	95	0.34	0.053		0.87	4.65	0.76	4.39	8.0	
	6	12.0-12.5	DS													97.1						
	7	14.5-15.0	US				26.2	14.9	2.71	108		0.626	125	0.21	0.039		91.5					
	8	16.5-17.0	DS	48	22	24																
	9	18.5-19.0	DS	37	21	16	23.7									39.8						
	10	21.0-21.5	DS													20.8						
	11	24.0-24.5	DS	Non-Plastic																		
	12	27.0-27.5	DS						2.66							15.7						
	13	30.0-30.5	DS	Non-Plastic			20.9															



SUMMARY OF TEST RESULTS

Borehole (8)

Site Borehole No. Al Basra Governorate Building
3

Sheet 3 of 4
Date August, 2013

Location of Specimen			Index Properties			Natural Water Content %	Dry Density KN/m ³	Specific Gravity	Strength Tests			Consolidation Test				Swelling Pressure kPa	Sieve Analysis % Passing No. 200	Chemical Test								
B.H. No.	Sample No.	Depth (m)	Sample Type	LL %	PL %				PI %	Unconfined Compression kPa	Triaxial Cohesion kPa	Friction Angle	e ₀	P _c	C _c			C _r	SO ₃ %	TSS %	Cl %	OM %	PH			
	3	1	1.5-2.0	US	53	24	29	22.4	14.8																	
		2	3.0-3.5	US				24.2	14.3	2.71	57				0.699	80	0.19	0.039	14	95.2	1.18	7.44	1.31	5.36	8.3	
		3	5.0-5.5	DS																	98.4	0.06	5.62	0.84	6.02	8.0
		4	7.0-7.5	DS	59	28	31																			
		5	9.5-10.5	DS																	97.0					
		6	12.0-12.5	US				30.1	13.4	2.70	52				0.879	105	0.29	0.044								
		7	14.0-14.5	DS	50	23	27																			
		8	15.5-16.0	DS	46	20	26																			
		9	18.0-18.5	US				25.2	15.3	2.72	148				0.561	145	0.16	0.041		95.6						
		10	19.5-20.0	DS																	41.7					
		11	21.0-21.5	DS	36	19	17																			
		12	24.0-24.5	DS						2.68											27.2					
		13	27.0-27.5	DS	Non-Plastic			21.4																		
		14	30.0-30.5	DS																	30.7					



SUMMARY OF TEST RESULTS

Site

Shatt Al-Basara Power Plant

Borehole (9)

Borehole No. 1

Sheet 1 of 4

Date Aug., 2014

Location of Specimen			Index Properties			Natural Water Content %	Dry Density KN/m ³	Specific Gravity	Strength Tests			Consolidation Test				Swelling Pressure kPa	Sieve Analysis % Passing No. 200	Chemical Test									
B.H. No.	Sample No.	Depth (m)	Sample Type	LL %	PL %				PI %	Unconfined Compression kPa	Triaxial Cohesion kPa	Friction Angle	e ₀	P _c	C _c			C _r	SO ₃ %	TSS %	Cl %	OM %	PH				
	1	1	0.0-0.5	DS																	97.8						
		2	1.5-2.0	US	58	25	33	29.0	14.2	2.71	23	0°	0.891	80	0.38	0.057	16				96.9	0.31	5.36	0.16	4.57	7.8	
		3	3.0-3.5	DS																							
		4	4.5-5.0	US				35.1	13.5	2.70	35				0.962	85	0.31	0.048									
		5	6.0-6.5	DS	54	26	28															0.37	5.82	0.14	2.94	7.9	
		6	7.5-8.0	US				38.8	13.7	2.71	29				1.198	100	0.37	0.052		97.1							
		7	9.0-9.5	DS	44	20	24																				
		8	11.0-11.5	DS				30.9														94.0					
		9	13.0-13.5	DS						2.67												39.7					
		10	15.0-15.5	DS	42	19	23	22.7																			
		11	18.0-18.5	DS																		46.3					
		12	21.0-21.5	DS	45	21	24	25.8																			
		13	24.0-24.5	DS						2.66												20.4					
		14	27.0-27.5	DS	Non Plastic																						
		15	30.0-30.5	DS	48	22	26	24.7														94.9					

SUMMARY OF TEST RESULTS

Site Shatt Al-Basara Power Plant Borehole (10) Sheet 3 of 4
Borehole No. 3 Date Aug., 2014

Location of Specimen			Index Properties			Natural Water Content %	Dry Density KN/m ³	Specific Gravity	Strength Tests			Consolidation Test				Swelling Pressure kPa	Sieve Analysis % Passing No. 200	Chemical Test				
B.H. No.	Sample No.	Depth (m)	Sample Type	LL %	PL %				PI %	Unconfined Compression kPa	Triaxial Cohesion kPa	Friction Angle	e ₀	P _c	C _c			C _r	SO ₃ %	TSS %	Cl %	OM %
3	1	0.0-0.5	DS	53	25	28									98.4	0.34	6.16	0.17	4.13	7.9		
	2	2.0-2.5	US				33.7	13.9	2.70	36					1.186	85	0.36	0.069	21			
	3	4.0-4.5	DS	56	26	30										0.31	4.56	0.15	3.85	7.9		
	4	6.0-6.5	US				35.5	13.7	2.70	27					0.976	95	0.32	0.064				
	5	8.0-8.5	DS	45	22	23										0.28	5.61	Nil	2.33	8.0		
	6	10.0-10.5	US				38.7	12.9	2.71		11	0°	1.078	100	0.38	0.059						
	7	12.0-12.5	DS	49	23	26																
	8	15.0-15.5	DS	Non Plastic			21.5									36.4						
	9	18.0-18.5	DS													92.1						
	10	21.0-21.5	DS	51	23	28	25.9															
	11	24.0-24.5	DS	Non Plastic																		
	12	27.0-27.5	DS					2.67								22.6						
	13	30.0-30.5	DS	42	20	22	24.7															
	14	35.0-35.5	DS													87.3						

SUMMARY OF TEST RESULTS

Site BWSIP Borehole (11) Sheet 3 of 4
Borehole No. 3 Date Oct. 2015

Location of Specimen			Index Properties			Natural Water Content %	Dry Density KN/m ³	Specific Gravity	Strength Tests		Consolidation Test				Swelling Pressure kPa	Coefficient of Permeability KV m/sec	Sieve Analysis % Passing No. 200	Chemical Test				
B.H. No.	Sample No.	Depth (m)	Sample Type	LL %	PL %				PI %	Unconfined Compression kPa	Pocket Penetrometer Test Kg/cm ²	e ₀	P _c	C _c				C _r	SO ₃ %	TSS %	Cl %	OM %
3	1	1.5-2.0	DS												97.2	1.39	4.52	0.43	3.37	7.7		
	2	3.0-3.5	US				40.1	12.5	2.70	0.28	1.298	70	0.39	0.071	7	98.0						
	3	4.5-5.0	DS	41	21	20																
	4	6.0-6.5	US				35.9	13.4	2.70	26	0.23	0.992	90	0.31	0.043	7.93x10 ⁻⁹	95.3	0.11	1.04	0.03	2.95	7.9
	5	7.5-8.0	DS	49	24	25																
	6	9.0-9.5	US				31.7	13.8		37	0.46					88.1						
	7	11.0-11.5	DS	46	22	24										90.4						
	8	13.0-13.5	DS	33	18	15										76.6						
	9	15.0-15.5	DS																			
	10	15.5-16.0	US				26.3	14.8		118	1.49											
	11	17.0-17.5	DS	37	18	19										80.2						
	12	19.0-19.5	DS	34	18	16			2.68													
	13	19.5-20.0	US				25.1									7.24x10 ⁻⁶						
	14	21.0-21.5	DS	43	20	23										86.5						
	15	23.0-23.5	DS													91.4						
	16	25.0-25.5	DS	47	23	24																



SUMMARY OF TEST RESULTS
Borehole (12)

Site BWSIP
Borehole No. 4

Sheet 4 of 4
Date Oct. 2015

Location of Specimen			Index Properties			Natural Water Content %	Dry Density KN/m ³	Specific Gravity	Strength Tests		Consolidation Test				Swelling Pressure kPa	Coefficient of Permeability kv m/sec	Sieve Analysis % Passing No. 200	Chemical Test				
B.H. No.	Sample No.	Depth (m)	Sample Type	LL %	PL %				PI %	Unconfined Compression kPa	Pocket Penetrometer Test Kg/cm ²	e ₀	P _c	C _c				C _r	SO ₃ %	TSS %	Cl %	OM %
4	1	1.5-2.0	DS												97.9							
	2	3.0-3.5	US	48	24	24	38.4	12.4	2.70	22	0.25	1.112	85	0.37	0.069	8	6.33x10 ⁻⁹	0.13	0.48	0.04	2.86	7.8
	3	4.5-5.0	DS															98.1				
	4	6.0-6.5	US	45	22	23	36.5	13.2		26	0.29							0.11	0.41	0.03	1.82	7.9
	5	7.5-8.0	DS	43	21	22																
	6	9.0-9.5	US				34.7	13.9		44	0.51							92.4				
	7	11.0-11.5	DS	44	23	21																
	8	11.5-12.0	US				28.2				0.83							64.8				
	9	13.0-13.5	DS	47	22	25																
	10	15.0-15.5	DS															91.7				
	11	17.0-17.5	DS	45	21	24												63.5				
	12	17.5-18.0	US				26.4										3.65x10 ⁻⁷					
	13	19.0-19.5	DS	59	26	33																
	14	21.0-21.5	DS	48	23	25	22.9															
	15	23.0-23.5	DS						2.69									85.3				
	16	25.0-25.5	DS															89.2				



SUMMARY OF TEST RESULTS

Borehole (13)
Site WQ (II) EPF Power Plant
Borehole No. 32

Sheet 6 of 13
Date Oct. 2013

Location of Specimen			Index Properties			Natural Water Content %	Dry Density KN/m ³	Specific Gravity	Strength Tests			Consolidation Test				Swelling Pressure kPa	Sieve Analysis % Passing No. 200	Chemical Test				
B.H. No.	Sample No.	Depth (m)	Sample Type	LL %	PL %				PI %	Unconfined Compression kPa	Triaxial Compression Cohesion kPa	Friction Angle	e ₀	P _c	C _c			C _r	SO ₃ %	TSS %	Cl %	OM %
32	1	1.5-2.0	DS	48	22	26										0.24	0.76	0.18	2.46	8.4		
	2	3.0-3.5	US				34.2	13.6	2.70	22	0°	0.847	70	0.31	0.046	21	99.0					
	3	4.5-5.0	DS	56	23	33											95.4					
	4	6.0-6.5	US				31.7	13.7	2.71	51		0.920	75	0.34	0.039	33		0.45	2.48	0.69	1.95	8.4
	5	7.5-8.0	DS	54	20	34																
	6	9.0-9.5	US				27.5	14.7		63												
	8	13.0-13.5	DS															96.3				
	9	15.0-15.5	DS	39	23	16																
	10	17.0-17.5	DS															84.1				
	11	19.0-19.5	DS	Non Plastic			20.8															
	13	24.0-24.5	DS						2.67									11.2				
	14	27.0-27.5	DS	Non Plastic																		
	15	30.0-30.5	DS															15.8				



SUMMARY OF TEST RESULTS

Borehole (14)
Site WQ (II) EPF Power Plant
Borehole No. 35

Sheet 9 of 13
Date Oct., 2013

Location of Specimen			Index Properties			Natural Water Content %	Dry Density KN/m ³	Specific Gravity	Strength Tests			Consolidation Test				Swelling Pressure kPa	Sieve Analysis % Passing No. 200	Chemical Test					
B.H. No.	Sample No.	Depth (m)	Sample Type	LL %	PL %				PI %	Unconfined Compression kPa	Triaxial Compression Cohesion kPa	Friction Angle	e _s	P _c	C _c			C _r	SO ₂ %	TSS %	Cl %	OM %	PH
35	1	1.5-2.0	DS												97.1								
	2	3.0-3.5	US	56	25	31	31.6	14.0	2.71		32	2*	0.889	75	0.29	0.037	16		0.46	1.32	0.39	2.51	8.4
	3	4.5-5.0	DS																90.2				
	4	6.0-6.5	US				30.3	13.7	2.70	52			0.903	85	0.32	0.041							
	5	7.5-8.0	DS	50	21	29													0.37	1.18	0.32	2.68	8.2
	6	9.0-9.5	DS																89.7				
	7	11.0-11.5	DS	54	23	31	25.8																
	8	13.0-13.5	DS	38	21	17													38.5				
	10	17.0-17.5	DS						2.68										27.3				
	12	21.0-21.5	DS	51	22	29	23.8																
	14	27.0-27.5	DS																83.5				



SUMMARY OF TEST RESULTS

Site Cluster 6Y at WQ (II)
Borehole No. 1B

Borehole (15)

Sheet 3 of 7
Date Dec., 2014

Location of Specimen			Index Properties			Natural Water Content %	Dry Density KN/m ³	Specific Gravity	Strength Tests			Consolidation Test				Swelling Pressure kPa	Sieve Analysis % Passing No. 200	Chemical Test					Coefficient of Permeability kv m/sec
B.H. No.	Sample No.	Depth (m)	Sample Type	LL %	PL %				PI %	Unconfined Compression kPa	Triaxial Compression Cohesion kPa	Friction Angle	e _s	P _c	C _c			C _r	SO ₂ %	TSS %	Cl %	OM %	
1B	1	0.5-1.0	DS												0.37	2.42	0.13	2.43	8.1				
	2	1.5-2.0	DS	54	23	31																	
	3	3.0-3.5	US				28.4	14.3	2.71	52			0.859	110	0.29	0.053	21					3.12 X 10 ⁻⁸	
	4	4.5-5.0	DS	57	24	33													0.34	1.18	0.11	3.81	8.2
	5	6.0-6.5	US				28.8	14.6		33	0*								90.4				
	6	7.5-8.0	DS	52	25	27													0.46	1.98	0.17	3.42	8.1
	7	9.0-9.5	US				26.7	14.8		89									93.6				
	8	12.0-12.5	DS																21.2				
	9	15.0-15.5	US	Non plastic			23.1	14.7		0	33***												
	10	18.0-18.5	DS					2.67											26.3				
	11	21.0-21.5	US	Non plastic			21.8	15.0		0	37***												
	12	24.0-24.5	DS	86	29	37																	
	13	27.0-27.5	US				24.6	15.4		174									91.8				
	14	30.0-30.5	DS																94.9				
	15	33.0-33.5	US				25.2	15.8		98	6.5**												
	16	36.0-35.5	DS	61	26	35																	

*CU Triaxial Test
**Direct Shear Test



SUMMARY OF TEST RESULTS

Site Cluster 6Y at WQ (II)

Borehole (16)

Sheet 5 of 7

Borehole No. 3B

Date Dec. 2014

Location of Specimen			Index Properties			Natural Water Content %	Dry Density KN/m ³	Specific Gravity	Strength Tests			Consolidation Test				Swelling Pressure kPa	Sieve Analysis % Passing No. 200	Chemical Test					Coefficient of Permeability KV m/sec
B.H. No.	Sample No.	Depth (m)	Sample Type	LL %	PL %				PI %	Unconfined Compression kPa	Triaxial Cohesion kPa	Triaxial Friction Angle	e ₀	P _c	C _c			C _r	SO ₃ %	TSS %	Cl %	OM %	
3B	1	0.5-1.0	DS	50	24	26																	
	2	1.5-2.0	DS												95.2	0.43	2.02	0.14	3.36	8.0			
	3	3.0-3.5	US				27.8	14.8	2.70	53				0.873	105	0.27	0.051	19					
	4	4.5-5.0	DS	41	19	22										0.82	2.92	0.23	3.49	7.9			
	5	6.0-6.5	US				28.9	14.3		38	0°					88.5							
	6	7.5-8.0	DS	39	18	21										91.7							
	7	9.0-9.5	US				29.2	14.8		34													
	8	12.0-12.5	DS													16.8							
	9	15.0-15.5	US	Non plastic			28.2	14.7		0	34°**												
	10	18.0-18.5	DS													91.4							
	11	21.0-21.5	US	47	22	25	28.6	15.2	2.70	148				0.738	145	0.21	0.038						8.67 X 10 ⁻⁹
	12	24.0-24.5	DS													96.0							
	13	27.0-27.5	US	49	23	26	25.0	15.6		82	4.5°**												
	14	30.0-30.5	DS	67	26	41																	
	15	33.0-33.5	US				23.5	15.8		183													
	16	35.0-35.5	DS													72.8							

*CU Triaxial Test
**Direct Shear Test



SUMMARY OF TEST RESULTS

Borehole (17)

Site BW S I P - P3

Borehole No. 15

Sheet 15 of 25

Date Dec. 2014

Location of Specimen			Index Properties			Natural Water Content %	Dry Density KN/m ³	Specific Gravity	Strength Tests			Consolidation Test				Swelling Pressure kPa	Sieve Analysis % Passing No. 200	Chemical Test						
B.H. No.	Sample No.	Depth (m)	Sample Type	LL %	PL %				PI %	Unconfined Compression kPa	Direct Shear		e ₀	P _c	C _c			C _r	SO ₃ %	TSS %	Cl %	OM %	PH	
15	1	2.5-3.0	US	40	28	12	35.2	12.9		14	2°					58.6								
	2	5.0-5.5	DS													91.3								
	3	7.5-8.0	US	42	20	22	33.4	13.6	2.70	40				0.902	105	0.28	0.033	10		0.12	0.56	Nil	3.76	7.8
	4	10.0-10.5	DS													72.4								
	5	12.5-13.0	US				31.8	13.5	2.70	38	23	0°		0.937	120	0.31	0.044							
	6	15.0-15.5	DS	34	16	18										80.4								
	7	17.5-18.0	US	36	17	19	27.7	14.2		5	11°					54.7								
	8	20.0-20.5	DS	45	24	21										86.3								
	9	22.5-23.0	US	49	25	24	26.4	14.9	2.68					0.815	145	0.22	0.041							
	10	25.0-25.5	DS																					
	11	27.5-28.0	US				29.2	14.0		157														
	12	30.0-30.5	DS	37	25	12																		
	13	32.0-32.5	DS				23.8									75.2								



SUMMARY OF TEST RESULTS

Borehole (18)

Site BWSLP-P3

Borehole No. 19

Sheet 19 of 25

Date Dec. 2014

Location of Specimen			Index Properties			Natural Water Content %	Dry Density KN/m ³	Specific Gravity	Strength Tests			Consolidation Test				Swelling Pressure kPa	Sieve Analysis % Passing No. 200	Chemical Test						
B.H. No.	Sample No.	Depth (m)	Sample Type	LL %	PL %				PI %	Unconfined Compression kPa	Triaxial Compression Cohesion kPa	Friction Angle	e ₀	P _c	C _c			C _r	SO ₃ %	TSS %	Cl %	OM %	PH	
19	1	2.5-3.0	US	45	20	25	38.2	12.6	2.70	28				1.238	85	0.39	0.056	8						
	2	5.0-5.5	DS																97.1					
	3	7.5-8.0	US	38	17	21	37.6	13.1		18	0°								0.06	0.60	Nil	2.35	7.9	
	4	10.0-10.5	DS																89.2					
	5	12.5-13.0	US	42	19	23	35.8	12.8	2.70	33				0.912	120	0.31	0.049							
	6	15.0-15.5	DS																74.5					
	7	17.5-18.0	DS	40	18	22	28.4																	
	8	20.0-20.5	DS																96.4					
	9	22.5-23.0	US				25.7	15.0	2.71	148				0.794	150	0.23	0.046							
	10	25.0-25.5	DS	51	23	28																		
	11	27.5-28.0	US	35	16	19	24.1	15.6		167									93.9					
	12	30.0-30.5	DS						2.67										41.3					
	13	32.0-32.5	DS	37	20	17																		



SUMMARY OF TEST RESULTS

Site Cluster 4Y at WQ (II)

Borehole No. 2B

Borehole (19)

Sheet 4 of 7

Date Dec. 2014

Location of Specimen			Index Properties			Natural Water Content %	Dry Density KN/m ³	Specific Gravity	Strength Tests			Consolidation Test				Swelling Pressure kPa	Sieve Analysis % Passing No. 200	Chemical Test					Coefficient of Permeability KV m/sec		
B.H. No.	Sample No.	Depth (m)	Sample Type	LL %	PL %				PI %	Unconfined Compression kPa	Triaxial Compression Cohesion kPa	Friction Angle	e ₀	P _c	C _c			C _r	SO ₃ %	TSS %	Cl %	OM %		PH	
2B	1	0.5-1.0	DS	52	24	28													98.0						
	2	1.5-2.0	DS																						
	3	3.0-3.5	US				29.0	14.0	2.71	47				0.844	115	0.28	0.033	17		0.49	2.16	0.16	1.83	8.1	
	4	4.5-5.0	DS	56	23	33													90.8						
	5	6.0-6.5	US				30.4	14.2	2.70	40				0.892	125	0.25	0.031								2.27 X 10 ⁻⁸
	6	7.5-8.0	DS																91.4						
	7	8.0-9.5	US	45	19	26	29.7	13.5		23	0°														
	8	12.0-12.5	DS	48	22	26													90.2						
	9	15.0-15.5	US				28.3	14.7		36	5°								72.9						
	10	18.0-18.5	DS	32	15	17																			
	11	21.0-21.5	US				23.4	15.3		4	29°														
	12	24.0-24.5	DS	34	16	18													47.8						
	13	27.0-27.5	US				19.8	15.8		0	33.5°														
	14	30.0-30.5	DS						2.69										64.6						
	15	33.0-33.5	US				22.7	15.4		184															
	16	36.0-36.5	DS	43	20	23																			

*CU Triaxial Test
**Direct Shear Test



SUMMARY OF TEST RESULTS

Site Cluster 4Y at WQ (II)
Borehole No. 3B

Borehole (20)

Sheet 5 of 7
Date Dec., 2014

Location of Specimen			Index Properties			Natural Water Content %	Dry Density KN/m ³	Specific Gravity	Strength Tests			Consolidation Test				Swelling Pressure kPa	Sieve Analysis % Passing No. 200	Chemical Test					Coefficient of Permeability kv m/sec
B.H. No.	Sample No.	Depth (m)	Sample Type	LL %	PL %				PI %	Unconfined Compression kPa	Triaxial Cohesion kPa	Compression Friction Angle	e _c	P _c	C _c			C _v	SO ₃ %	TSS %	Cl %	OM %	
3B	1	0.5-1.0	DS												90.7								
	2	1.5-2.0	DS	46	21	25										0.61	2.96	0.21	2.08	8.1			
	3	3.0-3.5	US				29.8	14.0		24	0°				95.8								
	4	4.5-5.0	DS	48	22	26										0.55	2.92	0.19	1.95	8.2			
	5	6.0-6.5	US				28.7	14.2	2.70	61		0.879	125	0.25	0.038	9						4.12 X 10 ⁻⁸	
	6	7.5-8.0	DS	47	26	21																	
	7	9.0-9.5	US				32.9	13.2		58						89.2							
	8	12.0-12.5	DS	49	22	27																	
	9	15.0-15.5	US	51	22	29	35.2	12.9	2.70	23		1.008	140	0.32	0.053								
	10	18.0-18.5	DS													97.1							
	11	21.0-21.5	US				29.4	14.1		43	4.5*												
	12	24.0-24.5	DS	57	24	33										75.8							
	13	27.0-27.5	US				25.7	14.9		149													
	14	30.0-30.5	DS	46	22	24										70.7							
	15	33.0-33.5	US				28.2	15.2		81	5.5***												
	16	35.0-35.5	DS	38	21	17			2.67							46.4							

*CU Triaxial Test
**Direct Shear Test

Appendix B: Borehole Logs



Borehole (1)

Site Western Breakwater /Al-Faw Grand Port Method of Boring Rotary
 Borehole No. 1 Ground Level+6.00 Date 02/07/2014

Water Table Level	Depth (m)	Sample Type & Depth	Litho logy	Thickness of Layer (m)	Soil Description	SPT Value N-Value					Remarks			
						20	40	60	80	100				
1.40	1.0			6.0	Soft to very soft brown to grayish brown lean Silty CLAY with little fine grained Sand in parts and reddish rusty traces of iron oxide compounds together with black spots of organic matter and white tiny marine shell pieces						1.0	(1)		
	1.5	D										2.0	(1)	
	2.0													
	3.0	D												
	4.0	U												
	5.0													
	6.0	D		5.0	Very soft brown to dark grayish brown fat Silty CLAY with reddish rusty traces of iron oxide compounds and black spots of organic matter together with white tiny marine shell pieces						6.0	(1)		
	7.0	D										7.0	(1)	
	7.5													
	8.0	U												
	9.0				4.0	Very soft to soft gray to brownish dark gray Sandy lean Silty CLAY with yellowish rusty traces of iron oxide compounds and black spots of organic matter						9.0	(1)	
	10.0													
	10.5	D												
	11.0													
	12.0			19.5	Soft to medium greenish gray to greenish dark gray lean Silty CLAY with white tiny marine shell pieces and black spots of organic matter						12.0	(2)		
	12.5													
	13.0	U												
	13.5	D												
	14.0			8.0	Medium to stiff grayish green Sandy fat Silty CLAY with black spots of organic matter						14.0	(4)		
	15.0	D												
16.0														
16.5	D													
17.0			21.0	Very dense gray to greenish gray fine grained Silty SAND with white tiny marine shell pieces						17.0	(4)			
18.0	D													
18.5														
19.0	D													
20.0			2.5	Very dense gray to greenish gray fine grained Silty SAND with white tiny marine shell pieces						20.0	(8)			
21.0	D													
22.0														
22.5	D													
23.0			2.0	Very dense gray to greenish gray fine grained Silty SAND with white tiny marine shell pieces						23.0	(13)			
24.0	D													
25.0														
25.5	D													
26.0			2.0	Very dense gray to greenish gray fine grained Silty SAND with white tiny marine shell pieces						26.0	(17)			
27.0	D													
28.0														
28.5	D													
29.0			2.5	Very dense gray to greenish gray fine grained Silty SAND with white tiny marine shell pieces						29.0	(18)			
30.0	D													
31.0														
31.5	D													
32.0			2.0	Very dense gray to greenish gray fine grained Silty SAND with white tiny marine shell pieces						32.0	(11)			
33.0	D													
34.0														
34.5	D													
35.0			2.0	Very dense gray to greenish gray fine grained Silty SAND with white tiny marine shell pieces						35.0	(73)			
36.0	D													
37.0														
37.5	D													
38.0			2.0	Very dense gray to greenish gray fine grained Silty SAND with white tiny marine shell pieces						38.0	(97)			
39.0	D													
40.0														
40.5	D													

Scale - 1 : 150 Undisturbed Sample - U Disturbed Sample : - D Bulk Sample - B Core Sample - C

Borehole (2)

Site *Western Breakwater /Al-Faw Grand Port* **Method of Boring** *Rotary*
Borehole No. *2* **Ground Level** *+8.00* **Date** *10/07/2014*

Water Table Level	Depth (m)	Sample Type & Depth	Soil Log	Thickness of Layer (m)	Soil Description	SPT Value N-Value					Remarks
						20	40	60	80	100	
1.00	1.0			4.5	Soft to very soft light brown to grayish brown lean Silty CLAY with reddish rusty traces of iron oxide compounds and black spots of organic matter						1.0
	2.0	D									2.0 (1)
	3.0	D		4.5	Very soft brown to grayish brown fat Silty CLAY with white tiny marine shell pieces and yellowish rusty traces of iron oxide compounds and black spots of organic matter						3.0 (1)
	4.5	U									4.5 (1)
	6.0	D		6.0							6.0 (1)
	7.5	D									7.5 (1)
	9.0	D		10.5	Very soft brown to brownish green Sandy lean Silty CLAY with yellowish rusty traces of iron oxide compounds and black spots of organic matter together with white sheets of mica minerals						9.0 (1)
	10.5	D									10.5 (1)
	12.0	U		4.5							12.0 (2)
	13.5	D									13.5 (2)
	15.0	D		15.0	Soft to medium greenish brown to grayish green lean Silty CLAY with white shiny traces of soluble salts and reddish rusty traces of iron oxide compounds						15.0 (3)
	16.5	D									16.5 (4)
	17.0	D		7.5							17.0 (7)
	18.0	U									18.0 (7)
	19.0	D		22.5	Medium to stiff grayish green Sandy fat Silty CLAY with black spots of organic matter						19.0 (7)
	22.5	D									22.5 (23)
	24.0	D		3.0							24.0 (13)
	25.0	D									25.0 (79)
	25.5	D		2.0	Very dense gray to greenish gray fine grained Clayey Silty SAND with rusty spots of iron oxide compounds						25.5 (79)
	27.0	D									27.0 (97)
28.0										28.0	
29.0										29.0	
30.0										30.0	

Scale - 1 : 150 Undisturbed Sample - U Disturbed Sample : - D Bulk Sample - B Core Sample - C

Borehole (3)

Site *WQ II - Mishrif CI-13* Method of Boring *Rotary*
Borehole No. *5* Ground Level ... *NGL* Date ... *06/03/2014* ...

Water Table Level	Depth (m)	Sample Type & Depth	No logy	Thickness of Layer (m)	Soil Description	SPT Value N-Value					Remarks	
						20	40	60	80	100		
3.20	1.0				Very stiff to stiff dark brown to brown lean Silty CLAY with black spots of organic matter and pieces of plant roots and white tiny marine shell pieces.						1.0	
	1.5	D		3.5							(25)	
	2.0					Stiff to medium gray to brownish gray Sandy lean Silty CLAY with little white tiny marine shell pieces and black spots of organic matter/roots.						2.0
	3.0	D		1.5								(22)
	4.0					Medium to stiff brownish gray lean Silty CLAY with black spots of organic matter and white tiny marine shell pieces .						4.0
	4.5	D		2.5								(14)
	5.0					Medium to stiff gray to grayish brown lean Silty CLAY with white tiny marine shell pieces.						5.0
	6.0	D		3.0								(13)
	7.0					Stiff to very stiff brown fat Silty CLAY with fine grained Sand seams and/or pockets and white tiny marine shell pieces.						7.0
	7.5	D		4.5								(15)
	8.0					Stiff to very stiff brown fat Silty CLAY with fine grained Sand seams and/or pockets and white tiny marine shell pieces.						8.0
	9.0	D		3.0								(12)
	10.0					Stiff to very stiff brown fat Silty CLAY with fine grained Sand seams and/or pockets and white tiny marine shell pieces.						10.0
	10.5	D		10.5								(13)
	11.0					Stiff to very stiff brown fat Silty CLAY with fine grained Sand seams and/or pockets and white tiny marine shell pieces.						11.0
	12.0	D		3.0								(17)
	13.0					Stiff to very stiff brown fat Silty CLAY with fine grained Sand seams and/or pockets and white tiny marine shell pieces.						13.0
	13.5	D		13.5								(27)
	14.0					Stiff to very stiff brown fat Silty CLAY with fine grained Sand seams and/or pockets and white tiny marine shell pieces.						14.0
	15.0	D		6.0								(29)
16.0				Stiff to very stiff brown fat Silty CLAY with fine grained Sand seams and/or pockets and white tiny marine shell pieces.						16.0		
16.5	D		16.0							(32)		
17.0				Stiff to very stiff brown fat Silty CLAY with fine grained Sand seams and/or pockets and white tiny marine shell pieces.						17.0		
18.0	D		18.0							(26)		
19.0				Stiff to very stiff brown fat Silty CLAY with fine grained Sand seams and/or pockets and white tiny marine shell pieces.						19.0		
19.5	D		19.5							(36)		
20.0				Very stiff brown to grayish brown Sandy lean Silty CLAY with reddish rusty traces of iron oxide compounds.						20.0		
21.0	D		4.5							(41)		
22.0				Very stiff brown to grayish brown Sandy lean Silty CLAY with reddish rusty traces of iron oxide compounds.						22.0		
22.5	D		22.5							(34)		
23.0				Very stiff to hard brown to reddish brown fat Silty CLAY interbedded by thin seams and/or pockets of fine grained Sand with reddish rusty traces of iron oxide compounds.						23.0		
24.0	D		24.0							(41)		
25.0				Very stiff to hard brown to reddish brown fat Silty CLAY interbedded by thin seams and/or pockets of fine grained Sand with reddish rusty traces of iron oxide compounds.						25.0		
25.5	D		25.5							(45)		
26.0				Very stiff to hard brown to reddish brown fat Silty CLAY interbedded by thin seams and/or pockets of fine grained Sand with reddish rusty traces of iron oxide compounds.						26.0		
27.0	D		6.5							(44)		
28.0				Very stiff to hard brown to reddish brown fat Silty CLAY interbedded by thin seams and/or pockets of fine grained Sand with reddish rusty traces of iron oxide compounds.						28.0		
28.5	D		28.5							(56)		
29.0				Very stiff to hard brown to reddish brown fat Silty CLAY interbedded by thin seams and/or pockets of fine grained Sand with reddish rusty traces of iron oxide compounds.						29.0		
30.0	D		30.0							(60)		

Scale - 1 : 150 Undisturbed Sample - U Disturbed Sample : - D Bulk Sample - B Core Sample - C

BOREHOLE LOG

Borehole (4)

Site *WQ II - Mishrif CI-13* **Method of Boring** *Rotary*

Borehole No. *6* **Ground Level** ... *NGL* **Date** ... *05/03/2014*

Water Table Level	Depth (m)	Sample Type & Depth	Photo log	Thickness of Layer (m)	Soil Description	SPT Value N-Value					Remarks
						20	40	60	80	100	
4.5	1.0				Very stiff dark brown to brown lean Silty CLAY with black spots of organic matter and rusty traces of iron oxide compounds.						1.5
	1.5	D		3.5							(24)
	2.0				Very stiff to stiff gray lean Silty CLAY with fine grained Sand and white tiny marine shell pieces together with black spots of organic matter.						2.5
	2.5	D		3.5							(22)
	3.0				Stiff to medium grayish dark brown lean Silty CLAY with white tiny marine shell pieces and black spots of organic matter.						3.5
	3.5	D		3.0							(23)
	4.0				Stiff to medium grayish dark brown lean Silty CLAY with white tiny marine shell pieces and black spots of organic matter.						4.5
	4.5	D		3.0							(19)
	5.0				Stiff to medium grayish dark brown lean Silty CLAY with white tiny marine shell pieces and black spots of organic matter.						5.5
	5.5	D		3.5							(15)
	6.0				Stiff to medium grayish dark brown lean Silty CLAY with white tiny marine shell pieces and black spots of organic matter.						6.5
	6.5	D		5.5							(16)
	7.0				Stiff to medium grayish dark brown lean Silty CLAY with white tiny marine shell pieces and black spots of organic matter.						7.5
	7.5	D		5.5							(16)
	8.0				Stiff to medium grayish dark brown lean Silty CLAY with white tiny marine shell pieces and black spots of organic matter.						8.5
	8.5	D		5.5							(16)
	9.0				Stiff to medium grayish dark brown lean Silty CLAY with white tiny marine shell pieces and black spots of organic matter.						9.5
	9.5	D		5.5							(16)
	10.0				Stiff to medium grayish dark brown lean Silty CLAY with white tiny marine shell pieces and black spots of organic matter.						10.5
	10.5	D		5.5							(16)
11.0				Stiff to medium grayish dark brown lean Silty CLAY with white tiny marine shell pieces and black spots of organic matter.						11.5	
11.5	D		5.5							(16)	
12.0				Medium to stiff gray to grayish brown lean Silty CLAY with white spots of soluble salts.						12.5	
12.5	D		12.0							(12)	
13.0				Medium to stiff gray to grayish brown lean Silty CLAY with white spots of soluble salts.						13.5	
13.5	D		4.5							(16)	
14.0				Medium to stiff gray to grayish brown lean Silty CLAY with white spots of soluble salts.						14.5	
14.5	D		4.5							(17)	
15.0				Medium to stiff gray to grayish brown lean Silty CLAY with white spots of soluble salts.						15.5	
15.5	D		4.5							(22)	
16.0				Stiff to very stiff brown lean Silty CLAY with yellowish rusty traces of iron oxide compounds.						16.5	
16.5	D		15.0							(23)	
17.0				Stiff to very stiff brown lean Silty CLAY with yellowish rusty traces of iron oxide compounds.						17.5	
17.5	D		15.0							(23)	
18.0				Stiff to very stiff brown lean Silty CLAY with yellowish rusty traces of iron oxide compounds.						18.5	
18.5	D		15.0							(28)	
19.0				Stiff to very stiff brown lean Silty CLAY with yellowish rusty traces of iron oxide compounds.						19.5	
19.5	D		6.0							(22)	
20.0				Stiff to very stiff brown lean Silty CLAY with yellowish rusty traces of iron oxide compounds.						20.5	
20.5	D		6.0							(34)	
21.0				Stiff to very stiff brown lean Silty CLAY with yellowish rusty traces of iron oxide compounds.						21.5	
21.5	D		22.0							(34)	
22.0				Very stiff brown to grayish brown fat Silty CLAY interbedded by thin seams of fine grained Sand with reddish rusty traces of iron oxide compounds.						22.5	
22.5	D		22.0							(38)	
23.0				Very stiff brown to grayish brown fat Silty CLAY interbedded by thin seams of fine grained Sand with reddish rusty traces of iron oxide compounds.						23.5	
23.5	D		4.5							(44)	
24.0				Very stiff brown to grayish brown fat Silty CLAY interbedded by thin seams of fine grained Sand with reddish rusty traces of iron oxide compounds.						24.5	
24.5	D		4.5							(44)	
25.0				Very stiff grayish dark brown fat Silty CLAY with rusty spots/lines of iron oxide compounds & shiny crystal of soluble salts.						25.5	
25.5	D		27.0							(51)	
26.0				Very stiff grayish dark brown fat Silty CLAY with rusty spots/lines of iron oxide compounds & shiny crystal of soluble salts.						26.5	
26.5	D		27.0							(51)	
27.0				Very stiff grayish dark brown fat Silty CLAY with rusty spots/lines of iron oxide compounds & shiny crystal of soluble salts.						27.5	
27.5	D		3.5							(55)	
28.0				Very stiff grayish dark brown fat Silty CLAY with rusty spots/lines of iron oxide compounds & shiny crystal of soluble salts.						28.5	
28.5	D		3.5							(55)	
29.0				Very stiff grayish dark brown fat Silty CLAY with rusty spots/lines of iron oxide compounds & shiny crystal of soluble salts.						29.5	
29.5	D		3.5							(51)	
30.0				Very stiff grayish dark brown fat Silty CLAY with rusty spots/lines of iron oxide compounds & shiny crystal of soluble salts.						30.5	
30.5	D		30.5							(51)	

Scale: - 1 : 150 Undisturbed Sample - U Disturbed Sample: - D Bulk Sample - B Core Sample - C

Borehole (5)

Site *New Transformer / FAO-Station* Method of Boring *Auger & Rotary*
Borehole No. *2* Ground Level ... *NGL* Date *02/06/2014*

Water Table Level	Depth (m)	Sample Type & Depth	Photo log	Thickness of Layer (m)	Soil Description	SPT Value N-Value					Remarks			
						20	40	60	80	100				
0.50														
	1.0	D		4.0	Very soft brown to brownish gray lean Silty CLAY interbedded by thin seams and/or pockets of fine grained Sand with reddish rusty traces of iron oxide compounds and black spots of organic matter							1.0		
	2.0	U												2.0
	3.0													3.0
	4.0	D		4.0	Very soft brownish gray to greenish gray fat Silty CLAY interbedded by thin seams and/or pockets of fine grained Sand together with black spots of organic matter							4.0 (1)		
	5.0													5.0
	6.0	U												6.0
	7.0			8.0								7.0		
	8.0	D												8.0 (1)
	9.0													9.0
	10.0	D										10.0 (1)		
	11.0													11.0
	12.0	D												12.0 (2)
	13.0			6.0	Very soft to soft grayish brown to brownish gray lean Silty CLAY interbedded by thin seams and/or pockets of fine grained Sand with black traces of organic matter							13.0		
	14.0													14.0
	15.0	D												15.0 (4)
	16.0											16.0		
	17.0													17.0
	18.0	D												18.0 (4)
	19.0			3.5	Soft to medium brown to brownish green lean Silty CLAY interbedded by thin seams and/or pockets of fine grained Sand with white tiny marine shell pieces and black spots of organic matter							19.0		
	20.0													20.0
	21.0	D												21.0 (13)
	22.0			5.5	Medium to stiff brown to brownish green lean Silty CLAY with reddish rusty traces of iron oxide compounds and black spots of organic matter							22.0		
	23.0													23.0
	24.0	D												24.0 (25)
	25.0											25.0		
	26.0													26.0
	27.0	D												27.0 (30)
	28.0			3.0	Very stiff light green lean Silty CLAY with black spots of organic matter and rusty traces of iron oxide compounds							28.0		
	29.0													29.0
	30.0	D												30.0 (51)

Scale: - 1:150 Undisturbed Sample - U Disturbed Sample - D Bulk Sample - B Core Sample - C

Continued...

BOREHOLE LOG

Site *New Transformer / FAO-Station* Method of Boring *Auger & Rotary*
Borehole No. *2* Ground Level ... *NGL* Date *02/06/2014*

Water Table Level	Depth (m)	Sample Type & Depth	Litho log	Thickness of Layer (m)	Soil Description	SPT Value N-Value					Remarks			
						20	40	60	80	100				
	31.0	D		12.0	Very stiff to hard light green to greenish yellow lean Silty CLAY with rusty traces of iron oxide compounds and white traces of marine shell			60			(51)			
	32.0													
	33.0													
	34.0	D												
	35.0													
	36.0													
	37.0													
	38.0	D												
	39.0													
	40.0													
	41.0													
	42.0	D					4.0	Hard greenish yellow to yellowish red Sandy lean Silty CLAY with reddish rusty traces of iron oxide compounds and black spots of organic matter						(100/20)
	43.0													
	44.0													
	45.0													
	46.0	D		4.0	Very dense yellowish gray fine grained Silty SAND with reddish rusty traces of iron oxide compounds and white shiny traces of soluble salts together with black spots of organic matter						(100/24)			
	47.0													
	48.0													
	49.0													
	50.0	D		7.0	Very dense gray to yellowish gray fine grained Silty SAND with Silty Clay pockets and/or thin seam in parts and reddish rusty traces of iron oxide compounds						(100/25)			
	51.0													
	52.0													
	53.0													
	54.0													
	55.0	D												
	56.0			3.5	Very dense gray fine grained Silty SAND with reddish rusty traces of iron oxide compounds and white shiny traces of soluble salts						(50/5)			
	57.0													
	58.0													
	59.0													
	60.0	D												

Scale - 1 : 150 Undisturbed Sample - U Disturbed Sample : - D Bulk Sample - B Core Sample - C

Borehole (6)

Site *FOT Terminal (On Shore)* Method of Boring *Auger & Rotary*
Borehole No. *3* Ground Level *NGL* Date *04/06/2014*

Water Table Level	Depth (m)	Sample Type & Depth	Soil log	Thickness of Layer (m)	Description	SPT Value N _v -Value					Remarks
						20	40	60	80	100	
0.00	1.0	U		6.0	Very soft gray to light gray fat Silty CLAY interbedded by thin seams and/or pockets of fine grained Sand with black spots of organic matter and white spots of soluble salts						
	2.0	U									
	3.0										
	4.0	D									(1)
	5.0										
	6.0	U		4.0	Very soft brown to brownish dark gray fat Silty CLAY interbedded by thin seams and/or pockets of fine to medium grained Sand with white tiny marine shell pieces and black spots of organic matter						(1)
	7.0										
	8.0	D									(1)
	9.0										
	10.0	D		10.0	Very soft to soft brown to brownish gray Sandy lean Silty CLAY mixture with white tiny marine shell pieces and rusty spots of iron oxide compounds						(2)
	11.0										
	12.0	D									(1)
	13.0			8.0							
	14.0										
	15.0	D									(2)
	16.0										
	17.0										
	18.0	D		14.0	Soft to medium brown to brownish gray lean Silty CLAY interbedded by thin seams and/or pockets of fine grained Sand with rusty spots/lines of iron oxide compounds						(5)
	19.0										
	20.0			5.0							
	21.0	D									(6)
	22.0										
	23.0			23.0	Medium to stiff brown to brownish gray lean Silty CLAY interbedded by thin seams and/or pockets of fine grained Sand with reddish rusty traces of iron oxide compounds and black pockets of organic matter together with white tiny marine shell pieces						(21)
	24.0	D		4.0							
	25.0										
	26.0										
	27.0	D		27.0	Very stiff grayish brown to greenish brown lean Silty CLAY with reddish rusty traces of iron oxide compounds and black pockets of organic matter						(60)
	28.0			3.0							
	29.0										
	30.0	D									(30)

Scale - 1 : 100 Undisturbed Sample - U Disturbed Sample - D Bulk Sample - B Core Sample - C

Site FOT Terminal (On Shore) Method of Boring Auger & Rotary
 Borehole No. 3 Ground Level NGL Date 04/06/2014

Water Table Level	Depth (m)	Sample Type & Depth	litho log	Thickness of Layer (m)	Description	SPT Value N-Value					Remarks
						20	40	60	80	100	
		D			Ditto						(38)
	31.0			4.0							31.0
	32.0										32.0
	33.0										33.0
	34.0	D		8.0	Dense to very dense gray mixture of fine grained Clayey Silty SAND with black spots of organic matter						34.0 (35)
	35.0										35.0
	36.0										36.0
	37.0										37.0
	38.0	D		8.0							38.0 (72)
	39.0										39.0
	40.0										40.0
	41.0										41.0
	42.0	D		4.0	Very stiff to hard brownish yellow mixture of Sandy lean Silty CLAY with black spots of organic matter and red rusty traces of iron oxide compounds						42.0 (79)
	43.0										43.0
	44.0										44.0
	45.0										45.0
	46.0	D		8.0	Very dense green to greenish gray fine grained Silty SAND with Silty Clay pockets in part and reddish rusty traces of iron oxide compounds together with white shiny traces of soluble salts						46.0 (80)
	47.0										47.0
	48.0										48.0
	49.0										49.0
	50.0	D		8.0							50.0 (100/21)
	51.0										51.0
	52.0										52.0
	53.0										53.0
	54.0										54.0
	55.0										55.0
	56.0	D		5.5	Very dense light green to greenish gray fine grained Silty SAND with reddish rusty traces of iron oxide compounds and white shiny traces of soluble salts						56.0 (50/6)
	57.0										57.0
	58.0										58.0
	59.0										59.0
	60.0	D		5.5							60.0 (50/4)

Borehole (7)

Site *Basra Governorate Building* Method of Boring *Rotary*
Borehole No. *2* Ground Level NGL Date *22/08/2013*

Water Table Level	Depth (m)	Sample Type & Depth	Lithology	Thickness of Layer (m)	Soil Description	SPT Value N-Value					Remarks
						20	40	60	80	100	
1.10	1.0	U	X X X X	5.0	Medium to soft brownish yellow to brownish gray lean Silty CLAY with dark rusty traces of iron oxide compounds and white shiny traces of soluble salts together with black spots of organic matter and white tiny Marine shell pieces.						(3)
	2.0		X X X X								
	3.0	U	X X X X								
	4.0		X X X X								
	5.0	D	X X X X								
	6.0	D	X X X X	9.0	Soft brownish gray to grayish brown lean Silty CLAY with little fine grained Sand and white tiny marine shell pieces together with black spots of organic matter and white shiny traces of soluble salts.						(4)
	7.0	D	X X X X								
	8.0		X X X X								
	9.0	U	X X X X								
	10.0		X X X X								
	11.0		X X X X	14.0	Stiff to very stiff brownish gray to greenish gray lean Silty CLAY with fine grained Sand in parts and white shiny traces of soluble salts together with black areas of organic matter and yellow rusty traces of iron oxide compounds.						(5)
	12.0	D	X X X X								
	13.0		X X X X								
	14.0	U	X X X X								
	14.5		X X X X								
	15.0		X X X X	4.0	Stiff to very stiff brownish gray to greenish gray lean Silty CLAY with fine grained Sand in parts and white shiny traces of soluble salts together with black areas of organic matter and yellow rusty traces of iron oxide compounds.						(31)
	16.0		X X X X								
	16.5	D	X X X X								
	17.0		X X X X								
	17.5	D	X X X X								
	18.0		X X X X	3.0	Dense yellowish gray to yellowish green fine grained Clayey Silty SAND with white shiny traces of soluble salts and black spots of organic matter						(49)
	18.5	D	X X X X								
	19.0		X X X X								
	20.0		X X X X								
	21.0	D	X X X X								
	22.0		X X X X	8.5	Very dense dark gray to gray fine, medium to coarse grained Silty SAND with a lot of white tiny marine shell pieces and yellow rusty traces of iron oxide compounds together with white shiny traces of soluble salts.						(47)
	23.0		X X X X								
	24.0	D	X X X X								
	25.0		X X X X								
	26.0	D	X X X X								
	27.0		X X X X	30.0							(69)
	28.0		X X X X								
	29.0	D	X X X X								
	30.0		X X X X								
	31.0	D	X X X X								
	32.0		X X X X	30.0							(77)
	33.0		X X X X								
	34.0		X X X X								
	35.0		X X X X								
	36.0		X X X X								
	37.0		X X X X	30.0							(83)
	38.0		X X X X								
	39.0		X X X X								
	40.0		X X X X								
	41.0		X X X X								

Scale - 1 : 100 Undisturbed Sample - U Disturbed Sample - D Bulk Sample - B Core Sample - C

BOREHOLE LOG

Borehole (8)

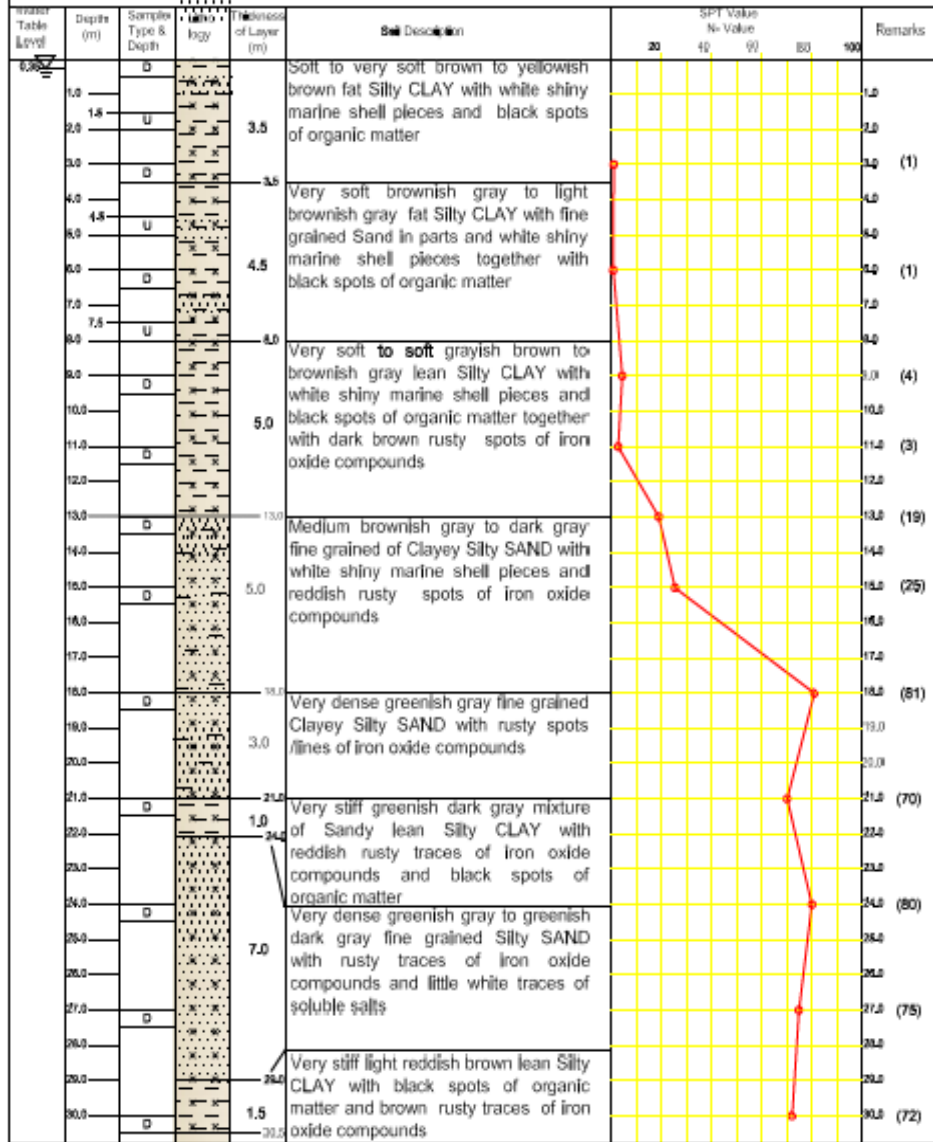
Site Basra Governorate Building Method of Boring Rotary
Borehole No. 3 Ground Level NGL Date 19/08/2013

Water Table Level	Depth (m)	Sample Type & Depth	Lithology	Thickness of Layer (m)	Description	SPT Value N-Value					Remarks	
						20	40	60	80	100		
1.30	1.0											
	1.4	U		5.0	Medium to soft greenish brown to brownish gray fat Silty CLAY with brown rusty traces of iron oxide compounds and white shiny traces of soluble salts together with black pockets of organic matter and green pockets of Marine shell pieces.							(4)
	2.0											(6)
	3.0											(6)
	4.0											
	5.0											
	6.0											
	7.0											
	8.0											
	9.0											
	10.0	D		10.5	Soft to medium brownish gray to grayish brown fat Silty CLAY with little fine grained Sand and white shiny traces of soluble salts together with black pockets of organic matter.							
	11.0											
	12.0											
	13.0											
	14.0											(9)
	15.0											
	15.5											
	16.0	D		3.0	Stiff to very stiff to hard greenish gray to gray lean Silty CLAY with fine grained Sand and white shiny traces of soluble salts together with black spots of organic matter and yellow rusty traces of iron oxide compounds.							(27)
	17.0											
	18.0											
	18.5											
	19.0	U		3.5	Very dense yellowish green to yellowish gray fine grained Clayey Silty SAND with white shiny traces of soluble salts and black spots of organic matter							(41)
	19.5											
	20.0	D										
	21.0											
	22.0											
	23.0											
	24.0											
	25.0											
	26.0											
	27.0											
	28.0											
	29.0											
	30.0	D		6.5	Very dense dark gray to grayish green fine, medium to coarse grained Silty SAND with little fine grained Gravel at bottom and yellowish red rusty traces of iron oxide compounds together with white shiny traces of soluble salts .							(100)
	31.0											
	32.0											
	33.0											
	34.0											
	35.0											
	36.0											
	37.0											
	38.0											
	39.0											
	40.0											
				30.4								(95)

Scale - 1 : 100 Undisturbed Sample - U Disturbed Sample - D Bulk Sample - B Core Sample - C

Borehole (9)

Site *Shatt Al-Basra Power Plant.....* Method of Boring *Rotary.....*
Borehole No. *1.....* Ground Level ... *NGL.....* Date *20/07/2014.....*



Scale - 1 : 150 Undisturbed Sample - U Disturbed Sample - D Bulk Sample - B Core Sample - C

Borehole (10)

Site *Shatt Al-Basra Power Plant.....* **Method of Boring** *Rotary*

Borehole No. *3* **Ground Level** ... *NGL* **Date** *19/07/2014*

Water Table Level	Depth (m)	Sample Type & Depth	Lithology	Thickness of Layer (m)	Soil Description	SPT Value N ₆₀ Value					Remarks
						20	40	60	80	100	
0.40	1.0	U		4.5	Soft to very soft brown fat Silty CLAY with white shiny marine shell pieces and fine grained Sand pockets in parts together with black spots of organic matter						1.0
	2.0	U									2.0
	3.0	U									3.0
	4.0	U		4.5	Very soft to soft light brown lean Silty CLAY with fine grained Sand in parts and white shiny marine shell pieces together with black spots of organic matter						4.0 (1)
	5.0	U									5.0
	6.0	U		6.0	Very soft to soft light brown lean Silty CLAY with fine grained Sand in parts and white shiny marine shell pieces together with black spots of organic matter						6.0 (3)
	7.0	U									7.0
	8.0	U									8.0
	9.0	U									9.0
	10.0	U									10.0
	11.0	U		11.0	Medium to stiff brownish dark gray Sandy lean Silty CLAY with white shiny marine shell pieces and black spots of organic matter together with brown rusty spots of iron oxide compounds						11.0
	12.0	U		4.5	Very soft to soft light brown lean Silty CLAY with fine grained Sand in parts and white shiny marine shell pieces together with black spots of organic matter						12.0 (19)
	13.0	U									13.0
	14.0	U									14.0
	15.0	U		15.0	Very dense dark greenish gray fine grained Clayey Silty SAND with black traces of organic matter						15.0 (51)
	16.0	U		3.0	Very dense dark greenish gray fine grained Clayey Silty SAND with black traces of organic matter						16.0 (38)
	17.0	U									17.0
	18.0	U		18.0	Very stiff greenish gray fat Silty CLAY with white shiny marine shell pieces and black traces of organic matter together with reddish rusty spots of iron oxide compounds						18.0 (50)
	19.0	U									19.0
	20.0	U									20.0
	21.0	U		6.0	Very stiff greenish gray fat Silty CLAY with white shiny marine shell pieces and black traces of organic matter together with reddish rusty spots of iron oxide compounds						21.0 (50)
	22.0	U									22.0
	23.0	U									23.0
	24.0	U		24.0	Very dense greenish dark gray fine grained Silty SAND with reddish rusty traces of iron oxide compounds						24.0 (75)
	25.0	U									25.0
	26.0	U		6.0	Very dense greenish dark gray fine grained Silty SAND with reddish rusty traces of iron oxide compounds						26.0 (83)
	27.0	U									27.0
	28.0	U									28.0
	29.0	U									29.0
	30.0	U		30.0	Very stiff light grayish brown lean Silty CLAY with white traces of carbonate compounds and brown rusty spots of iron oxide compounds						30.0 (69)
	31.0	U									31.0
	32.0	U									32.0
	33.0	U		5.5	Very stiff light grayish brown lean Silty CLAY with white traces of carbonate compounds and brown rusty spots of iron oxide compounds						33.0
	34.0	U									34.0
	35.0	U									35.0 (80)
	36.0	U		35.0							36.0
	37.0	U									37.0
	38.0	U									38.0
	39.0	U									39.0
	40.0	U									40.0

Scale - 1 : 200

Undisturbed Sample - U

Disturbed Sample: - D

Bulk Sample - B

Core Sample - C

Borehole (11)

Site *BWSIP* Method of Boring *Auger & Rotary*
Borehole No. *3* ... Ground Level *NGL* ... Date *11/10/2015* ...

Water Table Level	Depth (m)	Sample Type & Depth	Who logs	Thickness of Layer (m)	Soil Description	SPT Value N _v Value					Remarks	
						20	40	60	80	100		
0.35	1.0				Medium to soft brown to grayish brown lean Silty CLAY with little fine grained Sand in parts and white tiny marine shell pieces together with pieces of plant roots/organic matter and white traces of soluble salts.							
	1.5	D									(10)	
	2.0											
	3.0	U		6.0								
	4.0											
	4.5	D									(2)	
	5.0											
	6.0	U		4.0								
	7.0					Soft to very soft brown to brownish gray lean Silty CLAY interbedded by thin seams and/or pockets of fine grained Sand with white tiny marine shell pieces						
	7.5	D		3.0								(1)
	8.0				Very soft to soft brown to brownish gray lean Silty CLAY with little fine grained Sand with reddish rusty traces of iron oxide compounds.							
	9.0	U		4.0							(6)	
	10.0											
	11.0	D								(6)		
	12.0											
	13.0	D		13.0	Soft brown to brownish gray Sandy lean Silty CLAY .						(4)	
	14.0			1.5								
	15.0	D		14.0	Medium to stiff brown Sandy lean Silty CLAY with little white tiny marine shell pieces .						(37)	
	16.0	U		3.0								
	17.0											
	17.0	D		17.0	Medium brownish gray fine grained Clayey Silty SAND mixture with rusty spots of iron oxide compounds.						(23)	
	18.0											
	19.0	D		2.5						(21)		
	20.0	U		20.0	Stiff to very stiff brown to brownish gray lean Silty CLAY interbedded by thin seams and/or pockets of fine grained Sand.							
	21.0	D		3.0							(20)	
	22.0											
	23.0	D		23.0	Very stiff to hard brown to light brown lean Silty CLAY with little fine grained Sand and white tiny marine shell pieces.						(43)	
	24.0											
	24.0	D		2.5						(72)		
	25.0			24.0								
	26.0											
	27.0											
	28.0											
	29.0											
	30.0											

Scale - 1 : 150 Undisturbed Sample - U Disturbed Sample - D Bulk Sample - B Core Sample - C

BOREHOLE LOG

Borehole (12)

Site *BWSIP* Method of Boring *Auger & Rotary*
Borehole No. *4* Ground Level *NGL* Date *15/10/2015*

Water Table Level	Depth (m)	Sample Type & Depth	Lithology	Thickness of Layer (m)	Soil Description	SPT Value N ₆₀ Value					Remarks		
						20	40	60	80	100			
0.40	1.5			4.5	Soft to very soft brown to grayish brown lean Silty CLAY with black spots of organic matter .						7.5 (2)		
	2.0	D											
	3.0	U											
	4.0												
	4.5	D				14	Very soft to soft brown to grayish brown lean Silty CLAY with white tiny marine shell pieces.						9.0 (1)
	5.0												
	6.0	U				3.0							
	7.0												
	7.5	D				7.5	Very soft to soft brown to grayish brown lean Silty CLAY with little fine grained Sand and reddish rusty traces of iron oxide compounds .						9.0 (2)
	8.0												
	9.0	U				3.5							
	10.0												
11.0	D		11.0	Soft to medium brown to grayish dark brown Sandy lean Silty CLAY interbedded by thin seams and/or pockets of fine grained Sand with white tiny marine shell pieces.						11.0 (7)			
11.5	U		2.0										
13.0	D		13.0	Medium to stiff brown to grayish dark brown lean Silty CLAY interbedded by thin seams and/or pockets of fine grained Sand.						13.0 (11)			
14.0													
15.0	D		4.0	Stiff brown to grayish dark brown lean Silty CLAY interbedded by thin seams and/or pockets of fine grained Sand.						15.0 (13)			
16.0													
17.0	D		17.0	Stiff brown to grayish dark brown Sandy lean Silty CLAY mixture with white tiny marine shell pieces.						17.0 (25)			
17.5	U		2.0										
19.0	D		19.0	Stiff to very stiff brown fat Silty CLAY with little fine grained Sand and reddish rusty traces of iron oxide compounds.						19.0 (20)			
20.0													
21.0	D		21.0	Very stiff to hard brown to brownish gray lean Silty CLAY interbedded by thin seams and/or pockets of fine grained Sand with reddish rusty traces of iron oxide compounds.						21.0 (41)			
22.0													
23.0	D		4.5										
24.0													
25.0	D		24.5										
26.0													
27.0													
28.0													
29.0													
30.0													

Scale - 1 : 150 Undisturbed Sample - U Disturbed Sample: - D Bulk Sample - B Core Sample - C

BOREHOLE LOG

Borehole (13)

Site *WQ (II) EPF Power Plant* Method of Boring *Rotary*
Borehole No. *32* Ground Level NGL Date *19/09/2013*

Water Table Level	Depth (m)	Sample Type & Depth	Lithology	Thickness of Layer (m)	Description	SPT Value N-Value					Remarks	
						20	40	60	80	100		
▽	1.0		[Symbol]	4.5	Medium brown to light brown lean Silty CLAY with little yellow rusty traces of iron oxide compounds and black spots of organic matter and pieces of plant roots.						1.0	(12)
	1.5	D									2.0	
	3.0	U									3.0	
	4.0										4.0	
	5.0		[Symbol]	1.5	Medium to stiff grayish brown to brownish gray fat Silty CLAY with little fine grained Sand and white tiny marine shell pieces together with black spots of organic matter and yellow rusty traces of iron oxide compounds.						5.0	(11)
	6.0	D									6.0	
	7.0	U									7.0	
	8.0										8.0	
	9.0		[Symbol]	10.5							9.0	(16)
	10.0	U									10.0	
	11.0	D									11.0	
	12.0										12.0	
13.0		[Symbol]	16.0	Stiff to very stiff light brownish dark gray to dark gray Sandy lean Silty CLAY with white tiny marine shell pieces and black spots of organic matter together with yellow rusty traces of iron oxide compounds.						13.0	(19)	
14.0	D									14.0		
15.0	U									15.0		
16.0										16.0		
17.0		[Symbol]	3.0							17.0	(25)	
18.0	D									18.0		
19.0	U									19.0		
20.0										20.0		
21.0		[Symbol]	16.0	Stiff to very stiff light brownish dark gray to dark gray Sandy lean Silty CLAY with white tiny marine shell pieces and black spots of organic matter together with yellow rusty traces of iron oxide compounds.						21.0	(19)	
22.0	D									22.0		
23.0	U									23.0		
24.0										24.0		
25.0		[Symbol]	9.0	Very dense to dense yellowish gray to yellowish green fine to medium grained SAND with yellow rusty traces of iron oxide compounds and white shiny traces of soluble salts .						25.0	(65)	
26.0	D									26.0		
27.0	U									27.0		
28.0										28.0		
29.0		[Symbol]	27.0	Dense to very dense greenish gray to dark gray fine to medium grained Silty SAND with red rusty spots/lines if iron oxide compounds.						29.0	(72)	
30.0	D									30.0		
31.0	U									31.0		
32.0										32.0		
33.0		[Symbol]	3.5							33.0	(29)	
34.0	D									34.0		
35.0	U									35.0		
36.0										36.0		
37.0		[Symbol]	37.0	Dense to very dense greenish gray to dark gray fine to medium grained Silty SAND with red rusty spots/lines if iron oxide compounds.						37.0	(31)	
38.0	D									38.0		
39.0	U									39.0		
40.0										40.0		
41.0		[Symbol]	31.5							41.0	(40)	
42.0	D									42.0		
43.0	U									43.0		
44.0										44.0		

Scale - 1 : 100 Undisturbed Sample - U Disturbed Sample - D Bulk Sample - B Core Sample - C

BOREHOLE LOG

Borehole (14)

Site *WQ (II) EPF Power Plant* Method of Boring *Rotary*
Borehole No. *35* Ground Level NGL Date *17/09/2013*

Water Table Level	Depth (m)	Sample Type & Depth	Lithology	Thickness of Layer (m)	Soil Description	SPT Value N-Value					Remarks
						20	40	60	80	100	
1.02	1.0				Medium to soft brownish light green to light greenish brown fat Silty CLAY with yellow rusty traces of iron oxide compounds and black spots of organic matter and white tiny marine shell pieces.						(12)
	1.5	D		4.5							
	2.0	U									
	3.0				Soft to medium brown to brownish gray fat Silty CLAY with a lot of fine grained Sand in parts and white tiny marine shell pieces together with red rusty traces of iron oxide compounds.						(7)
	4.0	D		4.0							
	5.0	U		5.0							
	6.0				Stiff to very stiff grayish green to reddish light green fat Silty CLAY with a lot of fine grained Sand and white tiny marine shell pieces together with yellow rusty traces of iron oxide compounds.						(8)
	7.0	D		7.0							
	8.0	U		8.0							
	9.0				Stiff to very stiff grayish green to reddish light green fat Silty CLAY with a lot of fine grained Sand and white tiny marine shell pieces together with yellow rusty traces of iron oxide compounds.						(18)
	10.0	D		10.0							
	11.0	U		11.0							
	12.0				Dense greenish gray to dark green fine grained Clayey Silty SAND with a lot of white tiny marine shell pieces and black spots of organic matter.						(25)
	13.0	D		13.0							
	14.0	U		14.0							
15.0				Dense greenish gray to dark green fine grained Clayey Silty SAND with a lot of white tiny marine shell pieces and black spots of organic matter.						(32)	
16.0	D		16.0								
17.0	U		17.0								
18.0				Dense greenish gray to dark green fine grained Clayey Silty SAND with a lot of white tiny marine shell pieces and black spots of organic matter.						(77)	
19.0	D		19.0								
20.0	U		20.0								
21.0				Dense greenish gray to dark green fine grained Clayey Silty SAND with a lot of white tiny marine shell pieces and black spots of organic matter.						(70)	
22.0	D		22.0								
23.0	U		23.0								
24.0				Dense greenish gray to dark green fine grained Clayey Silty SAND with a lot of white tiny marine shell pieces and black spots of organic matter.						(92)	
25.0	D		25.0								
26.0	U		26.0								
27.0				Very stiff brown to light brown Sandy fat Silty CLAY with red rusty traces of iron oxide compounds and white crystal pieces of mica mineral compounds.						(39)	
28.0	D		28.0								
29.0	U		29.0								
30.0				Very stiff brown to light brown Sandy fat Silty CLAY with red rusty traces of iron oxide compounds and white crystal pieces of mica mineral compounds.						(38)	
31.0	D		31.0								
32.0	U		32.0								
33.0				Very stiff brown to light brown Sandy fat Silty CLAY with red rusty traces of iron oxide compounds and white crystal pieces of mica mineral compounds.						(44)	
34.0	D		34.0								
35.0	U		35.0								
36.0				Very stiff brown to light brown Sandy fat Silty CLAY with red rusty traces of iron oxide compounds and white crystal pieces of mica mineral compounds.						(58)	
37.0	D		37.0								
38.0	U		38.0								

Scale - 1 : 100 Undisturbed Sample - U Disturbed Sample - D Bulk Sample - B Core Sample - C

BOREHOLE LOG

Borehole (15)

Site Cluster 6Y at WQ-II Method of Boring Rotary

Borehole No. 1B..... Ground Level NGL Date 29/11/2014 ...

Water Table Level	Depth (m)	Sample Type & Depth	Lithology	Thickness of Layer (m)	Description	SPT Value N-Value					Remarks	
						20	40	60	80	100		
2.0	0.4				Medium to soft brown to brownish dark gray fat Silty CLAY with little fine grained Sand in parts and white tiny marine shell pieces together with reddish rusty traces of iron oxide compounds.						(7)	
	1.0	D									(7)	
	1.2											
	2.0	D										
	3.0	U										
	4.0											
	4.4											(4)
	5.0	D			Soft to medium brown fat Silty CLAY with little fine grained Sand and white tiny marine shell pieces together with reddish rusty traces of iron oxide compounds.							
	6.0	U										
	7.0											
	7.5	D									(9)	
	8.0											
	9.0	U										
	10.0											
	11.0											
12.0	D									(32)		
13.0												
14.0												
15.0	U											
16.0												
17.0												
18.0	D									(37)		
19.0												
20.0												
21.0	U											
22.0												
23.0												
24.0	D									(41)		
25.0												
26.0												
27.0	U											
28.0												
29.0												
30.0	D									(58)		
31.0												
32.0												
33.0												
34.0	U											
35.0	D									(58)		
36.0												
37.0												
38.0												
39.0												
40.0												

Scale - 1 : 200 Undisturbed Sample - U Disturbed Sample - D Bulk Sample - B Core Sample - C

Borehole (16)

Site Cluster 6Y at WQ-II Method of Boring Rotary

Borehole No. 3B.... Ground Level NGL Date 29/11/2014 ...

Water Table Level	Depth (m)	Sample Type & Depth	Lithology	Thickness of Layer (m)	Soil Description	SPT Value N-Value					Remarks
						20	40	60	80	100	
1.5	0.0				Medium to soft brown fat Silty CLAY with white shiny crystals of soluble salts and reddish rusty traces of iron oxide compounds together with black spots of organic matter.						(8)
	1.0	D		4.5							(3)
	1.5										
	2.0	D									
	3.0	U									
	4.0										
	4.4	D		4.5	Medium to soft brown lean Silty CLAY with little fine grained Sand and white tiny marine shell pieces together with reddish rusty traces of iron oxide compounds.						(10)
	5.0										
	6.0	U		3.0							
	7.0										
	7.5	D		7.5	Soft brown lean Silty CLAY with little fine grained Sand and white tiny marine shell pieces.						(5)
	8.0										
	9.0	U		3.5							
	10.0										
	11.0			11.1							
	12.0	D		4.5	Medium to dense gray to brownish gray fine grained Silty SAND with white shiny traces of soluble salts and yellowish rusty traces of iron oxide compounds.						(34)
13.0											
14.0											
15.0	U		10.5	Stiff brown lean Silty CLAY with little fine grained Sand and white crystals/sheets of mica minerals together with white shiny traces of soluble salts and reddish rusty spots of iron oxide compounds.						(26)	
16.0											
17.0											
18.0	D		6.0								
19.0											
20.0											
21.0	U		7.5	Stiff gray lean Silty CLAY with brownish rusty traces of iron oxide compounds and black spots of organic matter.						(26)	
22.0											
23.0											
24.0	D		8.5								
25.0											
26.0											
27.0	U										
28.0											
29.0											
30.0	D		31.4	Stiff to very stiff gray to greenish gray Sandy fat Silty CLAY with little yellowish rusty traces of iron oxide compounds and black spots of organic matter.						(25)	
31.0											
32.0											
33.0	U		5.5								
34.0											
35.0	D		35.0							(40)	
36.0											
37.0											
38.0											
39.0											
40.0											

Scale - 1 : 200 Undisturbed Sample - U Disturbed Sample - D Bulk Sample - B Core Sample - C

BOREHOLE LOG

Borehole (17)

Site BWSIP-P3 Method of Boring Rotary

Borehole No. 15 Ground Level +018m Date 29/11/2014

Water Table Level	Depth (m)	Sample Type & Depth	Thickn. of Layer (m)	Soil Description	SPT Value N-Value					Remarks	
					20	40	60	80	100		
1.0	1.0		3.0	Very soft to soft gray to brownish gray Clayey Sandy SILT mixture with white tiny marine shell pieces & black spots of organic matter.						1.0	
	2.0									2.0	
	3.0	U	5.0	Soft gray to grayish brown lean Silty CLAY with little fine grained Sand and black spots of organic matter together with rusty traces of iron oxide compounds.						3.0 (3)	
	4.0									4.0	
	5.0	D								5.0	
	6.0									6.0	
	7.0									7.0	
	7.5	U	5.0							7.5	
	8.0									8.0	
	9.0									9.0	
	10.0	D		10.0	Medium to soft gray to brownish dark gray Sandy lean Silty CLAY with black spots of organic matter.						10.0 (7)
	11.0									11.0	
	12.0									12.0	
	12.5	U		7.5						12.5	
13.0									13.0		
14.0									14.0		
15.0	D								15.0 (4)		
16.0									16.0		
17.0									17.0		
17.5	U		17.5	Medium brown to grayish brown mixture of fine grained Clayey Silty SAND with white spots of soluble salts.						17.5	
18.0									18.0		
19.0									19.0		
20.0	D		20.0	Very stiff brown to brownish gray lean Silty CLAY with little fine grained Sand.						20.0 (42)	
21.0									21.0		
22.0									22.0		
22.5	U		22.5	Very stiff to stiff brown to dark brown Sandy lean Silty CLAY mixture with white crystals of soluble salts and reddish rusty traces of iron oxide compounds.						22.5	
23.0									23.0		
24.0									24.0		
25.0	D								25.0 (38)		
26.0									26.0		
27.0									27.0		
27.5	U		7.5						27.5		
28.0									28.0		
29.0									29.0		
30.0	D		30.0	Stiff to very stiff gray to brownish gray mixture of Sandy Clayey SILT with white tiny marine shell pieces.						30.0 (14)	
31.0									31.0		
32.0	D		2.5						32.0 (68)		
33.0									33.0		
34.0									34.0		
35.0									35.0		
36.0									36.0		
37.0									37.0		
38.0									38.0		
39.0									39.0		
40.0									40.0		

Scale - 1 : 200 Undisturbed Sample - U Disturbed Sample - D Bulk Sample - B Core Sample - C

Borehole (18)

Site *B W S I P - P 3* **Method of Boring** *Rotary*

Borehole No. *19* **Ground Level** ... *+1.21m* **Date** *04/12/2014*

Water Table Level	Depth (m)	Sample Type & Depth	Litho logg	Thickness of Layer (m)	Description	SPT Value N-Value					Remarks
						20	40	60	80	100	
0.46	1.0				Very soft to soft gray to brownish gray lean Silty CLAY with white shiny traces of soluble salts and black spots of organic matter.						1.0
	2.0										2.0
	3.0	U			Soft gray to dark gray lean Silty CLAY with little fine grained Seams and/or pockets and reddish rusty traces of iron oxide compounds together with black spots of organic matter.						3.0
	4.0			7.5							4.0
	5.0	D									5.0 (2)
	6.0										6.0
	7.0				Soft gray to dark gray lean Silty CLAY with little fine grained Seams and/or pockets and reddish rusty traces of iron oxide compounds together with black spots of organic matter.						7.0
	7.5	U		7.5							7.5
	8.0										8.0
	9.0			5.0							9.0 (8)
	10.0	D			Soft to medium gray to brownish light gray lean Silty CLAY with white tiny marine shell pieces						10.0
	11.0										11.0
	12.0										12.0
	12.5	U		12.5							12.5
	13.0			2.5	Medium to stiff gray to grayish dark brown Sandy lean Silty CLAY with a lot of white tiny marine shell pieces and reddish rusty traces of iron oxide compounds .						13.0 (13)
	14.0										14.0
	15.0	D									15.0
	16.0			5.0							16.0 (26)
	17.0				Stiff to very stiff brown to dark brown fat Silty CLAY with white crystals of soluble salts and black traces of organic matter.						17.0
	17.5	D									17.5
	18.0										18.0
	19.0			7.5							19.0 (29)
	20.0	D			Very stiff brown to grayish brown brown to light brown lean Silty CLAY with little fine grained Sand and yellowish rusty traces of iron oxide compounds						20.0
	21.0										21.0
	22.0										22.0
	22.5	U		22.5							22.5
	23.0				Dense to very dense brownish gray to grayish green fine grained Clayey Silty SAND with white tiny marine shell pieces						23.0
	24.0			7.5							24.0 (44)
	25.0	D									25.0
	26.0										26.0
	27.0										27.0
	27.5	U		27.5							27.5
	28.0			2.5							28.0
	29.0										29.0
	30.0	D									30.0 (30)
	31.0			2.5							31.0
	32.0	D									32.0 (59)
	33.0			33.0							33.0
	34.0									34.0	
	35.0									35.0	
	36.0									36.0	
	37.0									37.0	
	38.0									38.0	
	39.0									39.0	
	40.0									40.0	

Scale - 1 : 200 Undisturbed Sample - U Disturbed Sample : - D Bulk Sample - B Core Sample - C

Borehole (19)

Site Cluster 4Y at WQ II Method of Boring Rotary
Borehole No. 2B Ground Level ... NGL Date 20/11/2014

Water Table Level	Depth (m)	Sample Type & Depth	Lithology	Thickness of Layer (m)	Description	SPT Value N-Value				Remarks		
						20	40	60	80		100	
1.35	0.4			2.0	Medium to soft brown to grayish brown fat Silty CLAY with white spots of soluble salts and reddish rusty traces of iron oxide compounds together with black spots of organic matter.						(10)	
	1.0	D		2.0							(2)	
	1.2	D		2.0								
	2.0			4.0	Soft to medium brown to reddish brown fat Silty CLAY with little fine grained Sand and white tiny marine shell pieces together with reddish rusty traces of iron oxide compounds and black pockes of organic matter.							(7)
	3.0	U		4.0								
	4.0			6.0	Soft to medium gray to brownish dark gray lean Silty CLAY with little fine grained Sand in parts and white tiny marine shell pieces							(8)
	4.8	D		6.0								
	5.0			12.0	Medium to stiff gray to whitish gray lean Silty CLAY with little fine grained Sand and white crystal pieces of mica minerals together with white tiny marine shell pieces and reddish rusty traces of iron oxide compounds							(10)
	6.0	U		12.0								
	7.0			6.0	Medium to stiff gray to grayish brown Sandy lean Silty CLAY with white tiny marine shell pieces and reddish rusty traces of iron oxide compounds .							(26)
	7.8	D		6.0								
	8.0			21.0	Dense to very dense gray to brownish gray fine grained Clayey Silty SAND mixture with white shiny traces of soluble salts and white tiny marine shell pieces together with yellowish rusty traces of iron oxide compounds.							(78)
	9.0	U		21.0								
	10.0			33.0	Very stiff light brown to grayish brown Sandy lean Silty CLAY mixture with white spots of soluble salts and reddish rusty traces of iron oxide compounds							(41)
	11.0	D		33.0								
	12.0			5.5								(37)
	13.0	U		5.5								
14.0			35.0									
15.0	D		35.0									
16.0												
17.0												
18.0												
19.0												
20.0												

Scale - 1 : 200 Undisturbed Sample - U Disturbed Sample - D Bulk Sample - B Core Sample - C

Borehole (20)

Site Cluster 4Y at WQ II **Method of Boring** Rotary

Borehole No. 3B **Ground Level** NGL **Date** ... 22/11/2014

Water Table Level	Depth (m)	Sample Type & Depth	Lithology	Thickness of Layer (m)	Soil Description	SPT Value N-Value					Remarks	
						20	40	60	80	100		
1.70	0.0											
	1.0	D		3.0	Soft gray to grayish light green lean Silty CLAY with white shiny crystals of soluble salts and reddish rusty traces of iron oxide compounds together with black spots of organic matter.							(4)
	1.5	D										(5)
	2.0	D										
	3.0	U		1.0								
	4.0	D										
	4.5	D		5.0	Soft to medium brown to reddish brown lean Silty CLAY with black spots of organic matter.							(9)
	5.0	D										
	6.0	U										
	7.0	D										
	7.5	D										
	8.0	D		4.0	Medium to soft brown lean Silty CLAY with fine grained Sand in parts and white tiny marine shell pieces together with reddish rusty traces of iron oxide compounds.							(11)
	9.0	U										
	10.0	D										
	11.0	D		7.0								
	12.0	D										
	13.0	D										
	14.0	D										
	15.0	D										
	16.0	U		15.5	Soft to very soft brown to brownish gray fat Silty CLAY with alot of fine grained Sand at bottom and reddish rusty traces of iron oxide compounds.							
17.0	D		3.5									
18.0	D		19.5	Medium to stiff brown mixture of Sandy fat Silty CLAY with reddish rusty traces of iron oxide compounds and black spots of organic matter.								(2)
19.0	D											
20.0	U											
21.0	D											
22.0	D		8.5									
23.0	D											
24.0	D											
25.0	D											
26.0	D											
27.0	U		27.5	Stiff to very stiff gray to brownish gray Sandy lean Silty CLAY with white shiny traces of soluble salts and white tiny marine shell piece together with reddish rusty traces of iron oxide compounds.								(21)
28.0	D											
29.0	D											
30.0	D		6.5									
31.0	D											
32.0	D											
33.0	U											
34.0	D		33.5	Dense greenish gray fine grained Clayey Silty SAND with rusty spots of iron oxide compounds.								(24)
35.0	D		2.0									
36.0	D											
37.0	D											
38.0	D											
39.0	D											
40.0	D											

Scale - 1 : 200 Undisturbed Sample - U Disturbed Sample - D Bulk Sample - B Core Sample - C